GENERALIZED LINEAR FILTERING OF SEISMIC ARRAY DATA

P. R. LINTZ
R. L. SAX
R. R. BLANDFORD
SEISMIC DATA LABORATORY

8 OCTOBER 1971

Prepared for
FORCE TECHNICAL APPLICATIONS CENTER
Washington, D.C.

Under
Project VELA UNIFORM

Sponsored by
ADVANCED RESEARCH PROJECTS AGENCY
Nuclear Monitoring Research Office
ARPA Order No.1714

TELEDYNE GEOTECH
XANDRIA LABORATORIES

APPROVED FOR PUBLIC RELEASE: DISTRIBUTION UNLIMITED.

DISCLAIMER NOTICE

Neither the Advanced Research Projects Agency nor the Air Force Technical Applications Center will be responsible for information contained herein which has been supplied by other organizations or contractors, and this document is subject to later revision as may be necessary. The views and conclusions presented are those of the authors and should not be interpreted as necessarily representing the official policies, either expressed or implied, of the Advanced Research Projects Agency, the Air Force Technical Applications Center, or the U S Government.

GENERALIZED LINEAR FILTERING OF SEISMIC ARRAY DATA

SEISMIC DATA LABORATORY REPORT NO. 269

AFTAC Project No.:	VELA T/2706
Project Title:	Seismic Data Laboratory
ARPA Order No.:	1714
ARPA Program Code No.:	2F-10
Name of Contractor:	TELEDYNE GEOTECH
Contract No.:	F33657-72-C-0009
Date of Contract:	01 July 1971
Amount of Contract:	$ 1,290,000
Contract Expiration Date:	30 June 1972
Project Manager:	Royal A. Hartenberger (703) 836-7647

P. O. Box 334, Alexandria, Virginia

APPROVED FOR PUBLIC RELEASE; DISTRIBUTION UNLIMITED.

UNCLASSIFIED

Security Classification

DOCUMENT CONTROL DATA - R&D

(Security classification of title, body of abstract and indexing annotation must be entered when the overall report is classified)

1. ORIGINATING ACTIVITY (Corporate author) TELEDYNE GEOTECH ALEXANDRIA, VIRGINIA	2a. REPORT SECURITY CLASSIFICATION Unclassified
	2b. GROUP

3. REPORT TITLE

GENERALIZED LINEAR FILTERING OF SEISMIC ARRAY DATA

4. DESCRIPTIVE NOTES (Type of report and inclusive dates)

5. AUTHOR(S) (Last name, first name, initial)

Lintz, P.R.; Sax, R.L.; and Blandford, R.R.

6. REPORT DATE 8 October 1971	7a. TOTAL NO. OF PAGES 88	7b. NO. OF REFS 17
8a. CONTRACT OR GRANT NO. F33657-70-C-0941	9a. ORIGINATOR'S REPORT NUMBER(S) 269	
b. PROJECT NO. VELA T/0706		
c. ARPA Order No. 624	9b. OTHER REPORT NO(S) (Any other numbers that may be assigned this report)	
d. ARPA Program Code No. 9F10		

10. AVAILABILITY/LIMITATION NOTICES

APPROVED FOR PUBLIC RELEASE; DISTRIBUTION UNLIMITED.

11. SUPPLEMENTARY NOTES	12. SPONSORING MILITARY ACTIVITY ADVANCED RESEARCH PROJECTS AGENCY NUCLEAR MONITORING RESEARCH OFFICE WASHINGTON, D. C.

13. ABSTRACT

The theory of generalized linear filtering (Oppenheim, [illegible], 1969) is applied to the problem of averaging the transfer functions between a seismic source and seismic recording stations on a continental-sized array.

To provide synthetic data for a test of the processor, a simple source signal is passed through nine different random perturbations of a velocity-depth structure yielding nine different synthetic seismograms. Two nuclear explosions (LONGSHOT and MILROW) and an Andreanoff Islands event (22 November 1965) are also processed using stations from the Long-Range-Seismic-Measurement net. Most of the reverberations are removed from the synthetic seismogram by generalized linear filtering. The explosions and the earthquake seismograms are simplified by this process.

The earthquake appears to have longer time terms remaining after generalized linear filtering and the nuclear events appear more similar (before the arrival of the depth phase).

14. KEY WORDS

Array Processing
Logarithmic Deconvolution
Generalized Linear Filtering
Homomorphic Filtering

UNCLASSIFIED

Security Classification

ABSTRACT

The theory of generalized linear filtering (Oppenheim, 1966, 1969) is applied to the problem of averaging the transfer functions between a seismic source and seismic recording stations on a continental-sized array.

To provide synthetic data for a test of the processor, a simple source signal is passed through nine different random perturbations of a velocity-depth structure yielding nine different synthetic seismograms. Two nuclear explosions (LONG SHOT and MILROW) and an Andreanoff Islands event (22 November 1965) are also processed using stations from the Long-Range-Seismic-Measurement net. Most of the reverberations are removed from the synthetic seismogram by generalized linear filtering. The explosion and the earthquake seismograms are simplified by this process.

The earthquake appears to have longer time terms remaining after generalized linear filtering and the nuclear events appear more similar (before the arrival of the depth phase).

TABLE OF CONTENTS

LIST OF FIGURES

LIST OF FIGURES (Cont'd.)

LIST OF FIGURES (Cont'd.)

LIST OF FIGURES (Cont'd.)

LIST OF FIGURES (Cont'd.)

LIST OF TABLES

INTRODUCTION

Seismic signal models

One difficulty encountered in beaming a short-period worldwide or continental-sized seismic array is that the signal coherency falls off markedly with distance* (Hartenberger, 1967; Klappenberger, 1967; Capon et al, 1967).

A possible model of the seismogram recorded at the jth instrument an array under excitation of a signal plus uncorrelated additive noise is

$$Y_j(t) = S(t) * h_j(t) + n_j(t) \tag{1}$$

where the * indicates convolution.

The Fourier transform of (1) yields

$$Y_j(f) = S(f) H_j(f) + N_j(f) \tag{2}$$

The $H_j(f)$ may be thought of as a source-receiver travel-path transfer function for the jth receiver.

---

*Amplitude anomalies may run as high as eight-to-one for LASA (Klappenberger, 1967; Mack, 1969), whereas time anomalies may run as high as 1.5 sec at LASA (Chiburis, 1966).

The probability density of the random transfer functions under the hypothesis of zero additive noise

If we make the assumption of large signal-to-additive noise ratio, equation (2) becomes

$$Y_j(f) \approx H_j(f)\, S(f) \tag{3}$$

If we further assume that $H_j(f)$ may be written as a product of a large number of small disturbances, then

$$Y_j(f) = \prod_{m=1}^{M} \mid A_{mj}(f) \mid \exp\left[i\phi_{mj}(f)\right] S(f) \tag{4}$$

where m is the index of each small disturbance and M is the total number of disturbances. Taking the logarithm of both sides of equation (4), gives

$$\log Y_j(f) = \log|S(f)| + \sum_{m=1}^{M} \log|A_{mj}(f)| + i\left\{\phi_s(f) + \sum_{m=1}^{M}\left[\phi_{mj}(f) \pm 2\pi M_{mj}(f)\right]\right\} \tag{5}$$

where $M_{mj}(f)$ is an integer which reflects the uncertainty in the correct Riemann sheet at each frequency. We see that the logarithm of the complex Fourier spectrum has converted our multiplicative variables into a new set of additive variables. If $A_{mj}(f)$ and the $\phi_{mj}(f)$ can be described by a probability density function, then we may invoke the weak law of large numbers and state that our new random variable $\log\ Y_j(f)$

is asymptotically normally distributed over the ensemble with the expected value of the real part equal to

$$\log|S(f)| + \log|\mu(f)|$$

where $\mu(f)$ is the geometric mean of the random transfer functions. The expected value of the imaginary part of log $Y_j(f)$ is equal to

$$\phi_s(f) + \phi_m(f)$$

where $\phi_m(f)$ is the phase of the mean of the random transfer functions. The maximum likelihood estimate of $\log|\mu(f)|$ is given by

$$\widehat{\log|\mu(f)|} = \frac{1}{N} \sum_{j=1}^{N} \sum_{m=1}^{M} \log|A_{mj}(f)| \tag{6a}$$

The maximum likelihood estimate of $\phi_\mu(f)$ is given by

$$\hat{\phi}_\mu(f) = \frac{1}{N} \sum_{j=1}^{N} \sum_{m=1}^{M} \left[\phi_{mj}(f) + M_{mj}(f)\right] \tag{6b}$$

The probability density function which describes the complex random variable y_i is a log-normal density function (Aitchinson and Brown, 1963). Note that if the signal

spectrum is white, then the estimates at different values of frequency are normally distributed and we have a stationary bivariate log-normal variable. If the signal spectrum is non-white we have a non-frequency-stationary bivariate log-normal variable.

The theory of logarithmic deconvolution has been developed by Oppenheim (1966) and Schafer (1967, 1969) as a specific case of Oppenheim's generalized linear filtering theory. For random transfer functions, the real difficulty with this method is the choice of the proper Riemann number $N_j(f)$ where $N_j(f) = \sum_{m=1}^{M} M_{mj}(f)$ for each recording site. If the phase changes rapidly with frequency, i.e., $\phi(f)$ has a large variance, we may find ourselves faced with an almost uniform distribution (over the ensemble of stations) for our estimate of the ensemble average of $\phi(f)$ due to the discontinuous Riemann transformation. This problem is illustrated in Figure 1 for a zero mean distribution. Our solution is to set the phase equal to zero zero at zero frequency for each recording site and then unwind the phase. Schafer (1969) has discussed techniques for unwinding the phase.

There is experimental evidence that the $A_j(f)$ are log-normally distributed. Klappenberger (1967) has shown that earthquakes have log-normally distributed peak-to-peak amplitudes at LASA and Freedman (1967) has shown the same distribution for earthquakes at worldwide recording sites. Figure 2 is the histogram of Klappenberger's data. Figure 3 is Klappenberger's best straight line fit to his data plotted on log-normal probability paper. If the data are log-normal, the cumulative frequency distribution should approximate a

straight line. The hypothesis that the data are log-normal cannot be rejected at the 95% confidence level.

Further indication of the log-normality of the station spectra may be obtained by passing a synthetic signal through ensembles of plane parallel-layered media with random reflection coefficients.

Figure 4 illustrates the problem of a seismic wave impinging upon a set of plain, parallel layered media. A subroutine given by Claerbout (1968) was programmed to yield the transmission seismogram of an arbitrary wavelet impinging upon the bottom layer. Figure 5 is the analog computer simulation of the transmission and reflection problem. Electrical engineers might recognize the circuit as a "ladder network" or as a parametric amplifier.

The optimum processor

Under the assumption of white, uncorrelated, zero-mean, equal variance, log-transfer functions and zero additive noise it can be demonstrated from maximization of the log-likelihood function that the likelihood estimator for the logarithm of the signal in the frequency domain is just the arithmetic average of the individual station log-spectra.

$$\widehat{\log S(f)} = \frac{1}{N} \sum_{j=1}^{N} \log Y_j(f) \tag{7}$$

or $$\widehat{S(f)} = \exp \left[\widehat{\log S(f)} \right] \tag{8}$$

so that $$\widehat{S(f)} = \left[\prod_{j=1}^{N} Y_j(f) \right]^{1/N} \tag{9}$$

Equation (9) is just the geometric mean of our individual station amplitude spectra. Figure 6 is a block diagram of the processor for this case. Figure 7 is a modification of the processor to filter out undesirable time components.

RESULTS

Simulated receiver site effects

Synthetic seismograms were generated by feeding a signal of the form $f(t) = t \exp(-\alpha t) \sin \omega_0 t$ into a stack of layers with random reflection coefficients. The velocity as a function of depth corresponds to a median of the models given in Figure 24 of SDL Report No. 243 (Glover and Alexander, 1970) with small perturbations in the velocity as a function of depth. In order to get reasonably complicated seismograms it was necessary to incorporate thin layers (Landers and Claerbout, 1969; Ali, 1966) into the model. Figures 8 through 16 are plots of (a), the reflection coefficients, (b), the seismogram and, (c), the velocity as a function of depth, for nine realizations of our random process. Since equal travel-time layers were taken, the spacing of sample points on the linear depth scale is not linear but is a function of the velocity. The following figures were all normalized to have the same peak values since only the shape of the seismograms and spectra was of concern. The first nine traces of Figure 17 are a plot of the nine synthetic seismograms as a function of time. The tenth trace is the signal before transmission through any of the nine random layer-stacks.

Figures 18 through 26 are the plots of (a), the seismogram versus time, (b), the logarithm of the amplitude versus frequency and, (c), the phase versus frequency.

Figure 27 is the result of the three processors.

The three traces under a are the result of weighted

beam summing. Trace

a1 is the weighted beam sum $\left(\sum_{i=1}^{N} W_i X_i(t) \Big/ \sum_{i=1}^{N} W_i\right)$; where $W_i = 1/\sigma_i$ and where σ_i is the sample standard deviation. Trace a2 is the log amplitude of the weighted beam sum versus frequency. Trace a3 is the phase of the weighted beam sum versus frequency. Trace b1 is the geometric mean; trace b2 is the averaged log-amplitudes versus frequency; and trace b3 is the average phases. Trace b4 is the complex cepstrum (Schafer, 1969). Trace b4 appears to be anti-symmetric about the midpoint because the phase (trace b3) is much larger than the log amplitude (trace b4). The unwound phase is the imaginary part of the log-spectra and is anti-symmetric about its midpoint (10 Hz), and the log amplitude is the real part of the log spectra and is symmetric about its midpoint (10 Hz). Since the numbers for the unwound phase are much larger than the numbers for the log-amplitude, the complex cepstrum appears to be antisymmetric.

The traces under c have been processed by tapering in the pseudo-time domain. Trace c2 is the smoothed averaged log-amplitudes, and trace c3 is the average unwound phase. Trace c4 is the first half of the tapered complex cepstrum. It would appear that the generalized filters have done a better job of estimating the signal than has the weighted beamed sum. The log amplitudes of the geometric beams and the phases of the geometric beams also show less variance than do the log-amplitude and phase of the weighted beam sum. Notice, however, the small precursor introduced by the generalized filters.

Observed data

Three events were processed on a continental sized array of LRSM (Long-Range-Seismic-Measurement) stations distributed throughout the continental United States and Canada. Two events (LONG SHOT and MILROW) were underground nuclear explosions which were detonated on Amchitka Island in the Aleutian Island Arc. The other event was an Andreanoff earthquake (22 November 1965) in the same island arc. Figure 28 is a map of the three events and the recording stations. Table I gives the seismic parameters of interest for the three events. Table II gives the locations of the recording stations used in this study. The processing results for LONG SHOT are given in Figure 29 through Figure 37. The formats are the same as for Figures 18 through 27. Figures 29 through 37 are for stations KN-UT, LC-NM, SV3QB, HL2ID, RK-ON, SJ-TX, TF-CL, KC-MO, and YR-CL, respectively. Notice the large variations in signal waveform from station-to-station in all traces. In Figure 39, note the small precursor introduced by the processor since we did not demand minimum phase as one of the attributes of our processor. The main signal of our processor (trace 39b1) seems to "ring" more than the signal form the weighted beam (trace 39a1), yet the coda dies out more rapidly for the first generalized linear filter compared to the weighted beam. The variance of trace b2 and trace b3 is seen to much less than the variance of trace a2 and a3.

The spectral null at 1.8 Hz in the LONG SHOT log- ... e amplitude spectra (traces a2, b2, and c2) has been interpreted (Cohen, 1969) as interference between the direct P wave and pP, the reflection from the free surface.

The processing results for the MILROW event are given in Figures 40 through 49. In Figure 40 through Figure 48, we have the results (in the same format as for the LONG SHOT event) for stations WQ-IL, BY-IO, SJ-TX, CR2NB, LC-NM, KN-UT, AS-PA, EU2AL, and PJ-PA. Figure 49 contains the results of our three processors in the same format as before. Notice that the first spectral null is shifted to a lower frequency from the LONG SHOT null (trace 37c2). This is consistent with the longer time delay for the reflected phase due to the deeper depth of MILROW compared to LONG SHOT. Notice the striking similarity between the processed LONG SHOT event (trace 37cl) and the processed MILROW event (trace 49cl) despite the great variablity of the individual stations. The decay times appear to be identical. The difference in the two waveforms appears to arise from the pP phase, since the first half cycle of motion (neglecting the precursor) is similar in shape and frequency. The results for the 22 November 1965 Andreanoff earthquake are contained in Figure 50 through Figure 58. Figures 48 through 55 are for stations EN-MO, HV-MA, KC-MO, KN-UT, MN-NV, RG-SD, RK-ON, and WN-SD.

Comparing the result for the Andreanoff Islands event (trace 58cl) with the MILROW event (trace 49cl) and the LONG SHOT event (trace 37cl), we see that the earthquake signal is more complex and exhibits a longer decay time than either MILROW or LONG SHOT. However, this fact is also apparent at the individual stations and on the weighted beams.

In conclusion we state that

The generalized linear filters did at least as well as

the weighted beam sum in the time domain in estimating our synthetic signal. No significant signal distortion in the first motion was present in our estimate.

The generalized linear filter traces for the explosions were similar despite substantial variations in the records for the same event at different stations. The explosion traces were simpler than the earthquake trace, but this was also true at the individual stations.

The codas are smaller for the output from the generalized filters than at the individual stations or on the weighted beam sums. The log-amplitude and phase spectra of the generalized linear filter output exhibited less variance from their mean compared to either individual station spectra or the weighted beam spectra. This might be expected since the geometric beam is the minimum variance estimator for uncorrelated equal variance random transfer functions.

The results suggest that continental beamforming or indeed even world-wide beamforming is possible for the initial P-wave using the theory of generalized linear filtering, and that complexity measurements and analysis of source dynamics might better be performed on the generalized beam.

III. REFERENCES

Aitchison, J., and Brown, J.A.C., The Log-normal Distribution; Cambridge University Press, 2nd Printing, 1963.

Aki, K., 1968, Seismological evidences for the existence of soft thin layers in the upper mantle under Japan. Jour. Geo. Res. vol. 73, pp. 585-994.

Capon, J.C., Greenfield, R.J., Kolker, R.J., and Lacoss, R.T., 1968, "Short-Period signal processing results for the large aperture seismic array," Geophysics, vol. 33, no. 3, pp. 452-472.

Chiburis, E.F., 1966, "LASA Travel-time anomalies for various epicentral regions," Seismic Data Laboratory Report No. 159.

Claerbout, Jon F., 1968, "Synthesis of a layered medium from its acoustic transmission response," Geophysics, Vol. 33, No. 2 pp. 264-269.

Cohen, T.J., 1969, Determination of source depth by spectral, pseudo-autocovariance, and cepstral analysis: Seismic Data Laboratory Report No. 229, Teledyne Geotech, Alexandria, Virginia.

Freedman, Helen, W., 1967, "Estimating Earthquake Magnitude," Bull. Seis. Soc. Am. 57, No. 4, pp. 747-760.

Glover, P., and Alexander, S.S., 1970, "A comparison of the Lake Superior and Nevada Test Site Source Regions," Seismic Data Laboratory Report No. 243.

Hartenberger, R.A., 1967, "The effect of the number and spacing of elements on the efficiency of LASA beams," Seismic Data Laboratory Report No. 203.

Haskell, N.A., 1953, "The Dispersion of Surface Waves on Multilayered Media," Bull. Seis. Soc. Am., Vol. 43, p. 17-34

Klappenberger, F.A., 1967, "Distribution of Short-Period P-Phase Amplitudes over LASA, Seismic Data Laboratory Report No. 195.

Landers, T., and Claerbout, Jon F., 1969, "Effects of thin soft layers on Body Waves," Bull. Seis. Soc. Amer., Vol 59, No. 5, pp. 2071-2078, October, 1969.

Mack, Harry, 1969, "Nature of Short-period P-wave variations at LASA; Jour. Geo. Res., 74, No. 12, pp. 3161-3170.

Noll, A.M., 1964, "Short-time spectrum and "cepstrum" techniques for vocal-pitch detection," Journal Acoust. Soc. Am., Vol. 36, No. 2, pp. 296-302.

Oppenheim, A.V., 1966, "Nonlinear Filtering of Convolved Signals," Quarterly Progress Report No. 80, Research Laboratory of Electronics, M.I.T.

________________, 1969, "Generalized Linear Filtering," Chapter 8 of Digital Processing of Signals; Gold and Rader, McGraw Hill, 1969.

Schafer, R.W., 1967, Echo removal by generalized linear filtering, 1967 NEREM Record Boston, 1967.

________________, 1969, Echo removal by discrete generalized linear filtering. Tech. Report No. 466, Research Lab. of Electronics, M.I.T.

TABLE 1

SEISMIC PARAMETERS

EVENT	DATE	ORIGIN TIME	MAGNITUDE	DEPTH	LAT.	LONG.
LONGSHOT	29 Oct. 65	21:00:00.08Z	5.85	2343 ft.	51°26'12" N	179°10'57" E
MILROW	02 Oct. 69	22:06:00.0 Z	6.32	3992 ft.	51°25'02" N	179°10'50" E
ANDREANOFF EQ.	22 Nov. 65	20:25:30.8 Z	5.90	60 km	51°39' N	179°48' W

TABLE II

Stations Used in this Study

Station	Location	Events		
SV3QB	Schefferville Quebec	LS		
RK-ON	Redlake Ontario	LS		A
HV-MA	Havre Montana			A
YR-CL	Yreka California	LS		
HL2ID	Hailey Idaho	LS		
RG-SD	Redig South Dakota			A
WN-SD	Winner South Dakota			A
BY-IO	Bloomfield Iowa		M	
WQ-IL	Watseka Illinois		M	
AS-PA	Aspen Pennsylvania		M	
PJ-PA	Pottstown Pennsylvania		M	
CR2NB	Crete Nebraska		M	
KC-MO	Kansas City Missouri	LS		A
KN-UT	Kanab Utah	LS	M,A	
MN-NV	Mina Nevada			A
TF-CL	Taft California	LS		
LC-NM	Las Cruces Nevada	LS	M	
EN-MO	Ellsinore Missouri			A
EU-AL	Eutaw Alabama		M	
SJ-TX	San Jose Texas	LS	M	

Key: LS - LONGSHOT
M - MILROW
A - Andreanoff 22 Nov 65

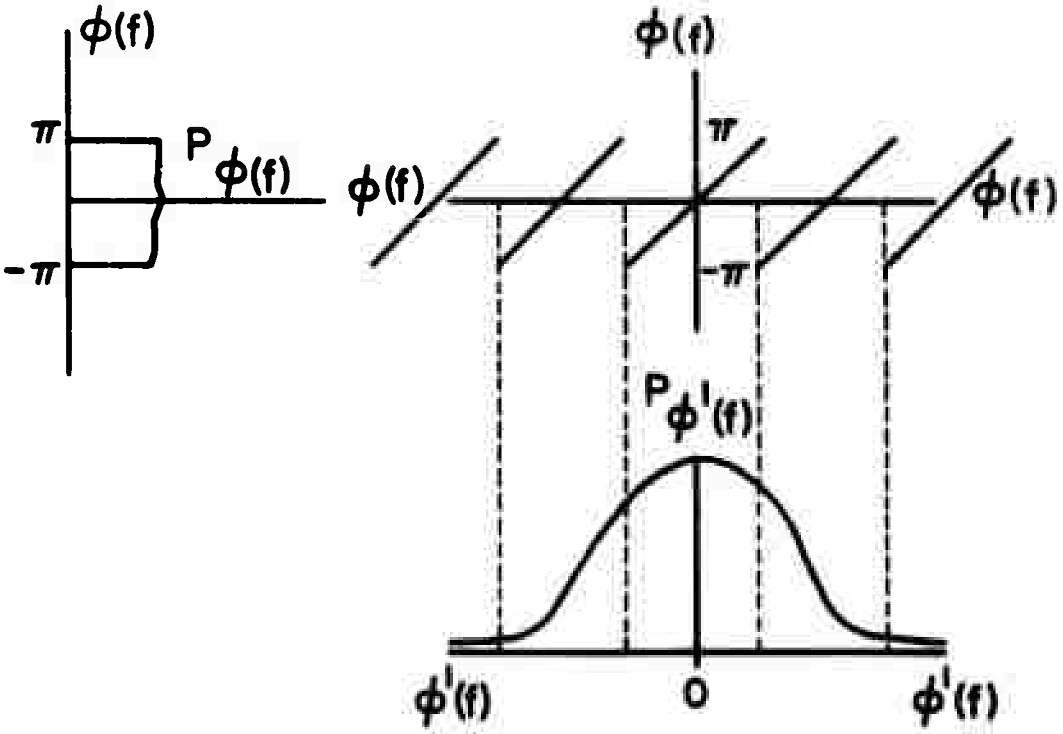

ϕ (f) IS WHAT WE MEASURE OUR PROBLEM IS TO RECOVER ϕ' (f)

Figure 1. Transformation of a normal probability density into an almost uniform probability density.

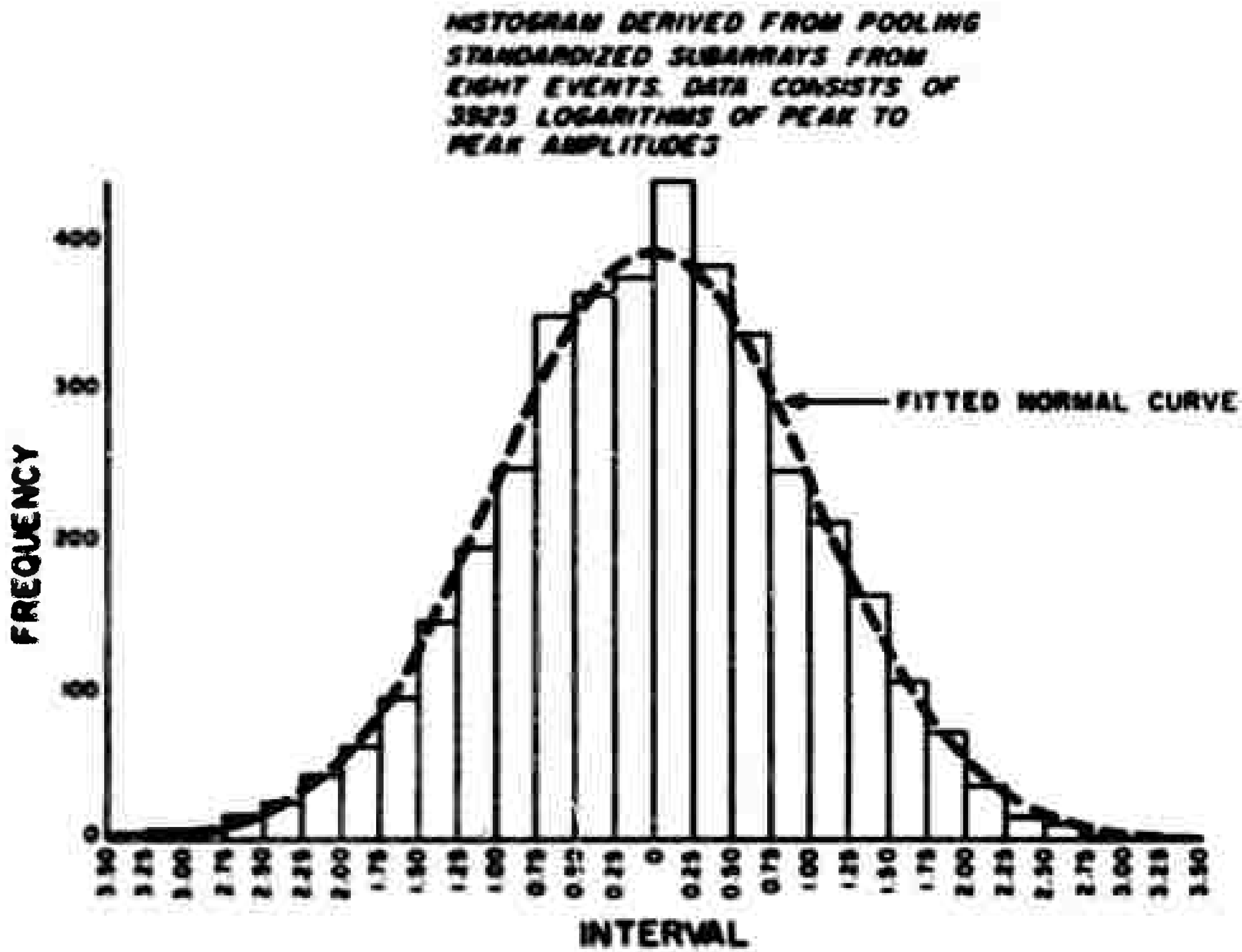

Figure 2. The best fit to a normal probability density of Klappenberger's (1967) data. (After Klappenberger, 1967).

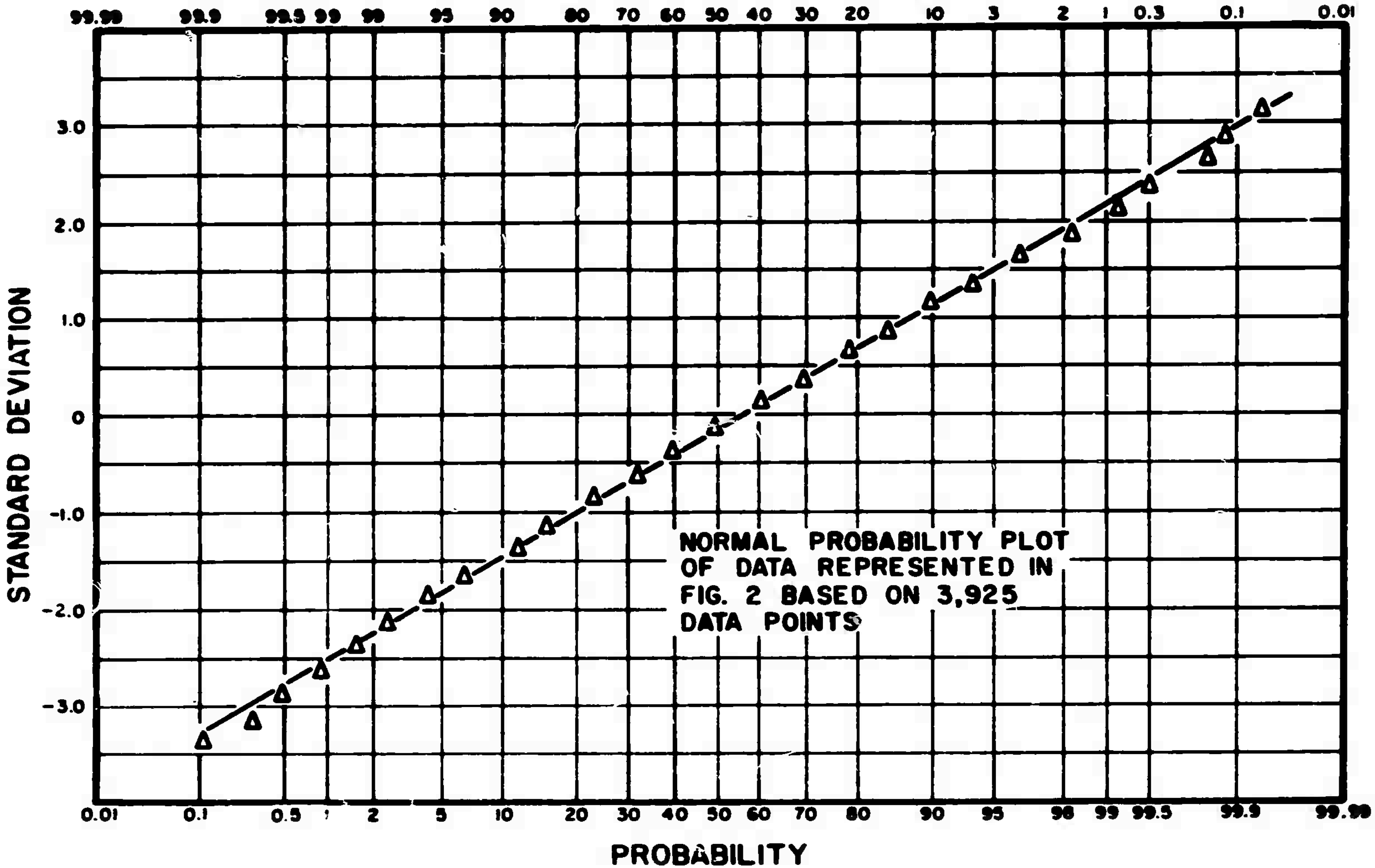

Figure 3. Klappenberger's best fit of LASA peak-to-peak amplitude data to a cumulative normal distribution function.

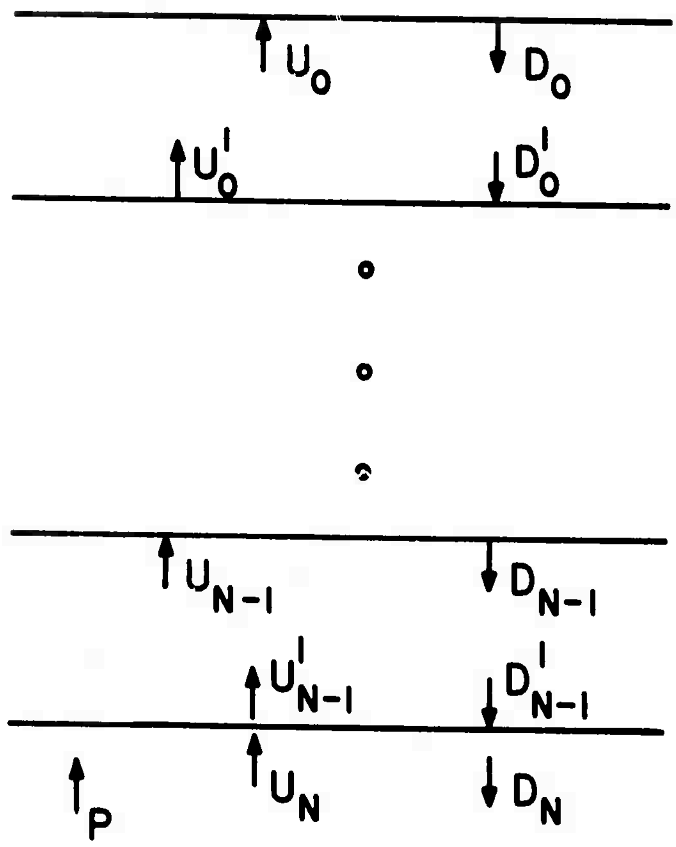

Figure 4. A schematic representation of the normal incident P-wave layering problem.

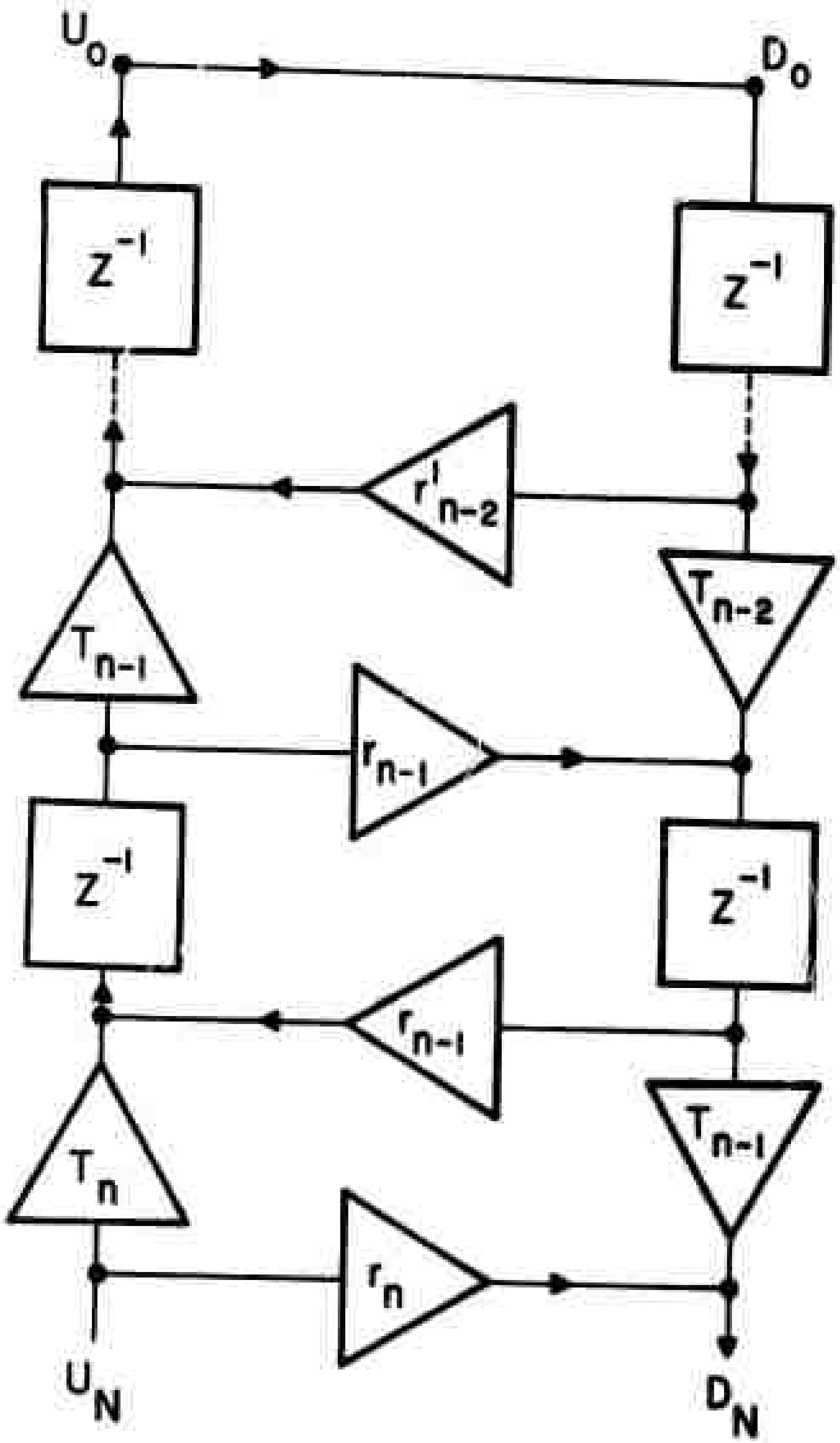

Figure 5. Analog computer simulation of the transmission problem. Note the similarity of this problem to the parametric amplifier problem. Also note that S-waves could be handled by designing another ladder network with different delays and reflection coefficients, and interconnecting the nodes of both networks with the proper conversion factors.

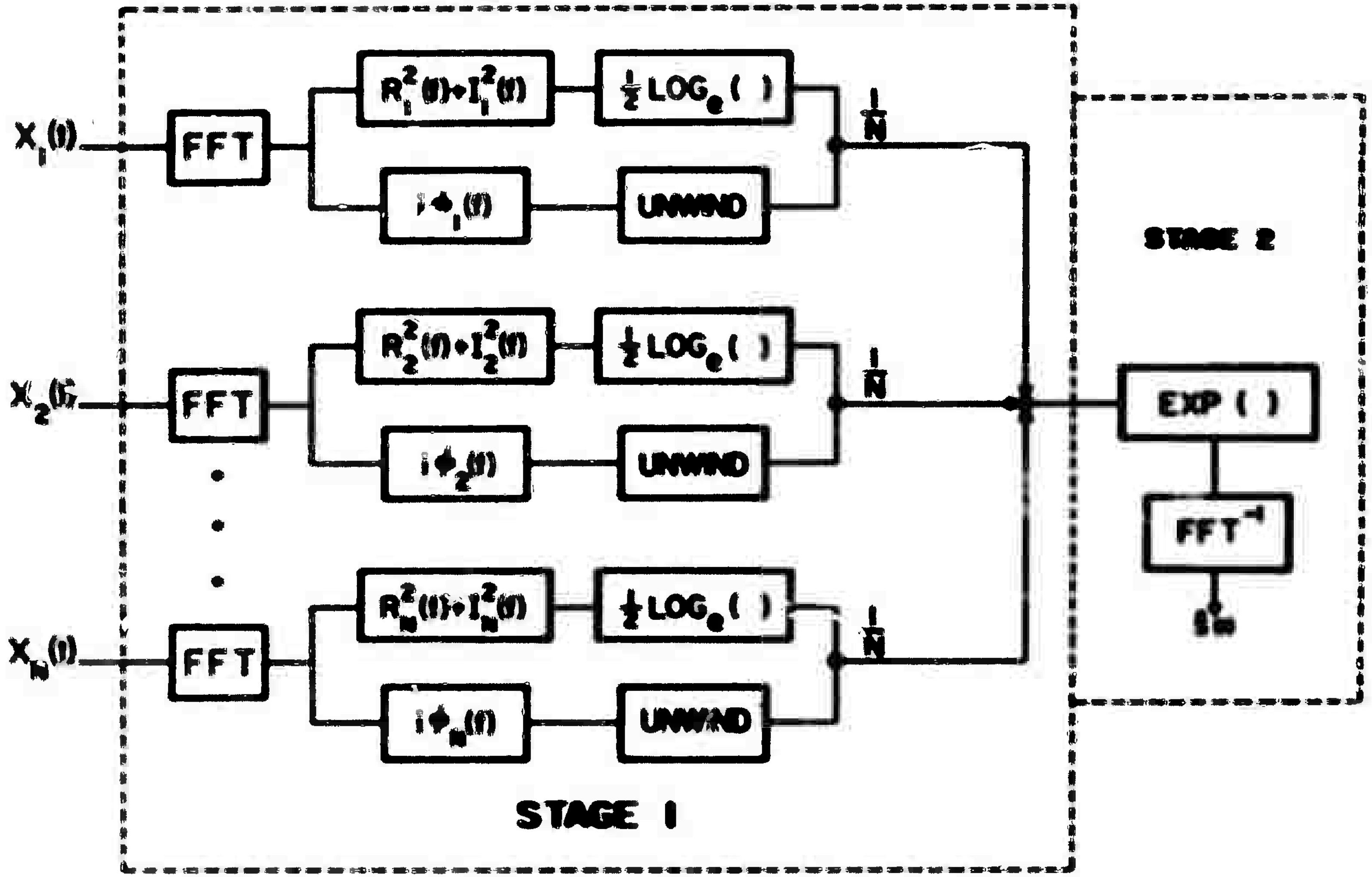

Figure [illegible]. A two-stage generalized-linear filter for the estimation of a signal convolved with equal variance, log-normally distributed, uncorrelated transfer functions.

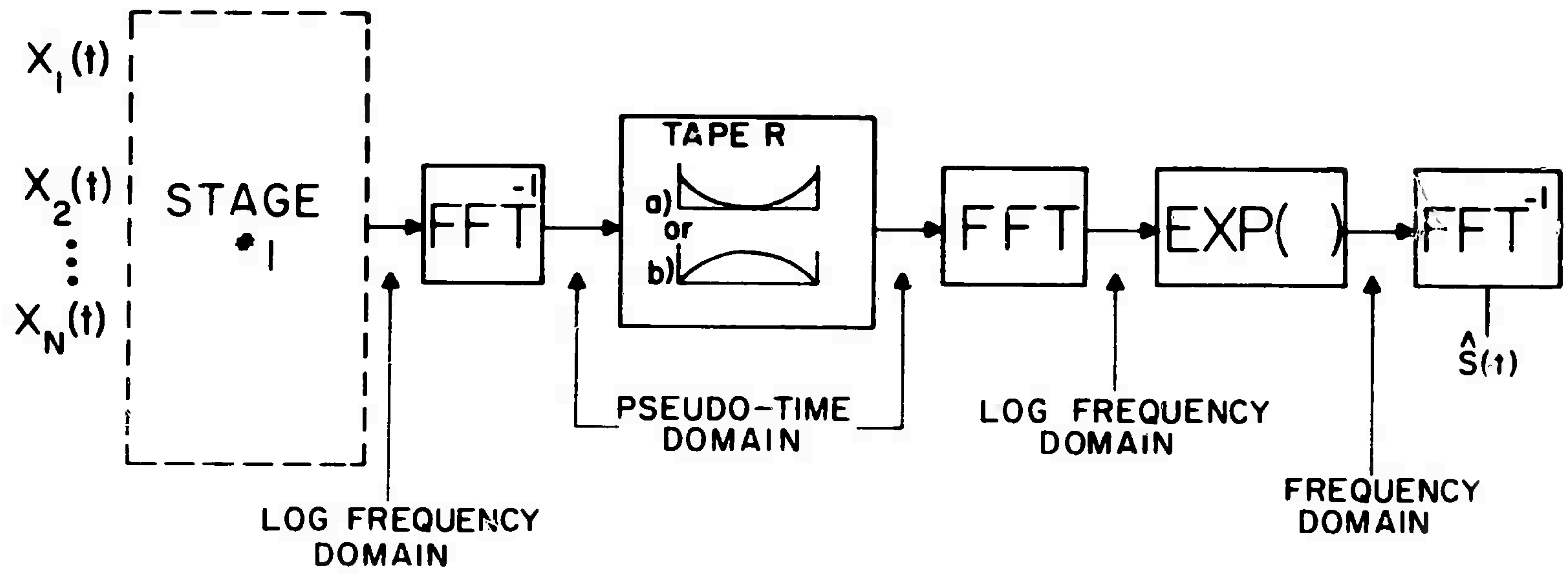

Figure 7. A modification of stage 2 of the GLF in Figure 6 to delineate long or short time components. Tapering the complex cepstrum is quite often done in speech processing (Noll, 1964; Oppenheim, 1968).

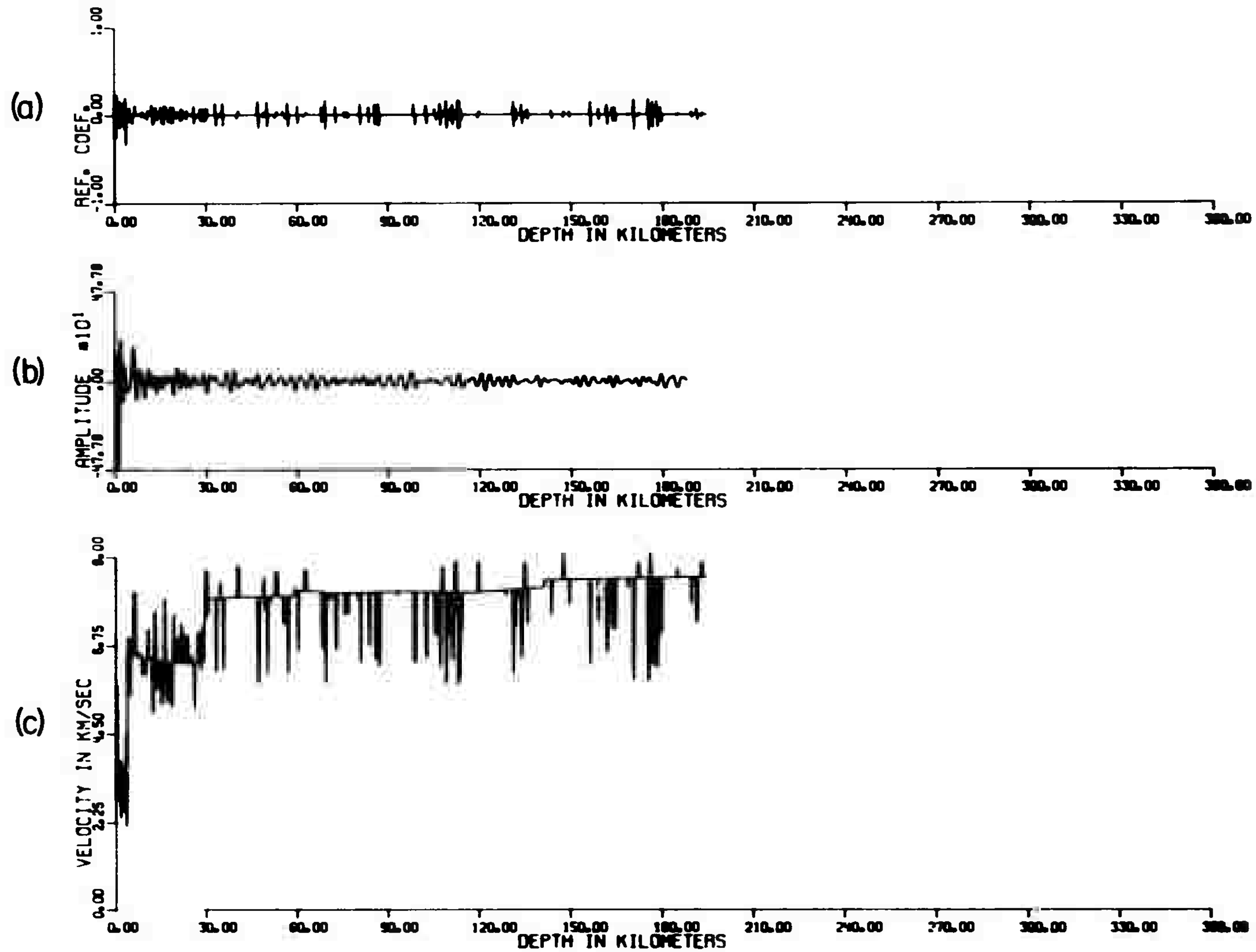

Figure 8. Synthetic seismogram 1 (a) Reflection coefficients vs. depth (b) Seismogram vs. depth (c) Velocity vs. depth.

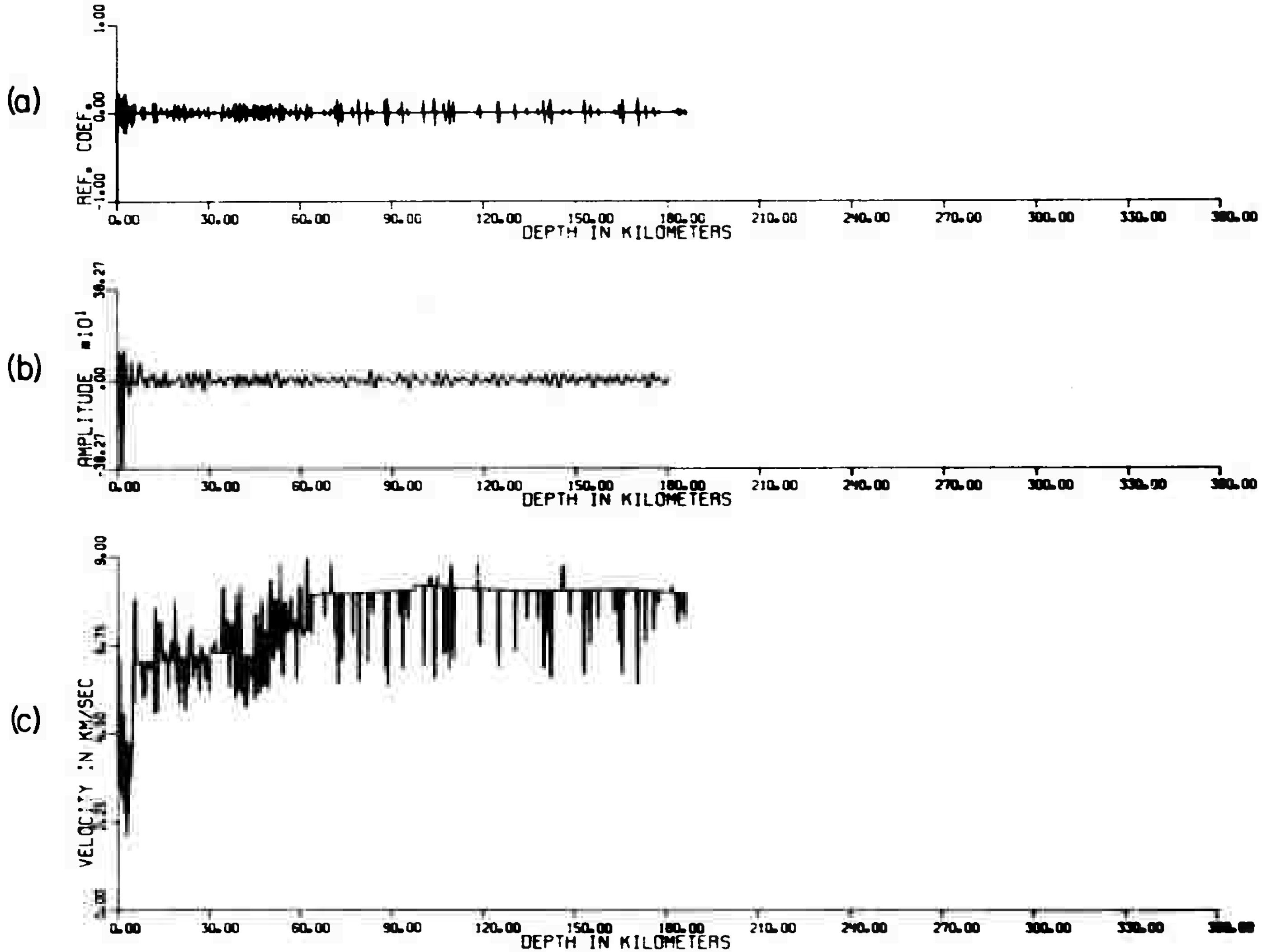

Figure 9. Synthetic seismogram 2 (a) Reflection coefficients vs. depth
(b) Seismogram vs. depth (c) Velocity vs. depth.

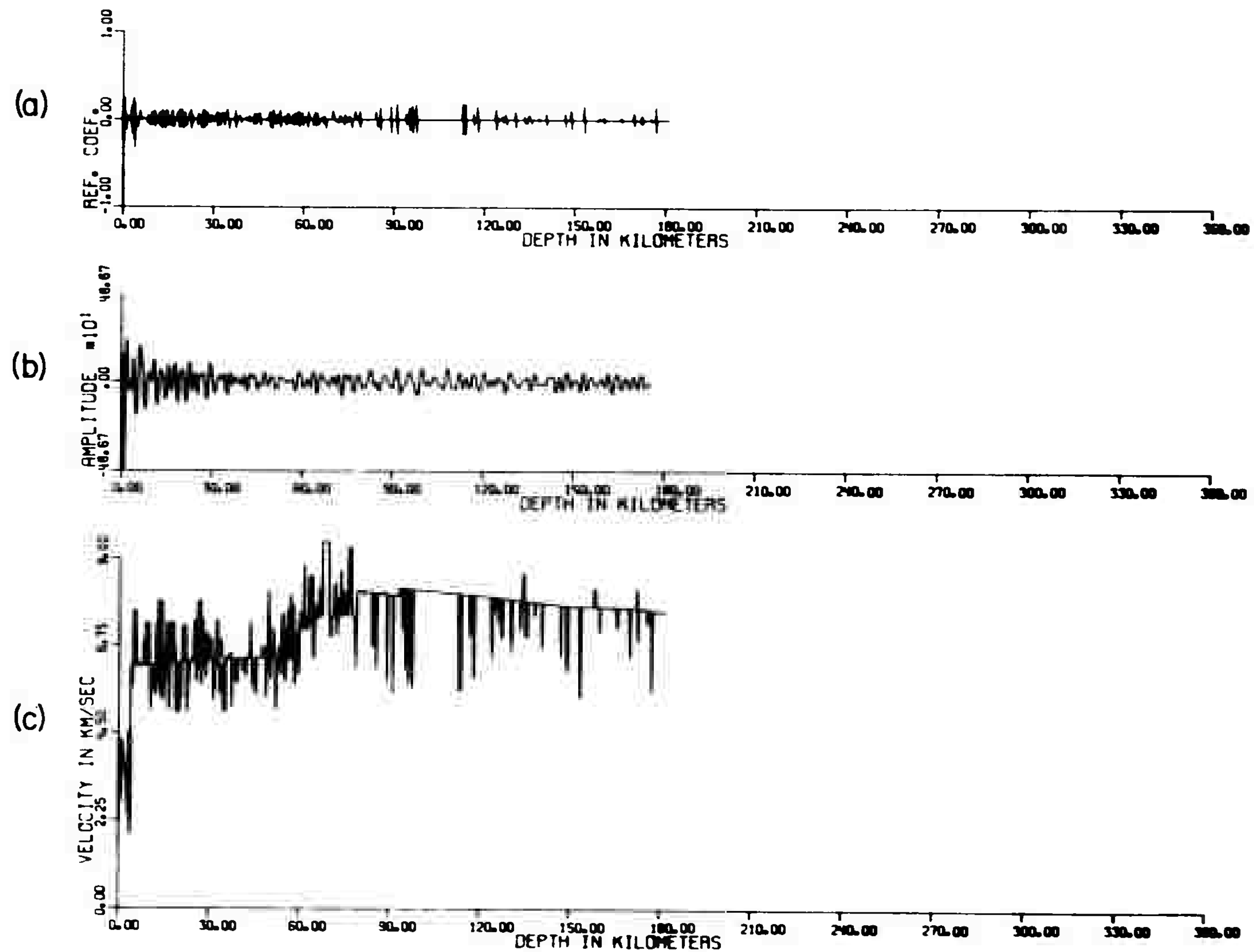

Figure 10. Synthetic seismogram 3 (a) Reflection coefficients vs. depth (b) Seismogram vs. depth (c) Velocity vs. depth.

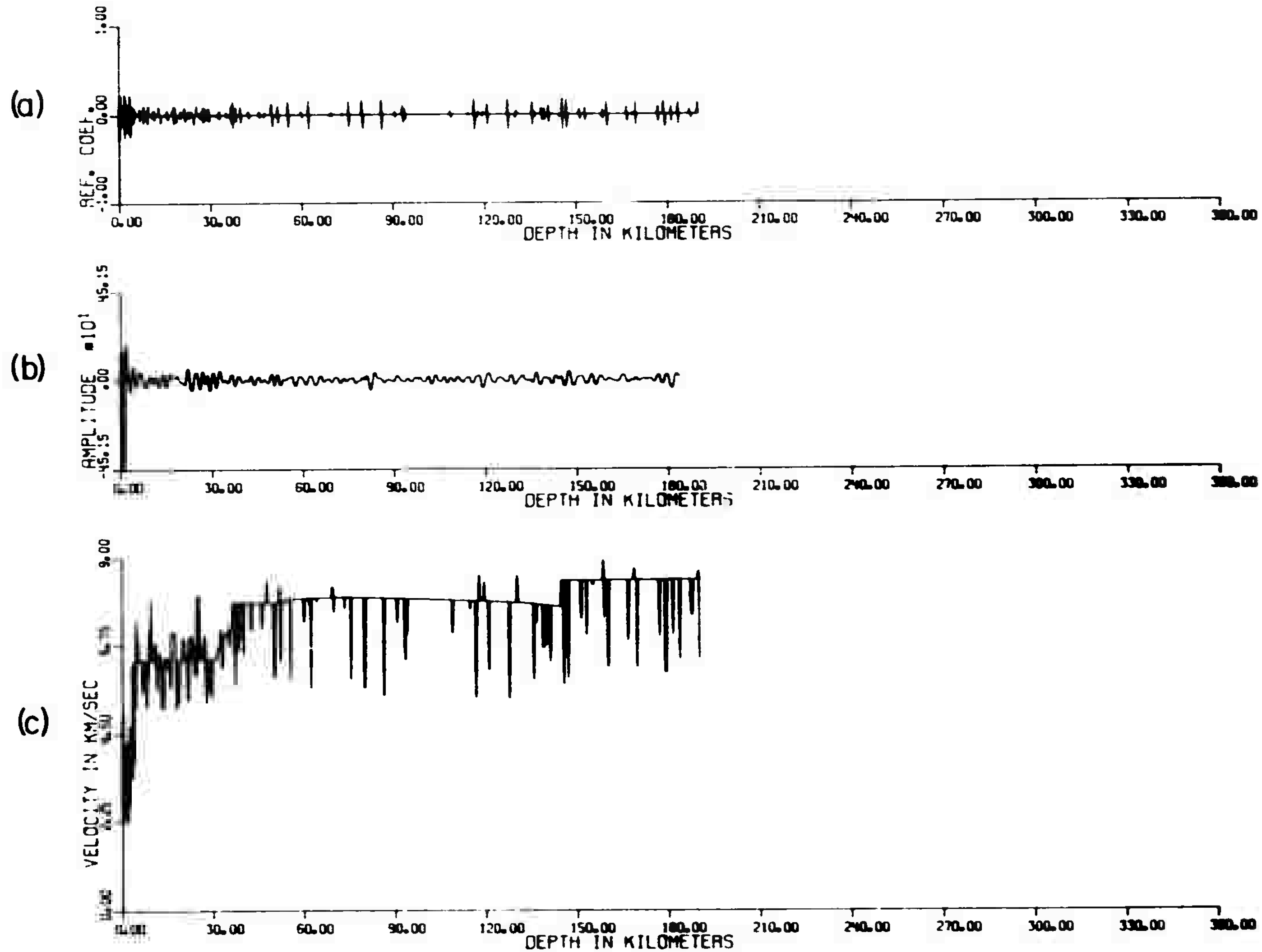

Figure 11. Synthetic seismogram 4 (a) Reflection coefficients vs. depth (b) Seismogram vs. depth (c) Velocity vs. depth.

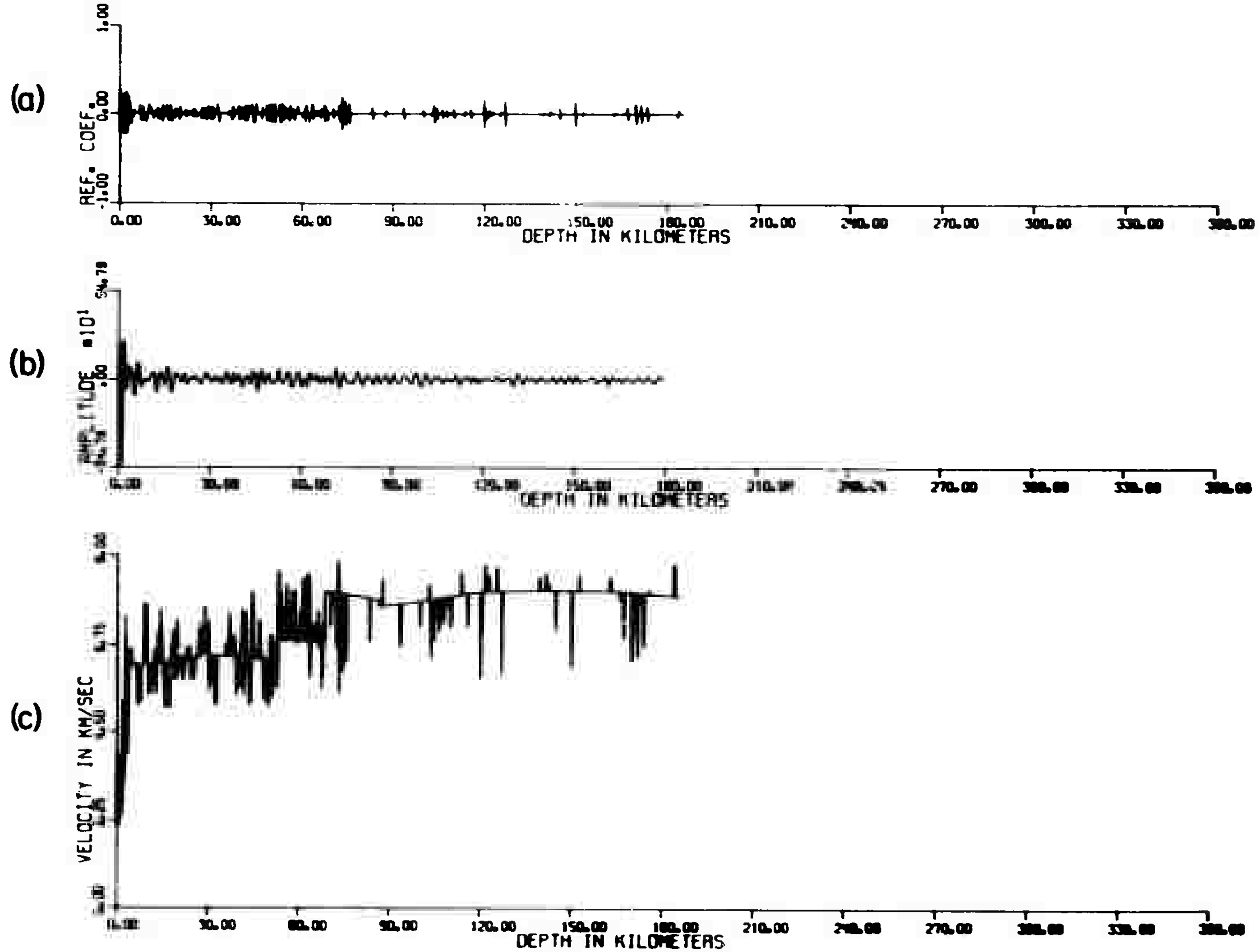

Figure 12. Synthetic seismogram 5 (a) Reflection coefficients vs. depth (b) Seismogram vs. depth (c) Velocity vs. depth.

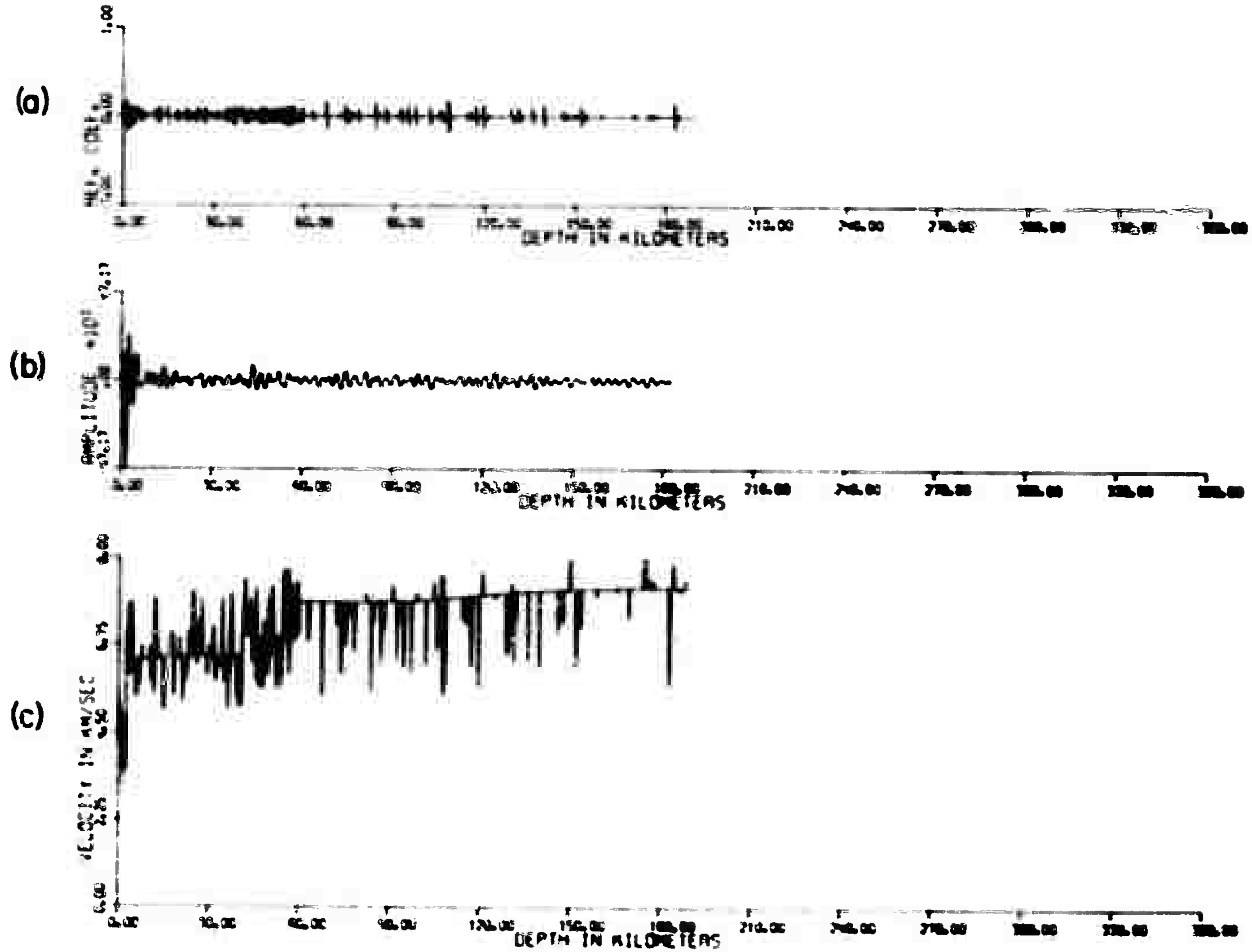

Figure 13. Synthetic seismogram 6 (a) Reflection coefficients vs. depth (b) Seismogram vs. depth (c) Velocity vs. depth.

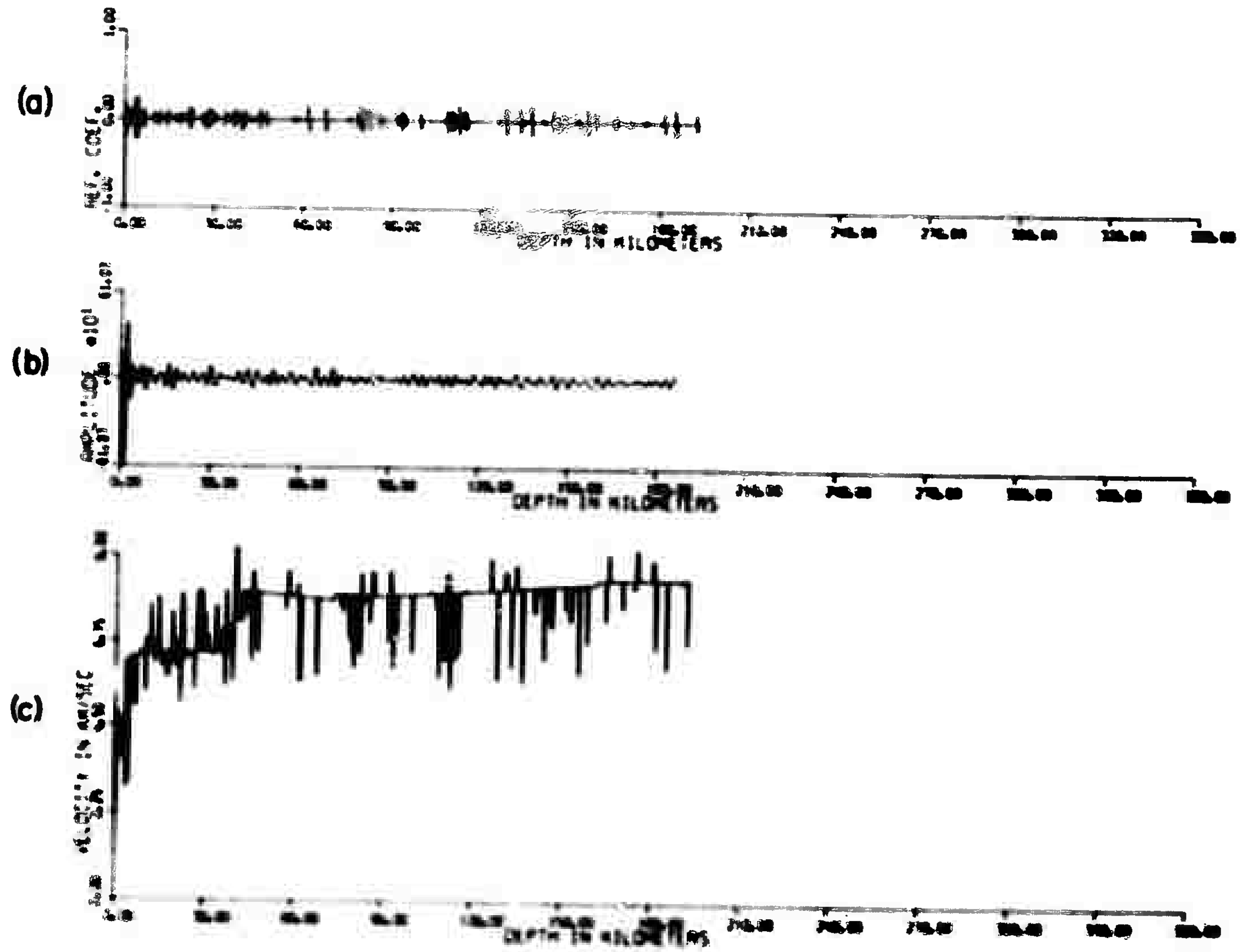

Figure 11. Synthetic seismogram 7 (a) Reflection coefficients vs. depth (b) Seismogram vs. depth (c) Velocity vs. depth.

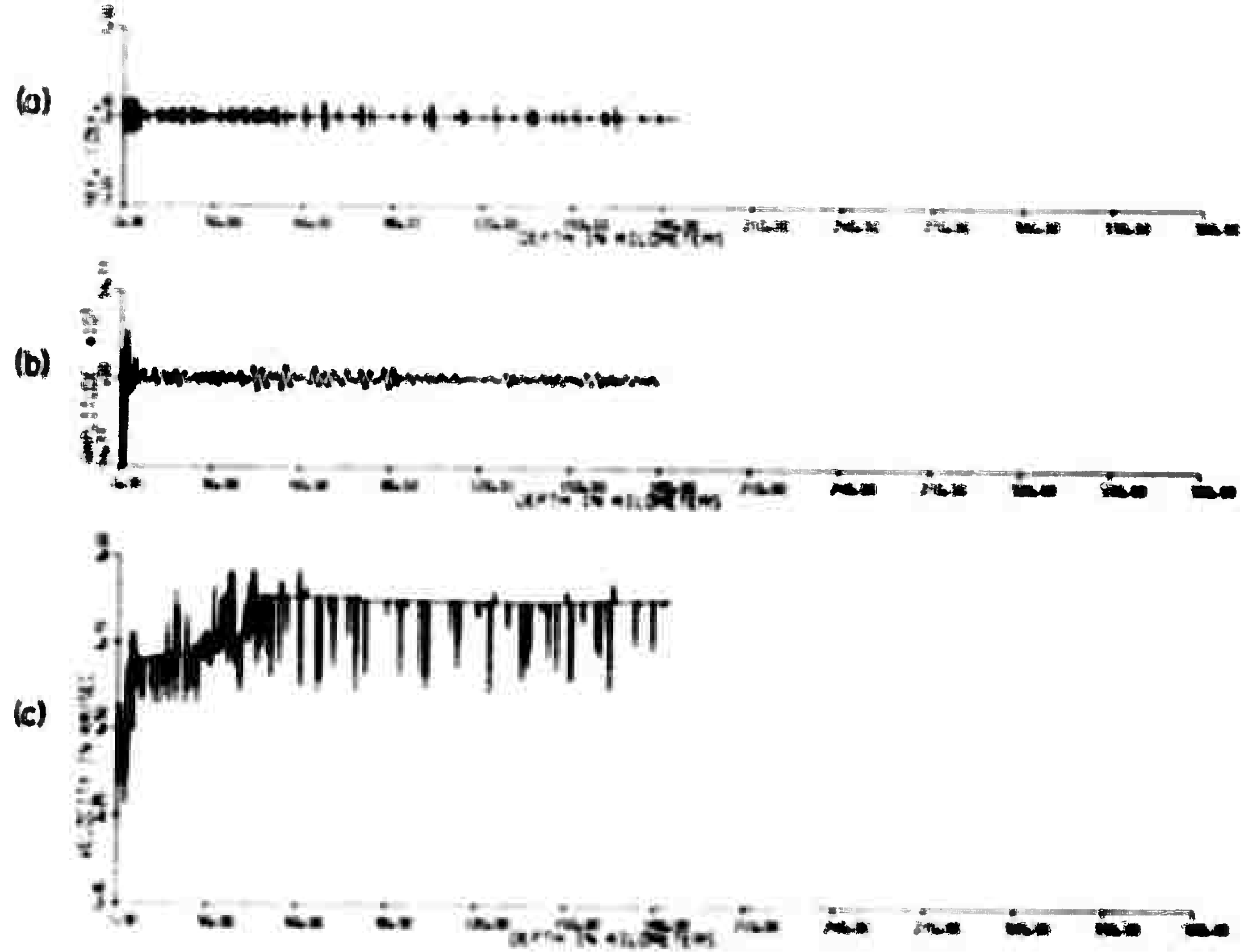

Figure 15. Synthetic seismogram 4 (a) Reflection coefficients vs. depth (b) Seismogram vs. depth (c) Velocity vs. depth.

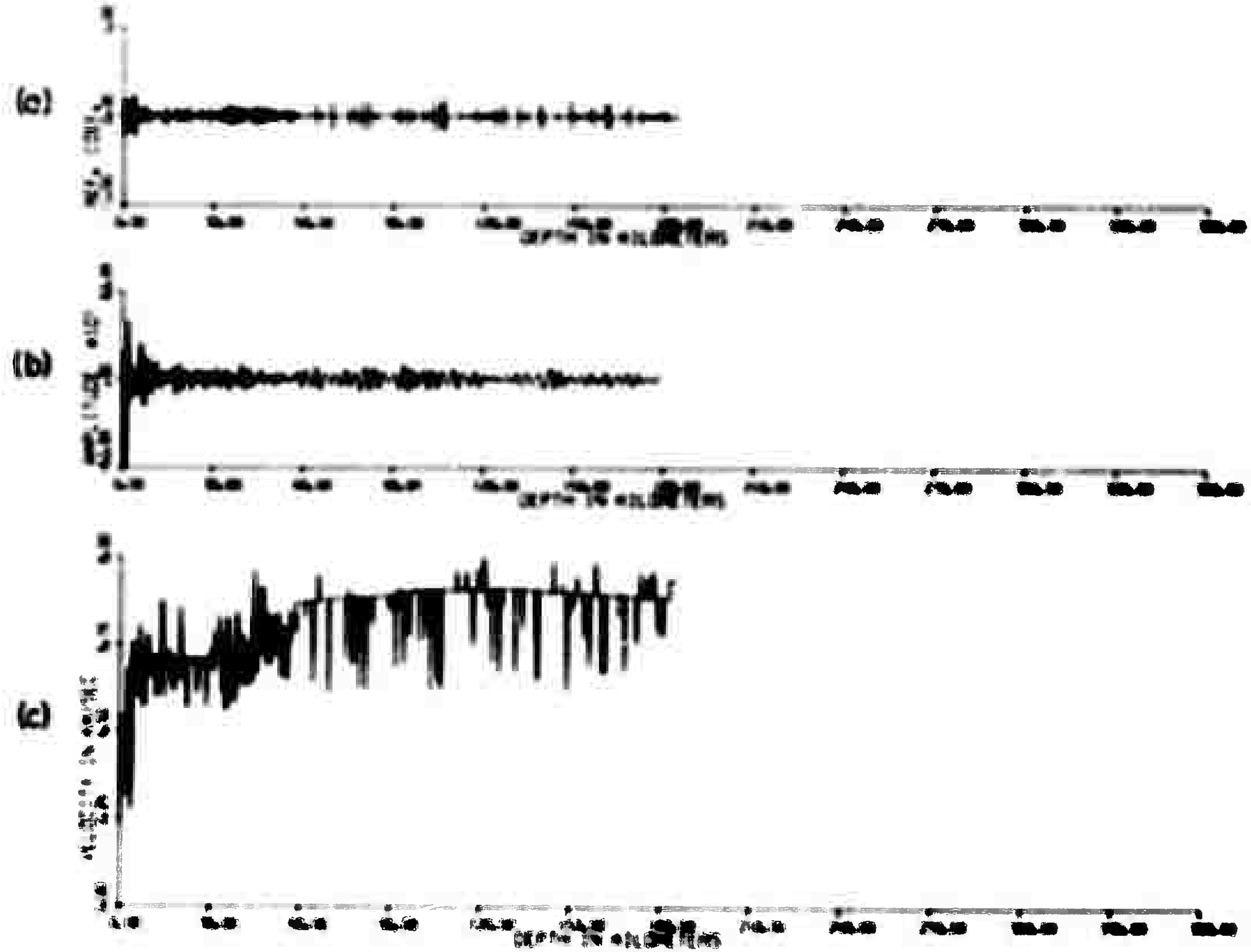

Figure 19. Synthetic seismogram 9 (a) Reflection coefficients vs. depth (b) Seismogram vs. depth (c) Velocity vs. depth.

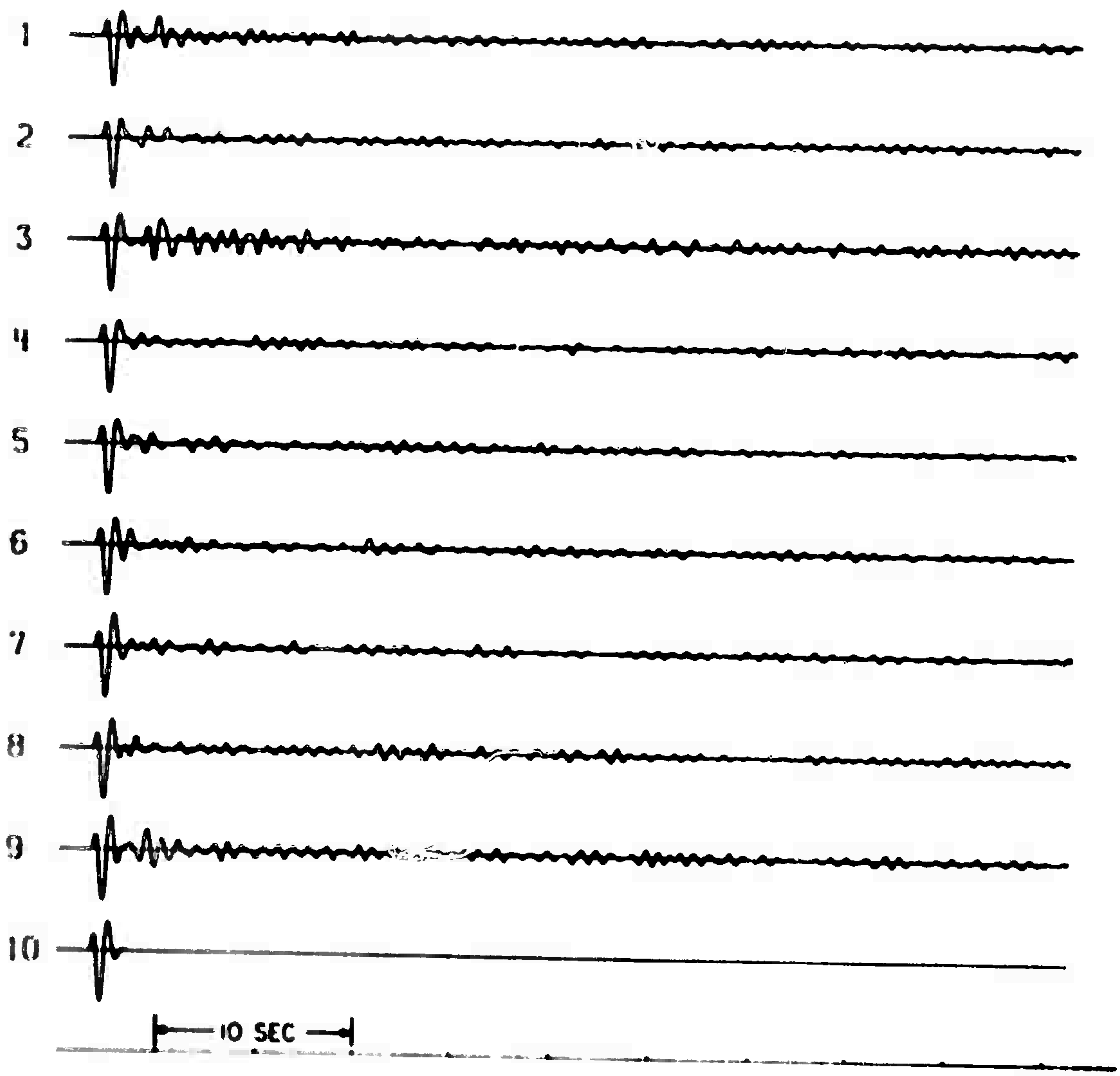

Figure 17. The nine synthetic seismograms and the source signal vs. time.

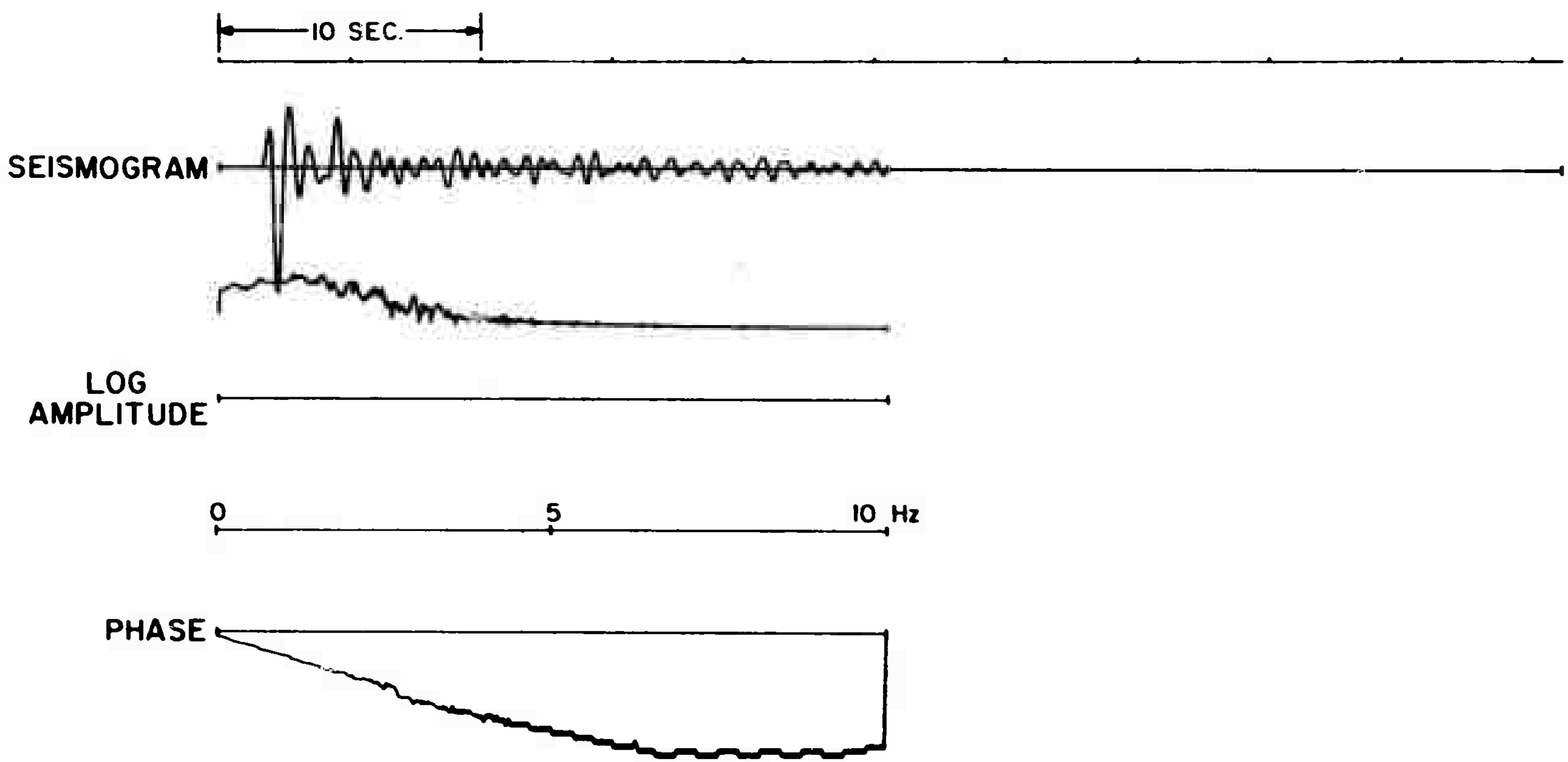

Figure 18. Synthetic seismogram 1 (a) Seismogram vs. time (b) Log-amplitude vs. frequency (c) Unwound phase vs. frequency.

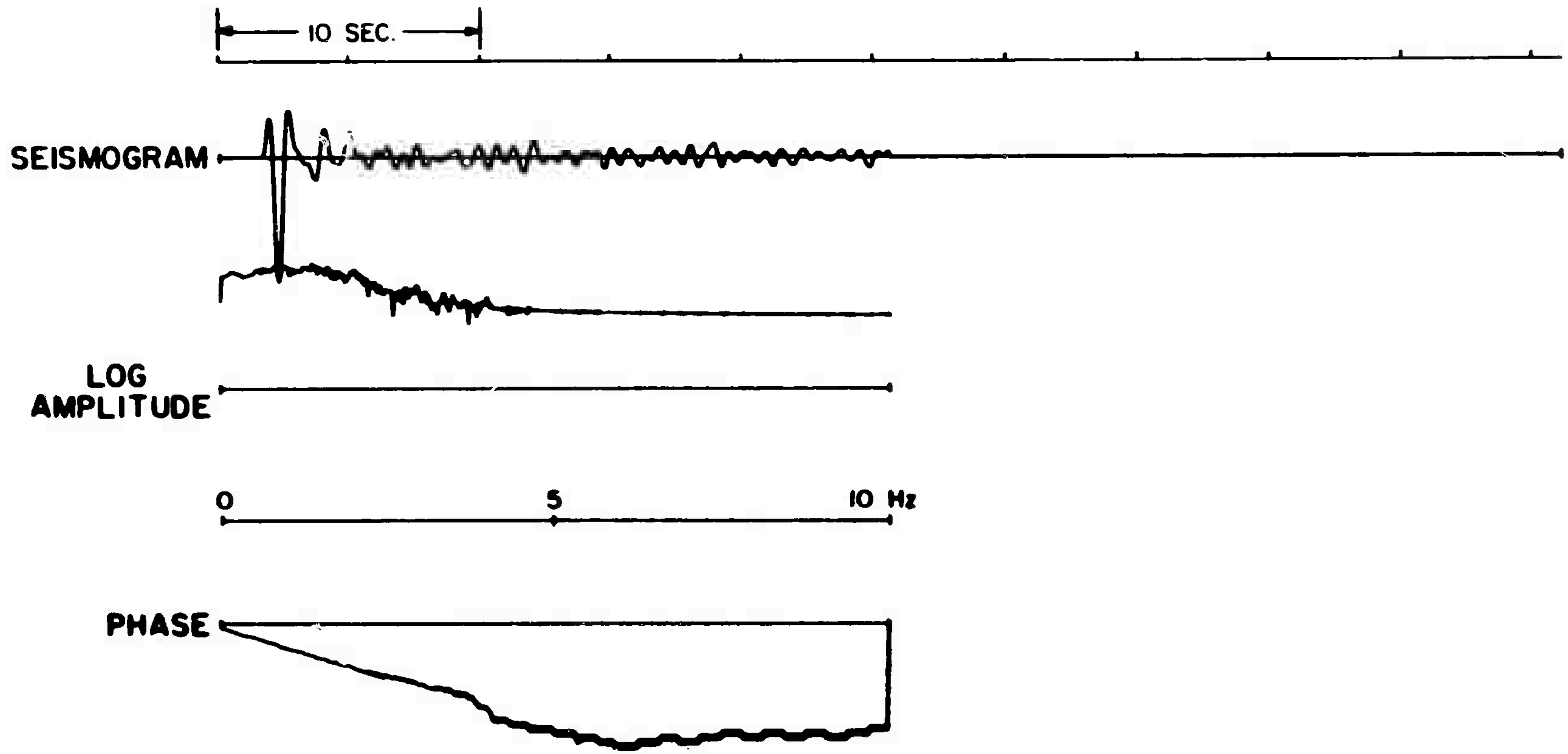

Figure 19. Synthetic seismogram 2 (a) Seismogram vs. time (b) Log-amplitude vs. frequency (c) Unwound phase vs. frequency.

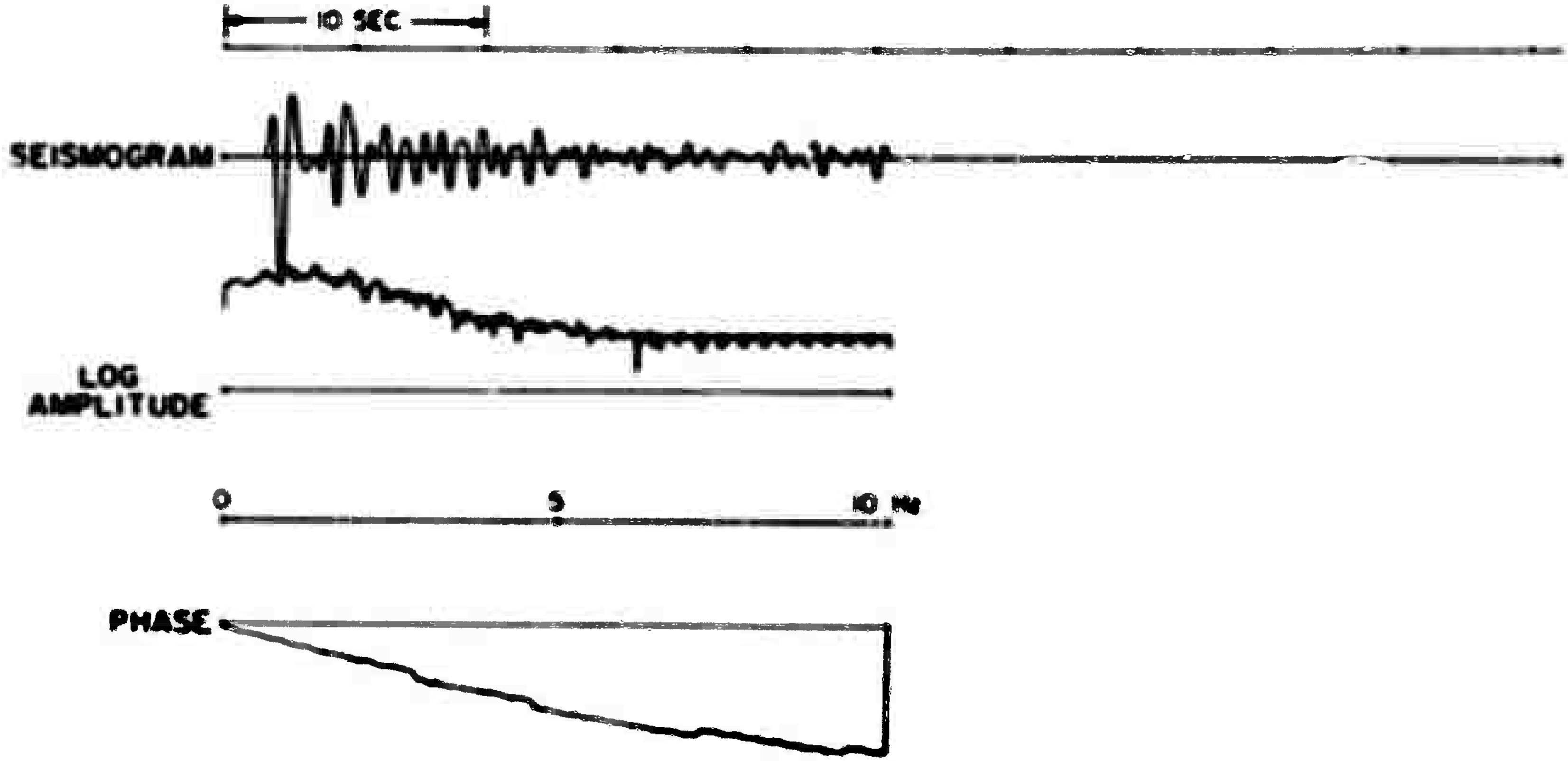

Figure 20. Synthetic seismogram 3 (a) Seismogram vs. time (b) Log-amplitude vs. frequency (c) Unwound phase vs. frequency.

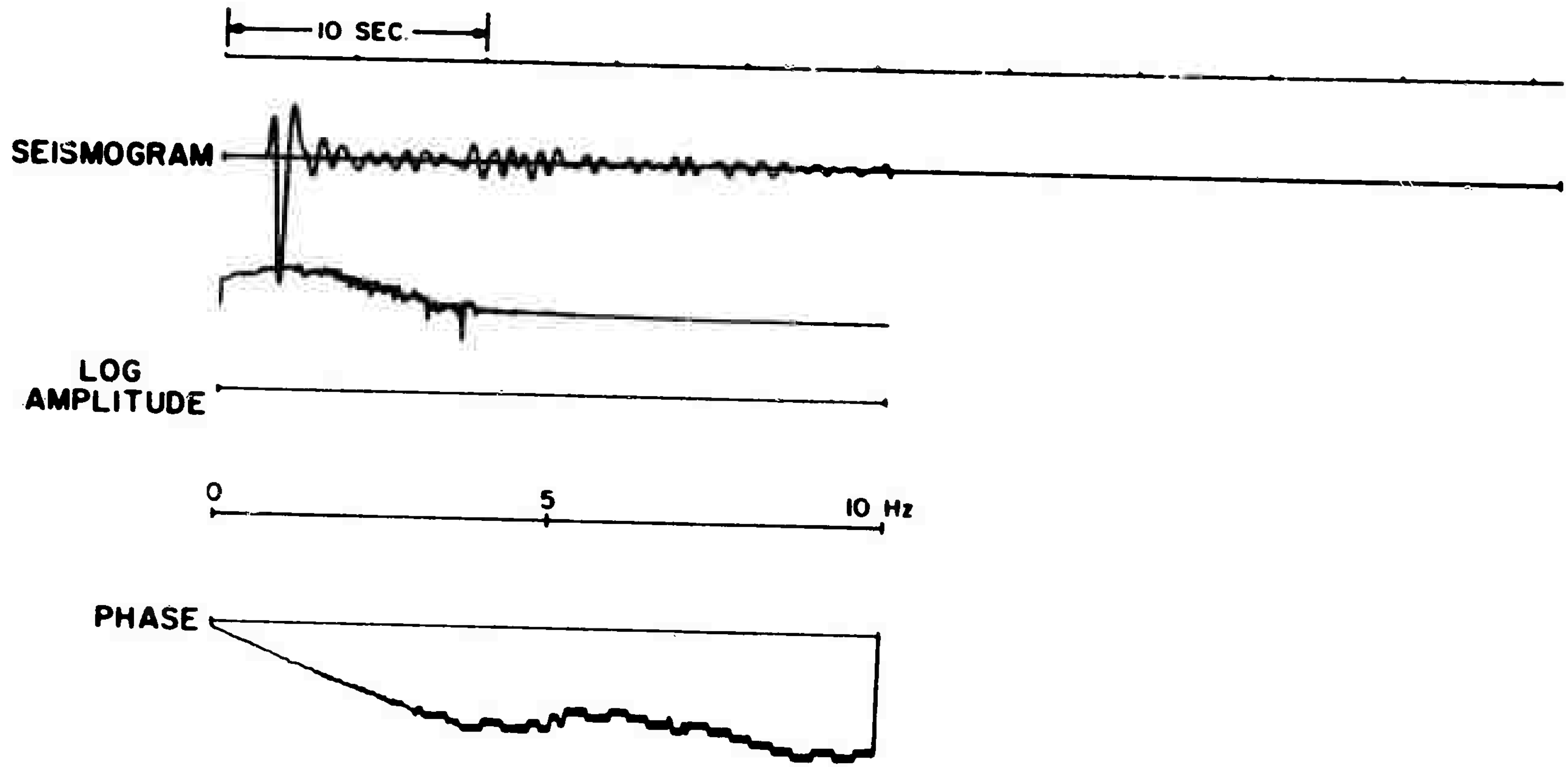

Figure 21. Synthetic seismogram 4 (a) Seismogram vs. time (b) Log-amplitude vs. frequency (c) Unwound phase vs. frequency.

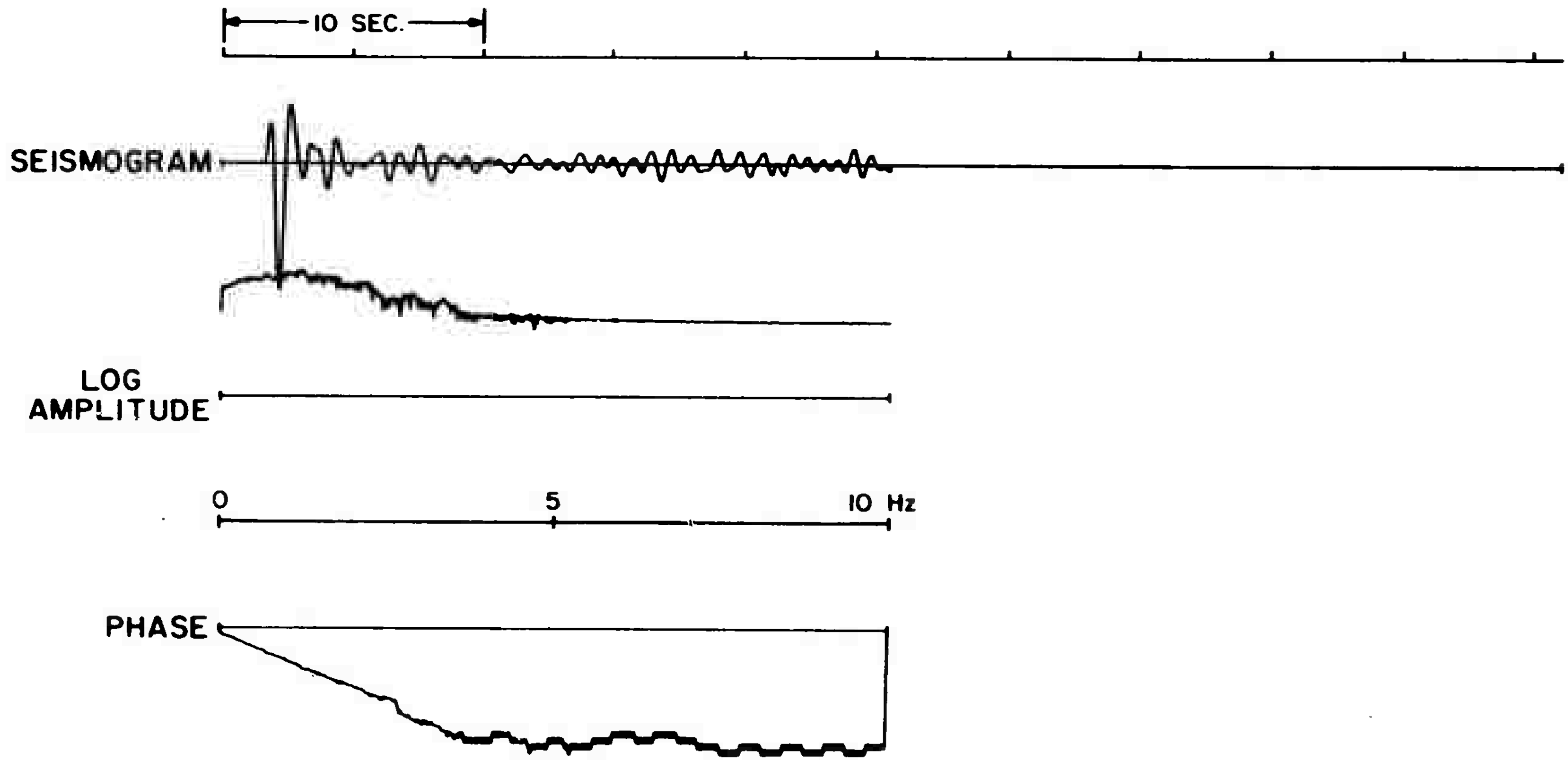

Figure 22. Synthetic seismogram 5 (a) Seismogram vs. time (b) Log-amplitude vs. frequency (c) Unwound phase vs. frequency.

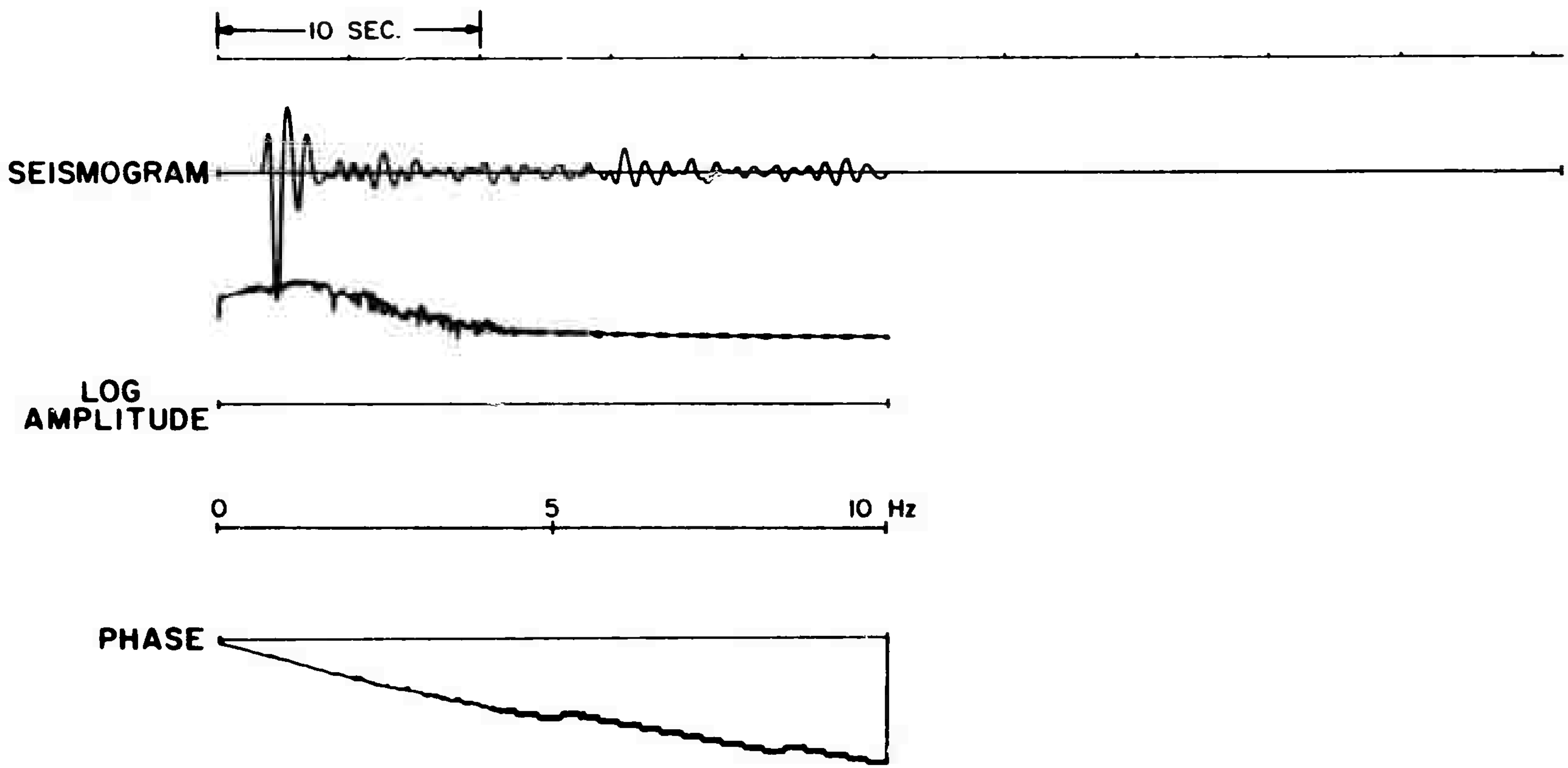

Figure 23. Synthetic seismogram 6 (a) Seismogram vs. time (b) Log-amplutide vs. frequency (c) Unwound phase vs. frequency.

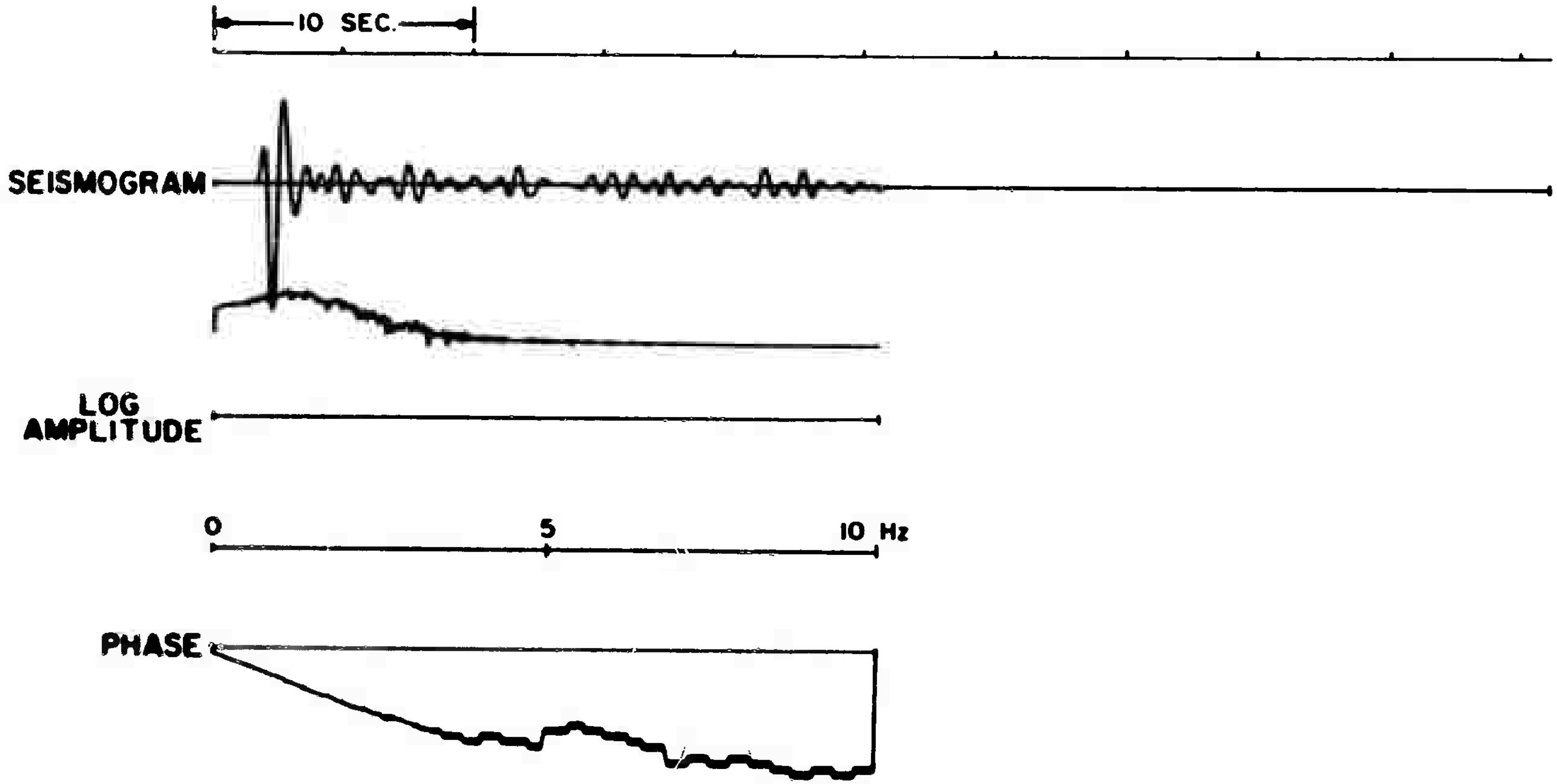

Figure [illegible]. Synthetic seismogram [illegible] (a) Seismogram vs. time (b) Log-amplitude vs. frequency (c) Unwound phase vs. frequency.

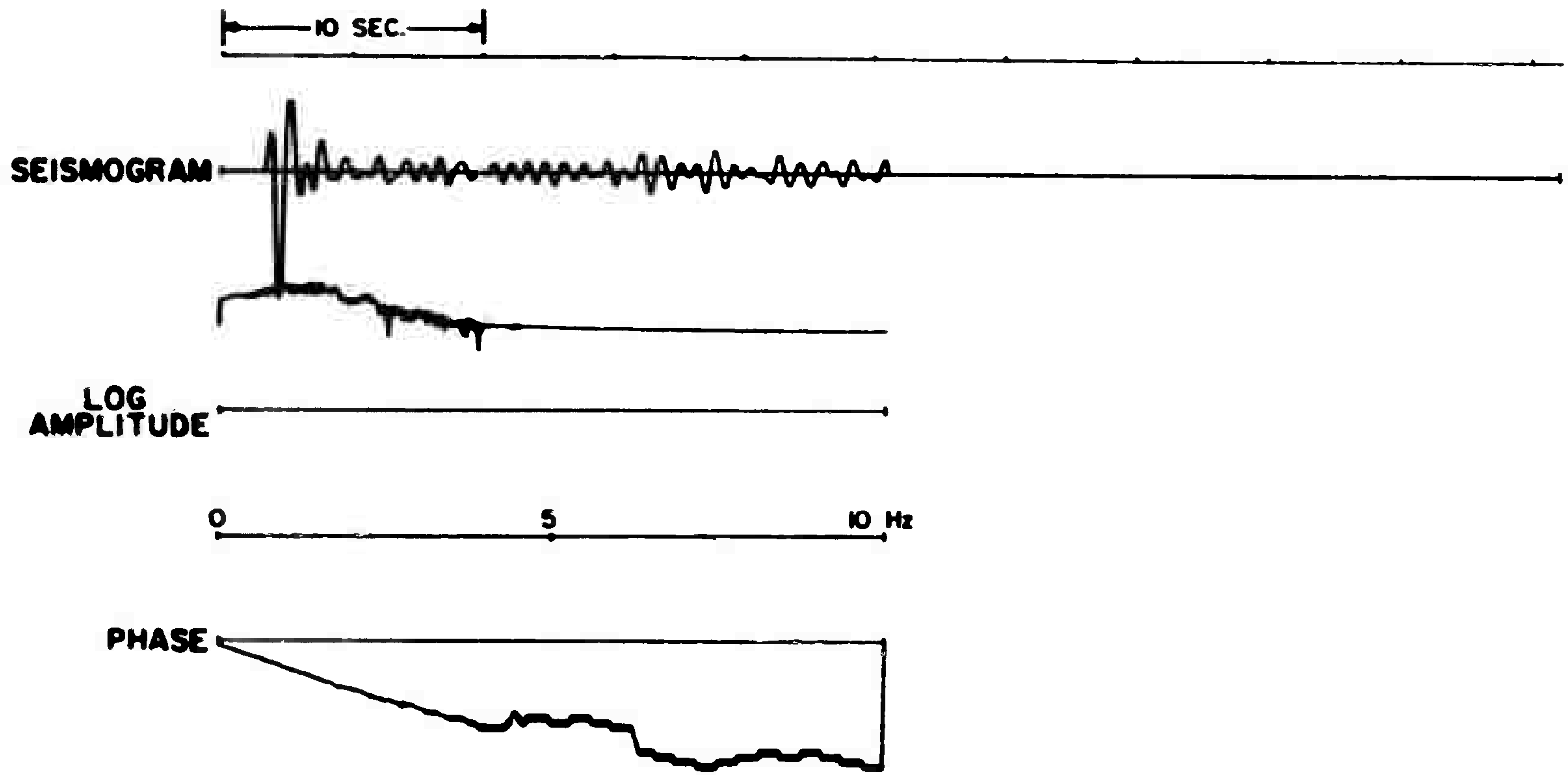

Figure 25. Synthetic seismogram S (a) Seismogram vs. time (b) Log-amplitude vs. frequency (c) Unwound phase vs. frequency.

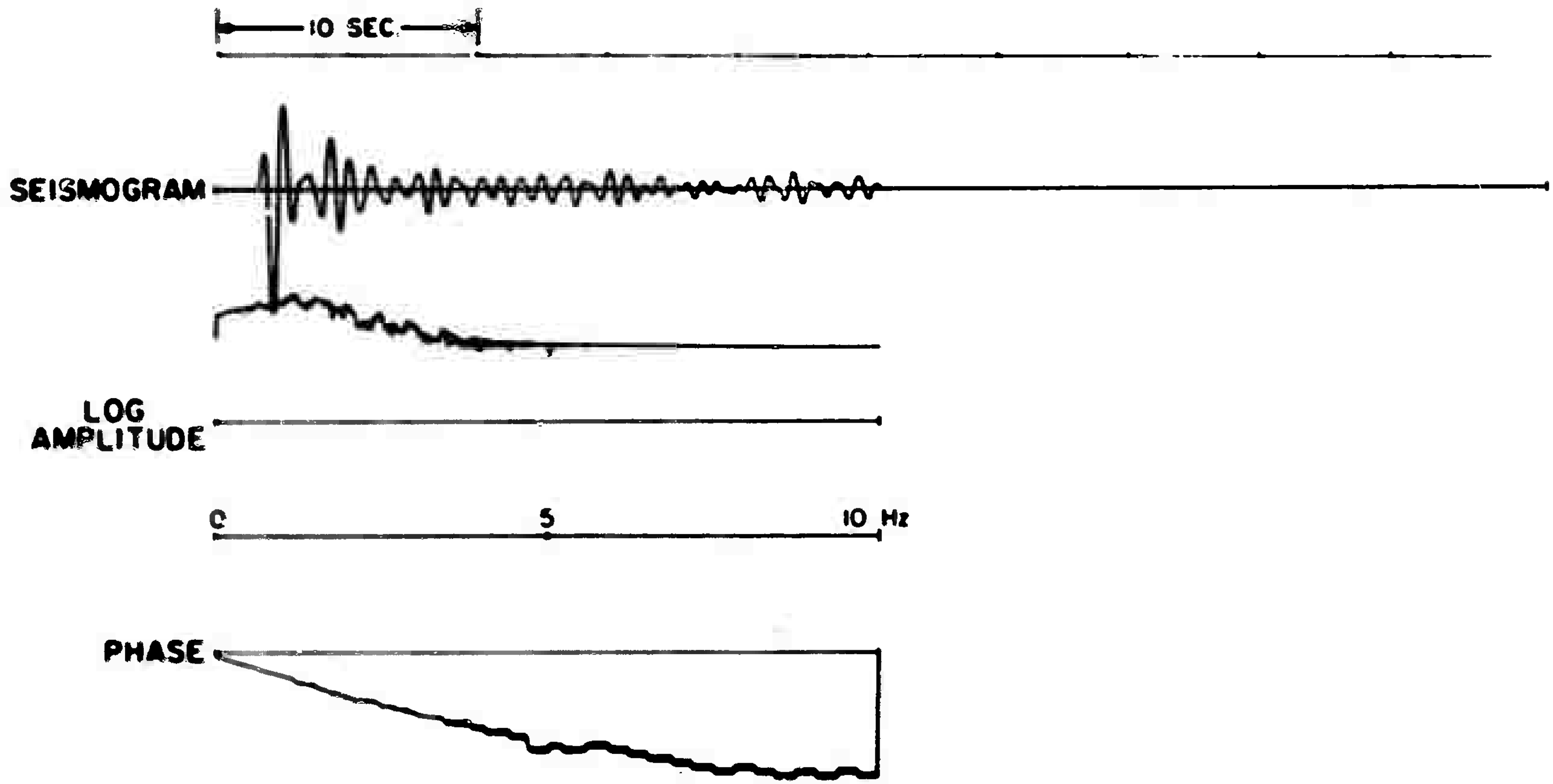

Figure 26. Synthetic seismogram 3 (a) Seismogram vs. time (b) Log-amplitude vs. frequency (c) Unwound phase vs. frequency.

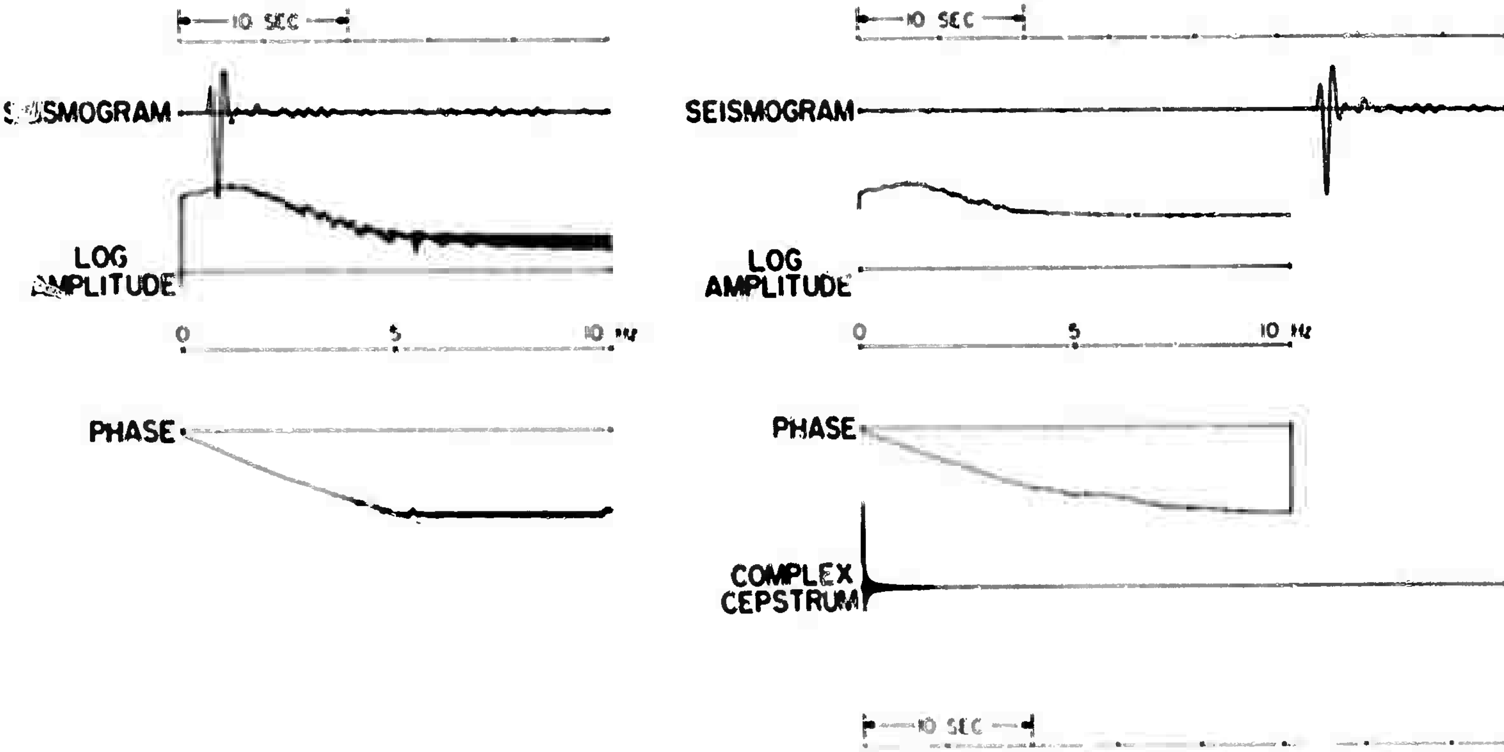

10 SEC
SEISMOGRAM
LOG AMPLITUDE
0
5
10 Hz
PHASE
10 SEC
SEISMOGRAM
LOG AMPLITUDE
0
5
10 Hz
PHASE
COMPLEX CEPSTRUM
10 SEC

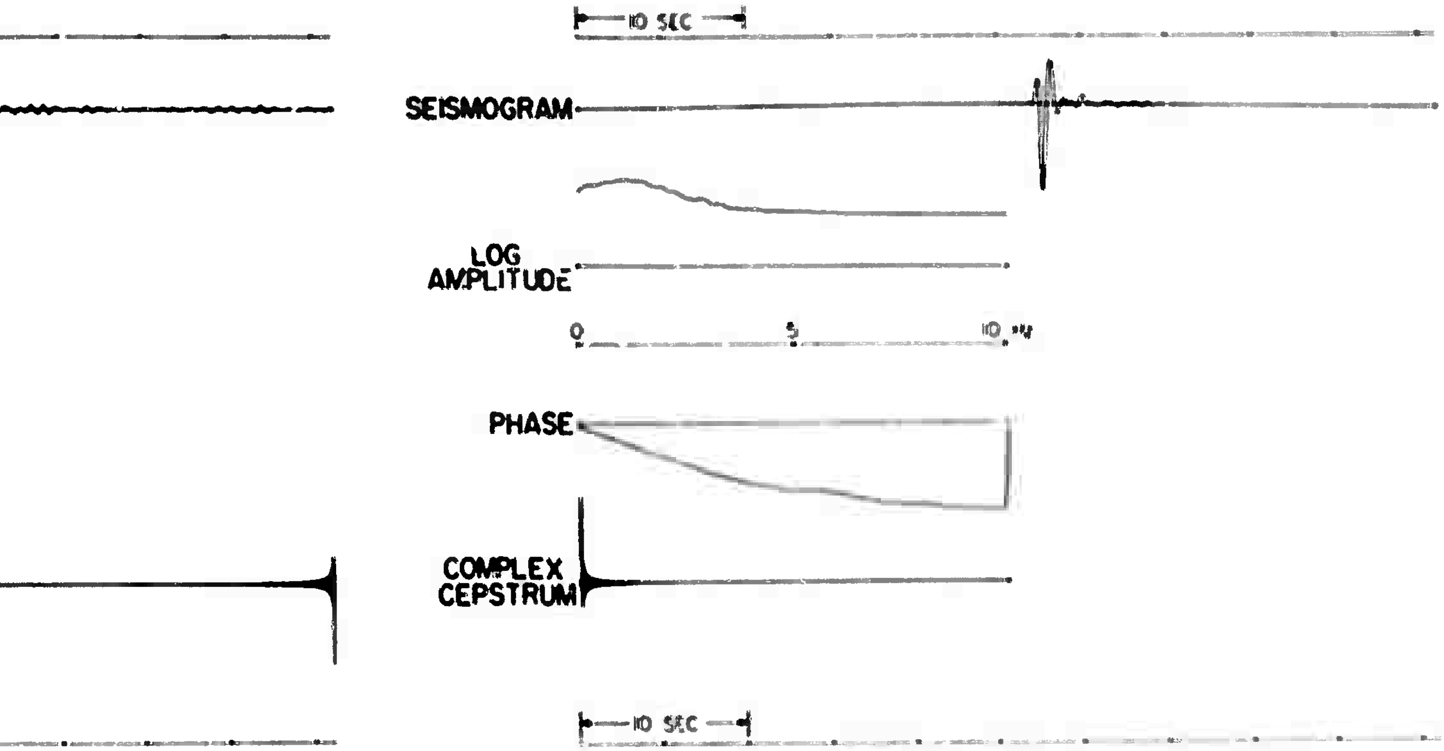

Figure 27. Results of processing the nine synthetic seismograms
(a) Weighted beamforming
1. Seismogram vs. time
2. Log-amplitude vs. frequency
3. Unwound phase vs. frequency
(b) Generalized linear filter 1
1. Seismogram vs. time
2. Log-amplitude vs. frequency
3. Unwound phase vs. frequency
4. Complex cepstrum vs. time
(c) Generalized linear filter 2
1. Seismogram vs. time
2. Log-amplitude vs. frequency
3. Unwound phase vs. frequency
4. Tapered complex cepstrum

β

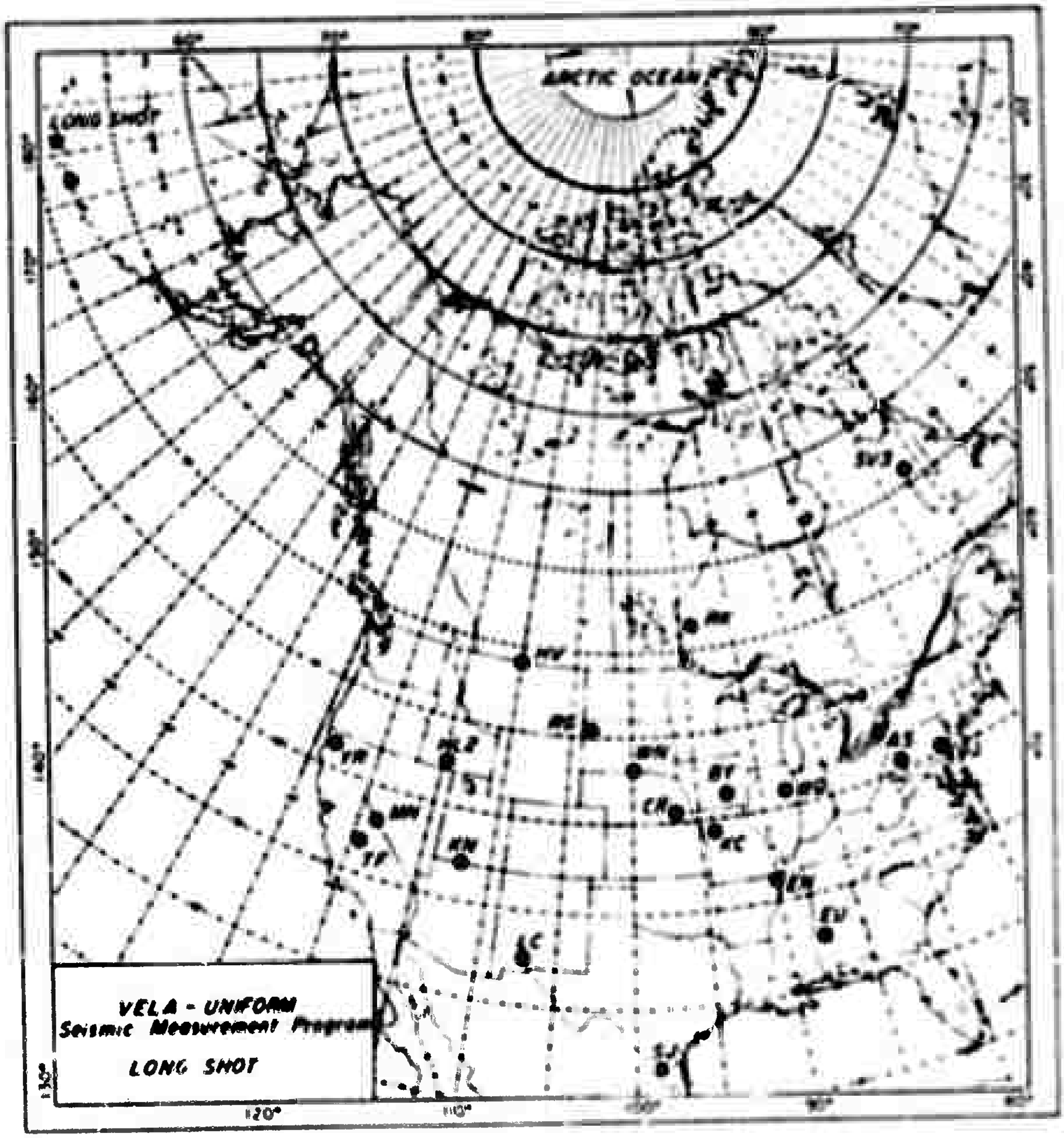

Figure 28. Location of events and stations.

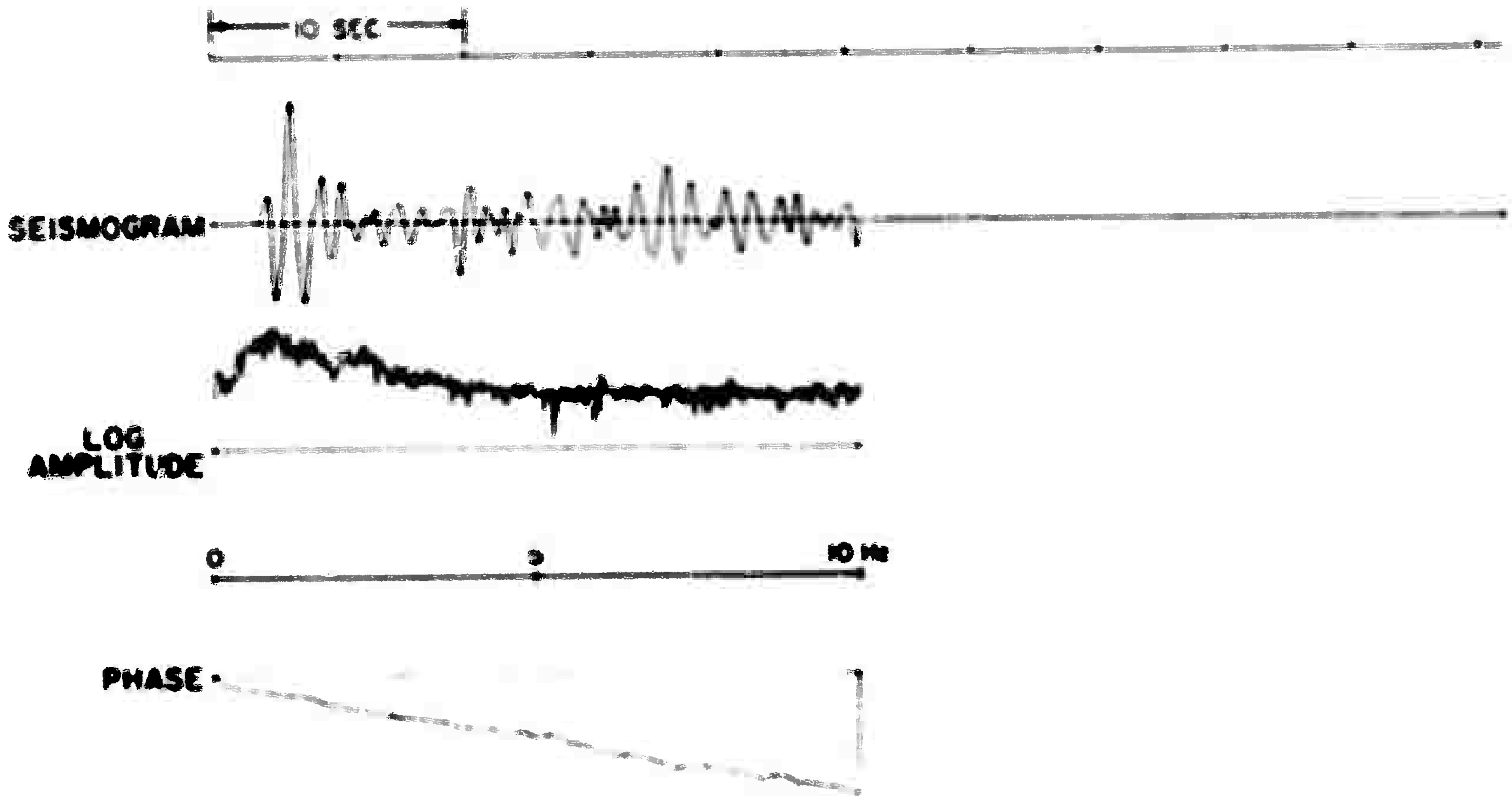

Figure 2[illegible]. [illegible], Station [illegible] (a) Seismogram vs. time, (b) log-amplitude vs. frequency, (c) Unwound phase vs. frequency.

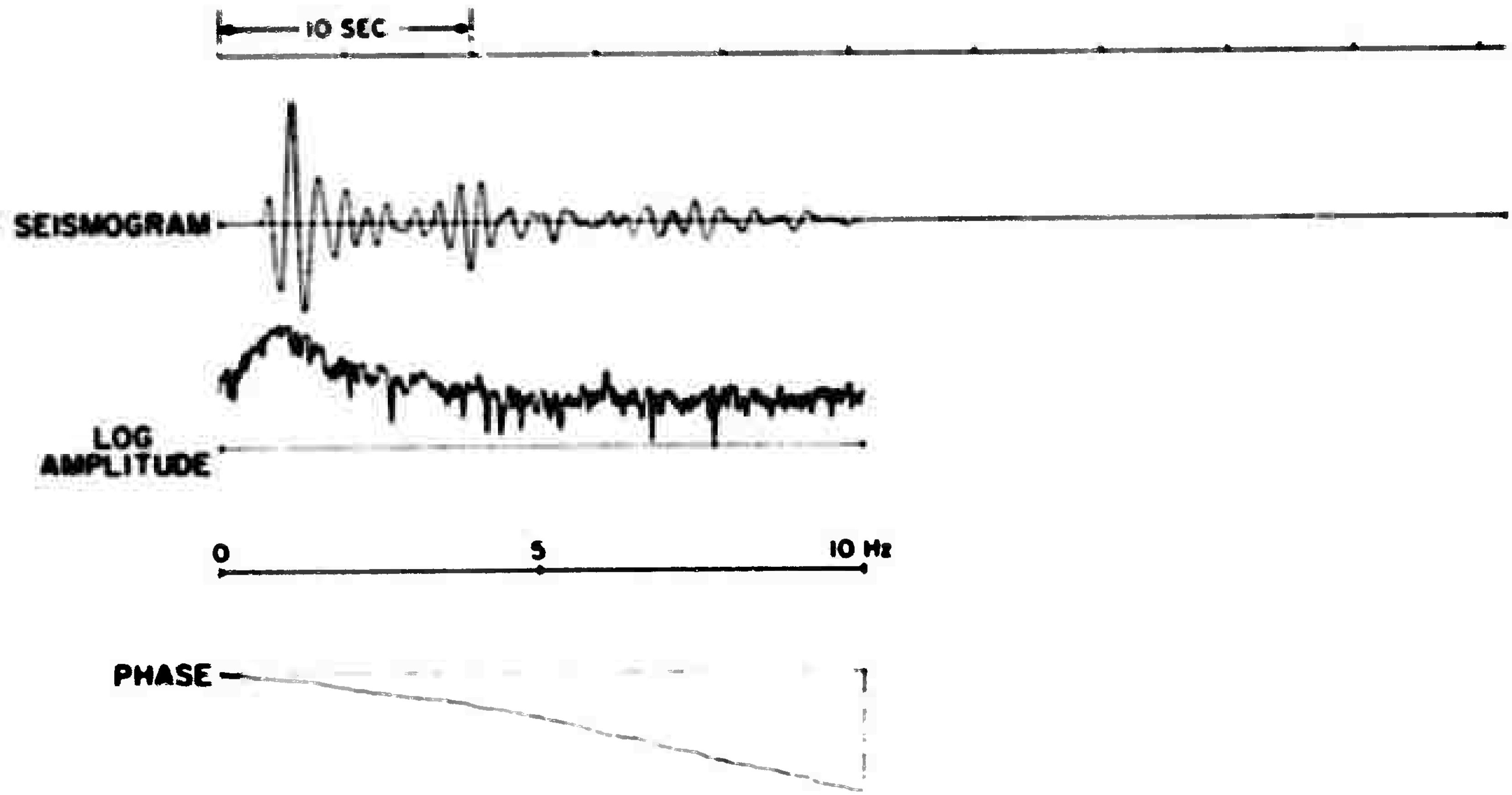

Figure 30. LONGSHOT, Station LC-NM (a) Seismogram vs. time, (b) Log-amplitude vs. frequency, (c) Unwound phase vs. frequency.

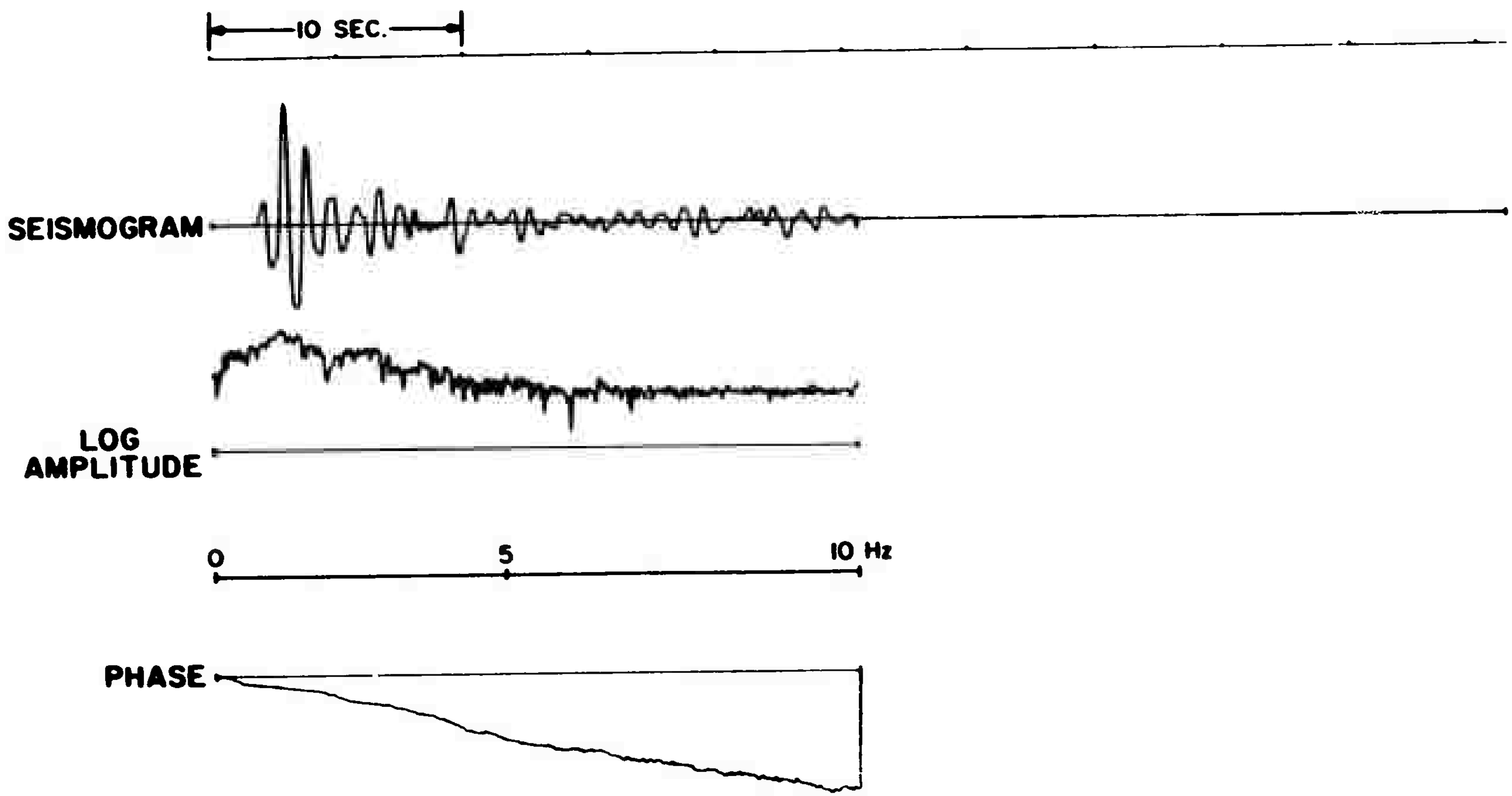

Figure 31. LONGSHOT, Station SV3QB (a) Seismogram vs. time, (b) Log-amplitude vs. frequency, (c) Unwound phase vs. frequency.

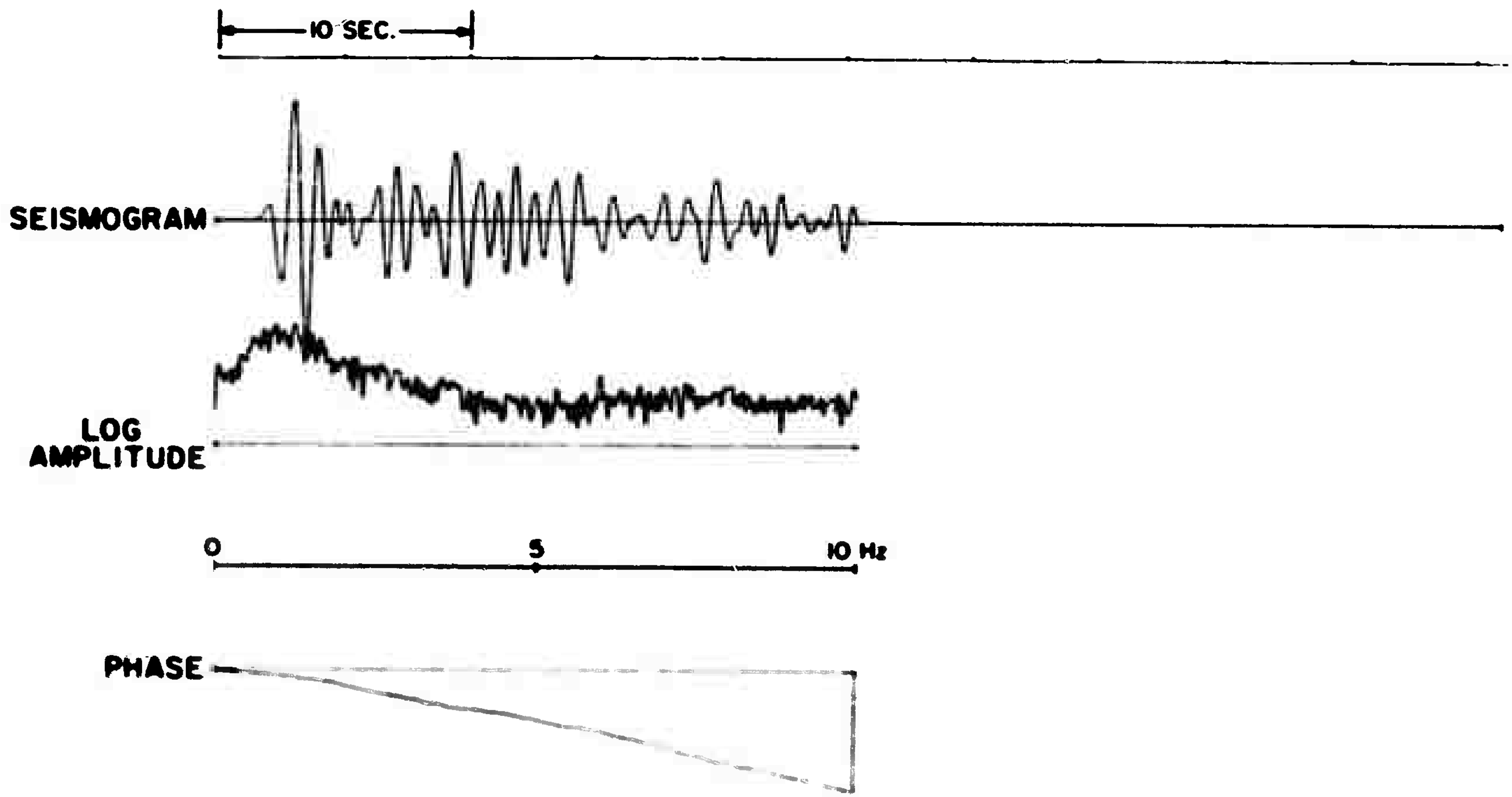

Figure 32. LONGSHOT, Station HN2ID (a) Seismogram vs. time, (b) Log-amplitude vs. frequency, (c) Unwound phase vs. frequency.

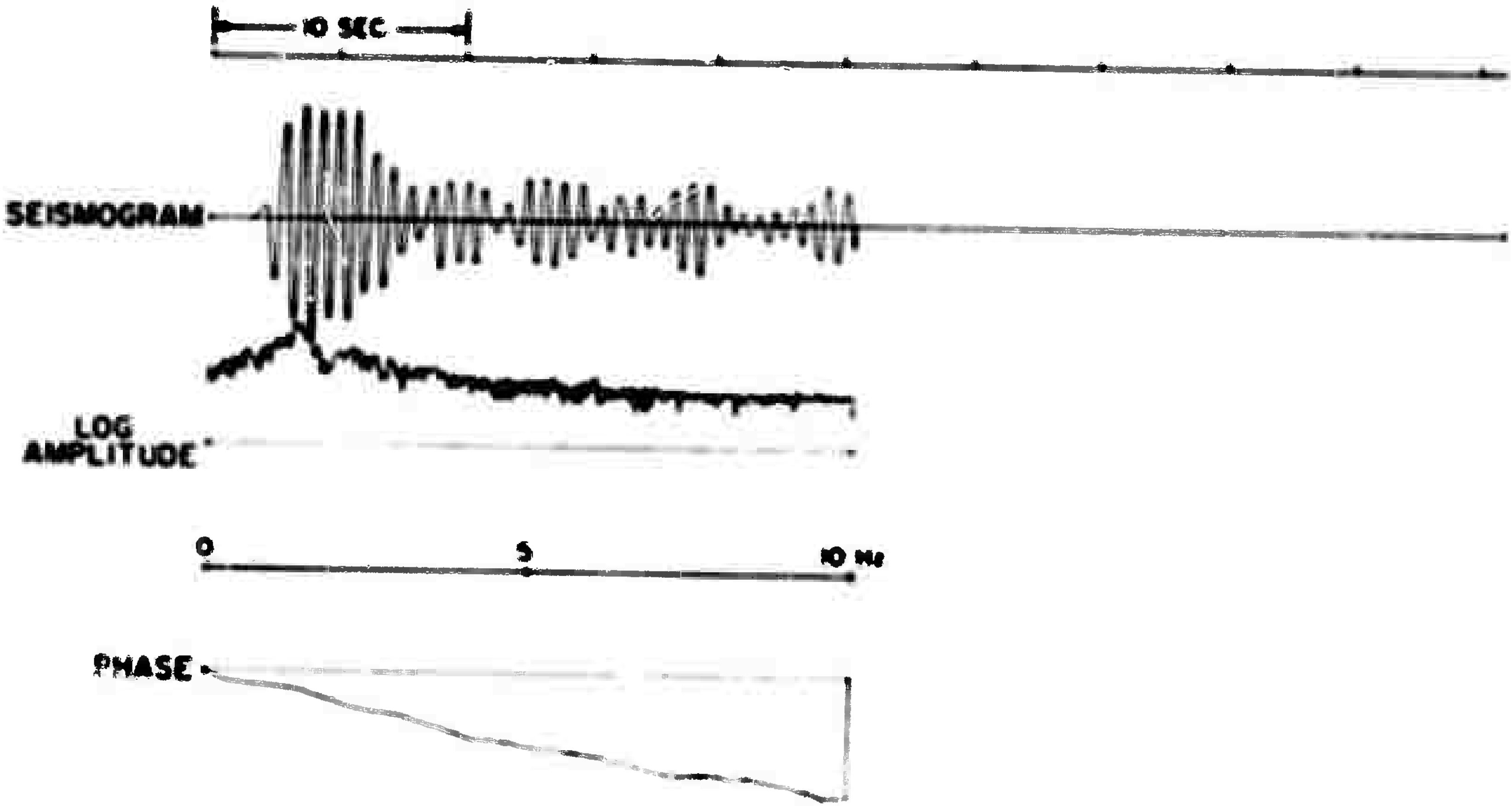

Figure 33. LONGSHOT, station NC-50 (a) Seismogram vs. time, (b) Log-amplitude vs. frequency, (c) Unwound phase vs. frequency.

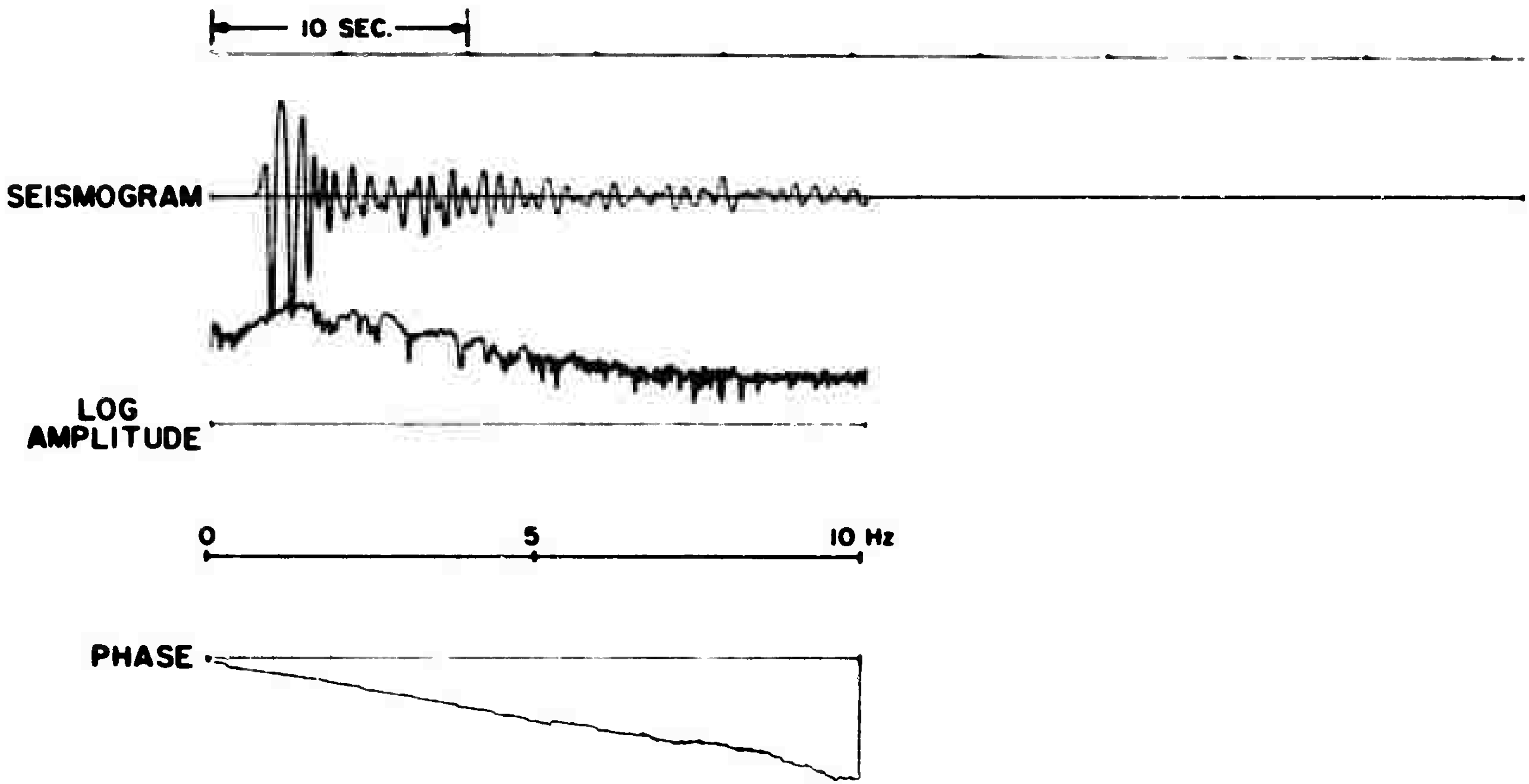

Figure 34. LONGSHOT, Station RK-ON (a) Seismogram vs. time, (b) Log-amplitude vs. frequency, (c) Unwound phase vs. frequency.

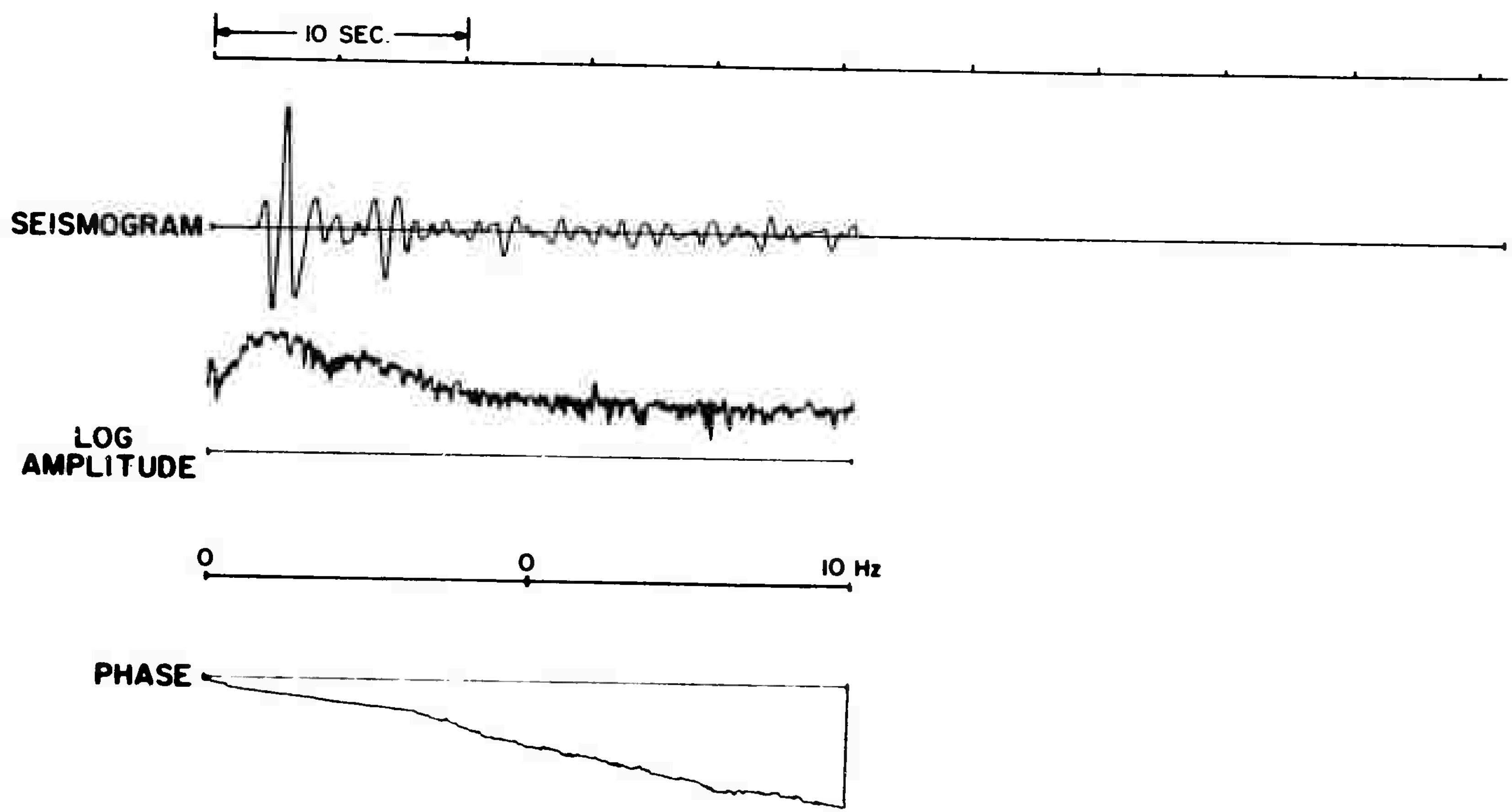

Figure 35. LONGSHOT, Station SJ-TX (a) Seismogram vs. time, (b) Log-amplitude vs. frequency, (c) Unwound phase vs. frequency.

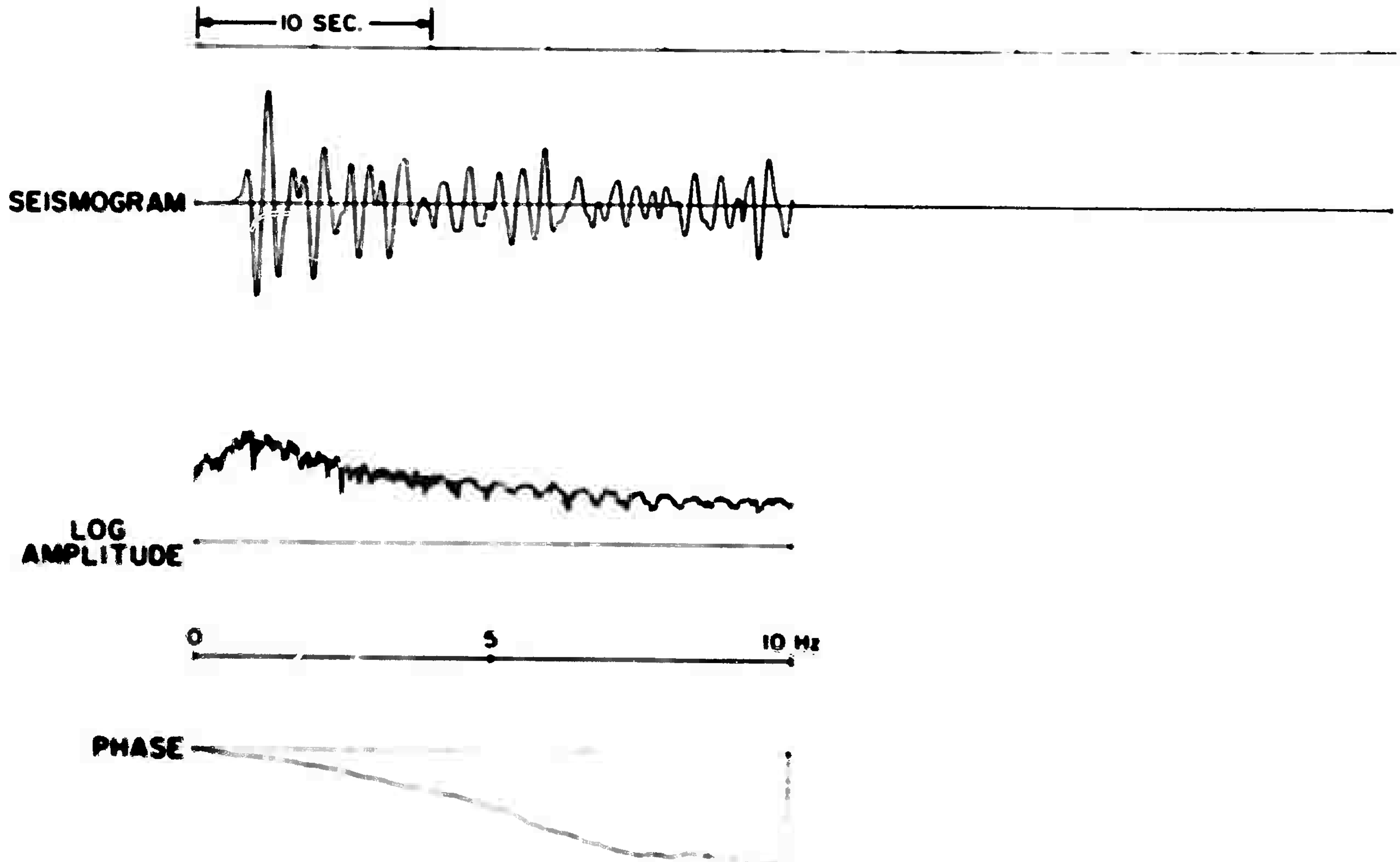

Figure [illegible]. [illegible], Station [illegible] (a) Seismogram vs. time, (b) Log-amplitude vs. frequency, (c) [illegible] phase vs. frequency.

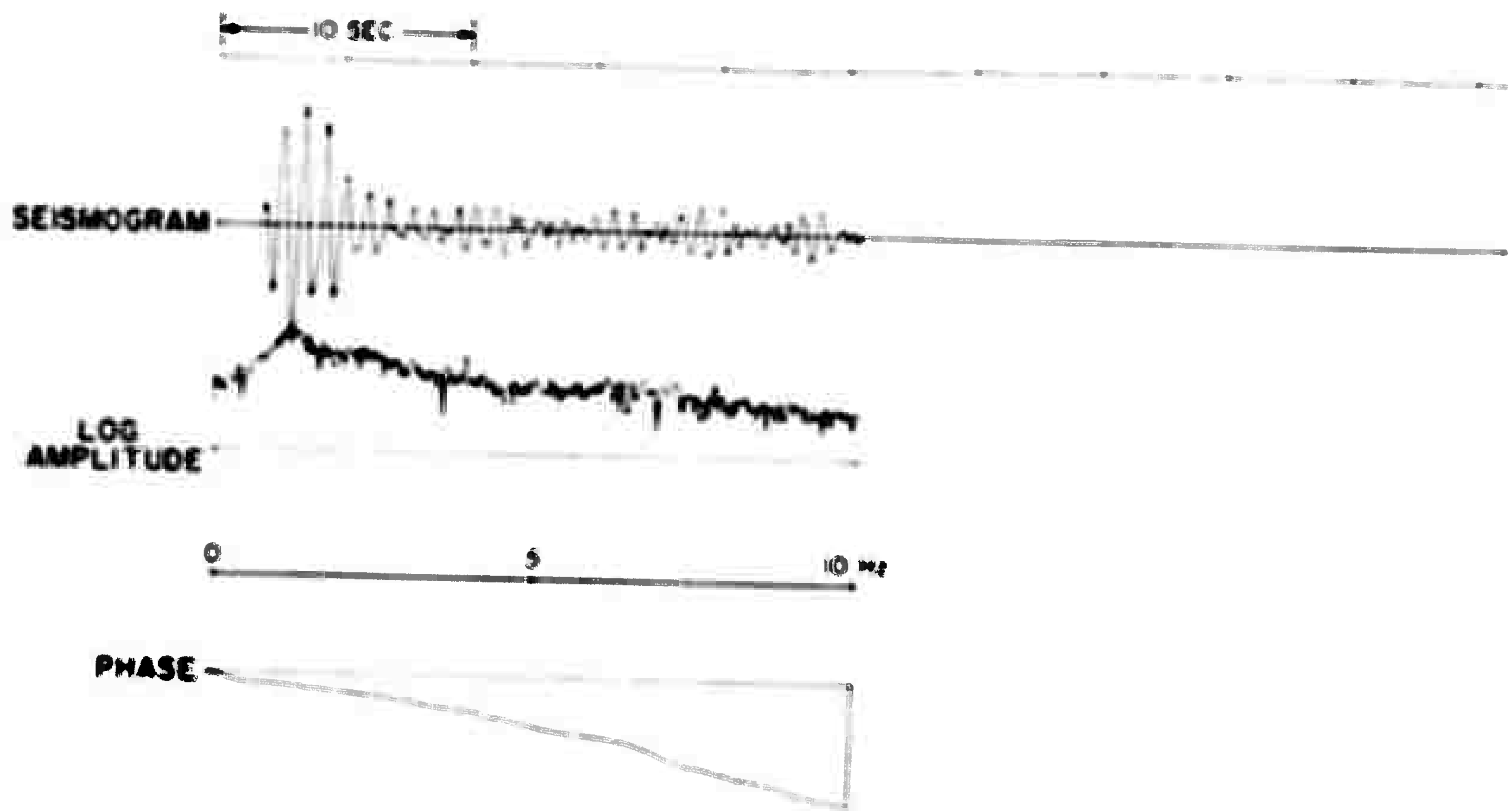

Figure [illegible]. [illegible] (a) Seismogram vs. time. (b) Log amplitude vs frequency. (c) [illegible] phase vs. frequency.

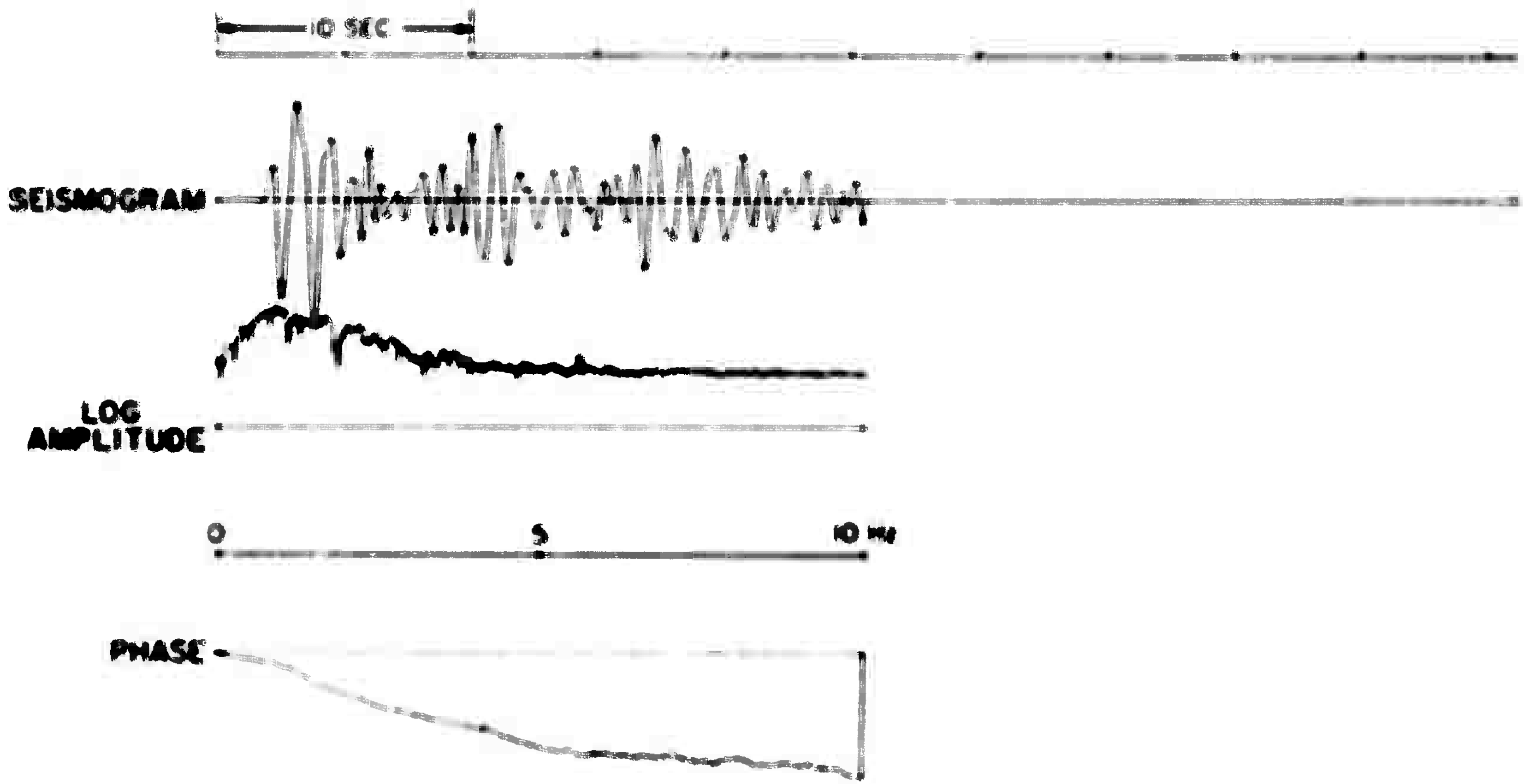

Figure [illegible]. [illegible] (a) Seismogram vs. time, (b) Log amplitude vs. frequency, (c) Unwound phase vs. frequency.

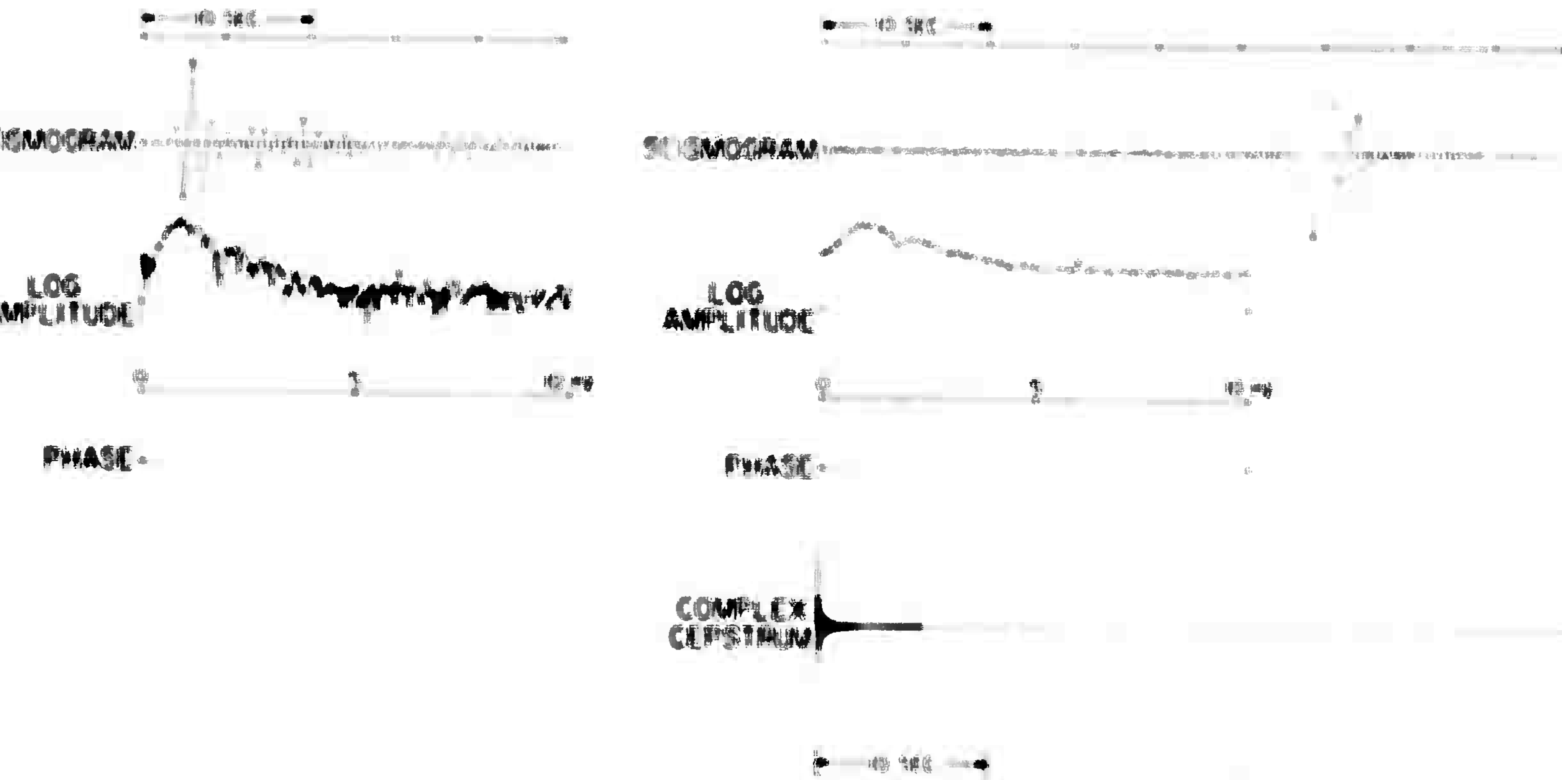
10 SEC
SEISMOGRAM
LOG AMPLITUDE
PHASE
10 SEC
SEISMOGRAM
LOG AMPLITUDE
PHASE
COMPLEX CEPSTRUM
10 SEC

A

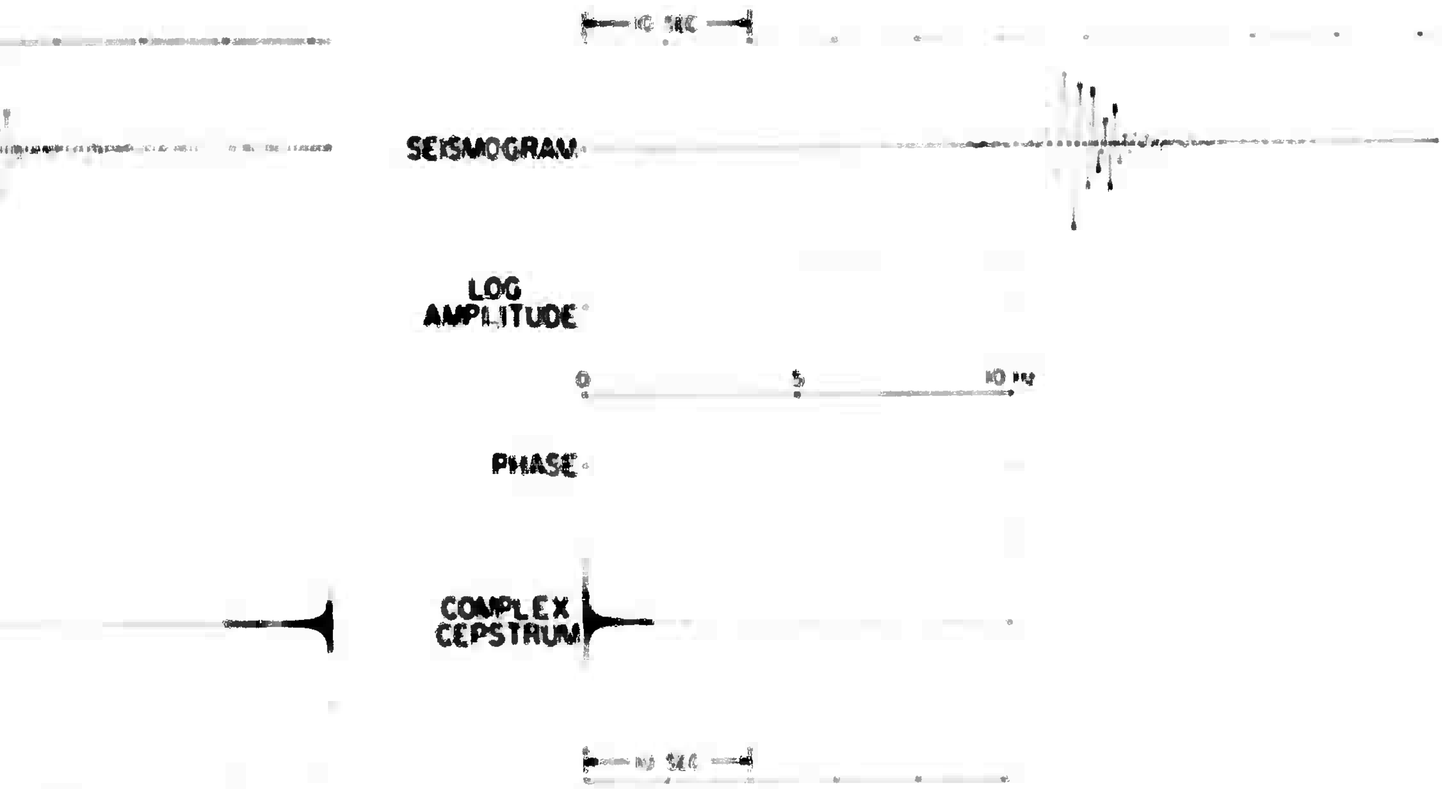

Figure 39. LONGSHOT processing results
(a) Beamforming
1. Seismogram vs. time
2. Log-amplitude vs. frequency
3. Unwound phase vs. frequency
(b) Generalized linear filter 1
1. Seismogram vs. time
2. Log-amplitude vs. frequency
3. Unwound phase vs. frequency
(c) Generalized linear filter 2
1. Seismogram vs. time
2. Log-amplitude vs. frequency
3. Unwound phase vs. frequency.

6

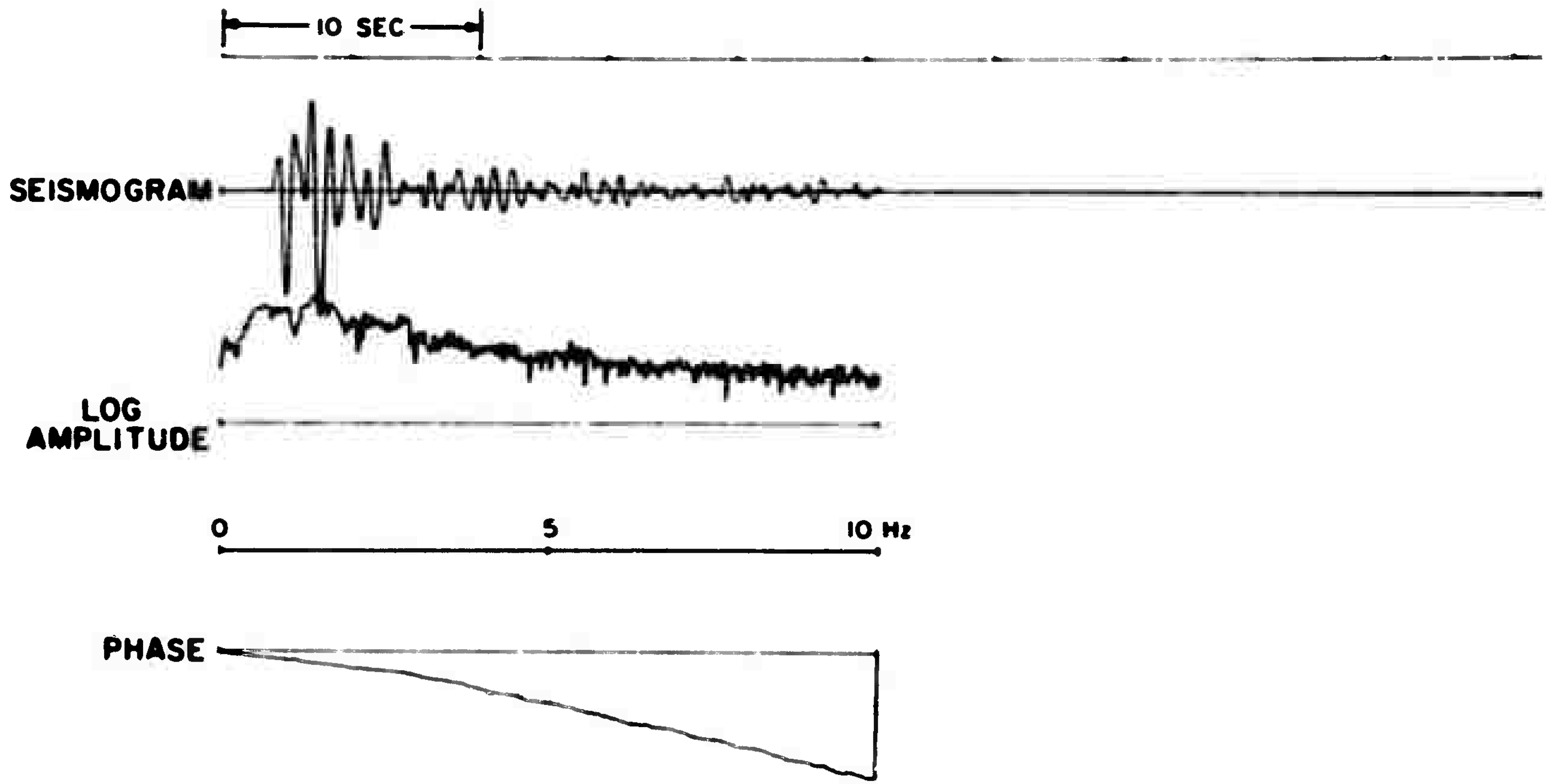

Figure [illegible]. MILROW, Station NQ-11. (a) Seismogram vs. time, (b) Log-amplitude vs. frequency, (c) Unwound phase vs. frequency.

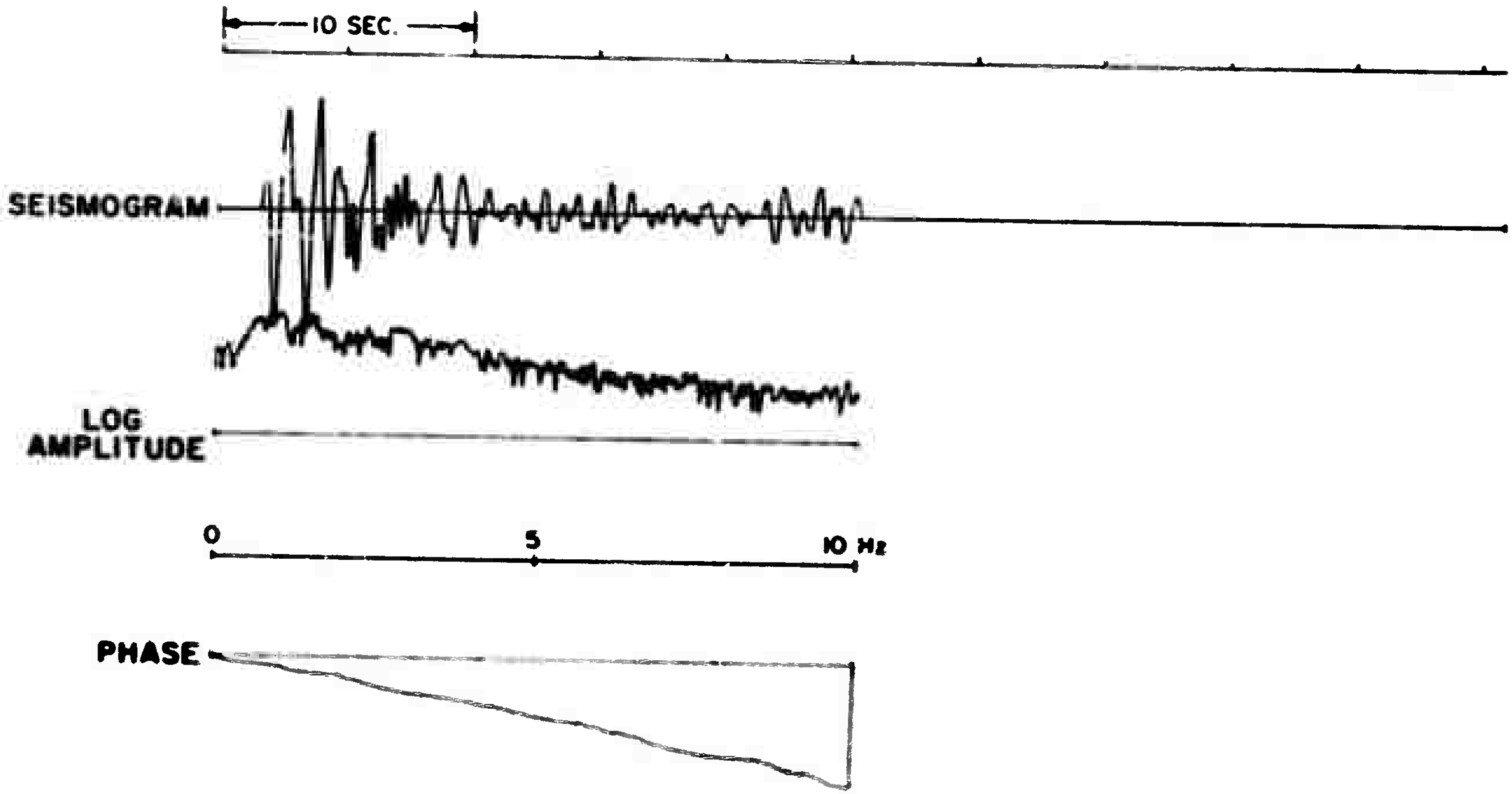

Figure 11. MILROW, Station A1-10 (a) Seismogram vs. time, (b) Log-amplitude vs. frequency, (c) Unwound phase vs. frequency.

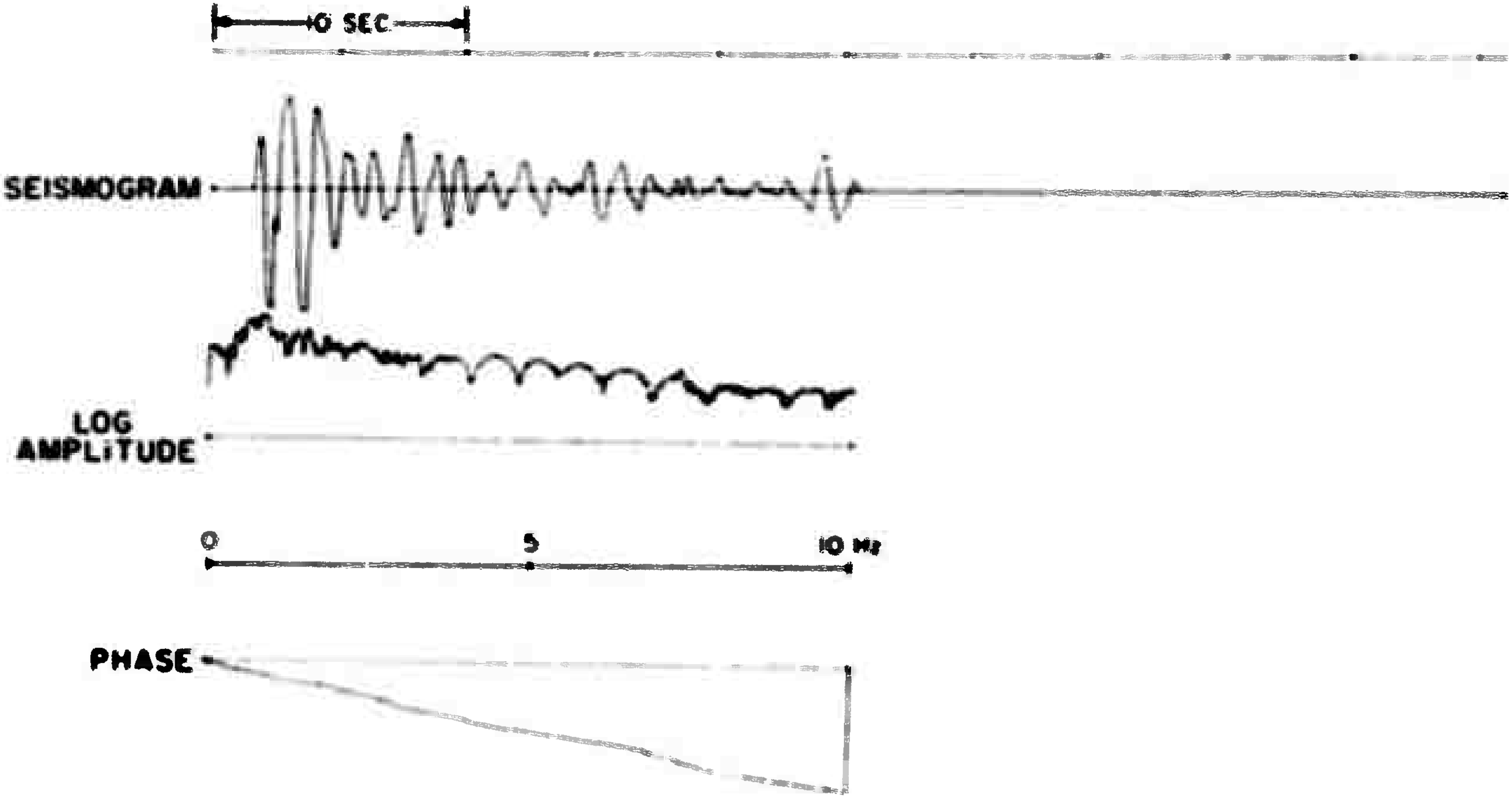

Figure [illegible]. [illegible], station [illegible] (a) Seismogram vs. time. (b) Log-amplitude vs. frequency. (c) Unwound phase vs. frequency.

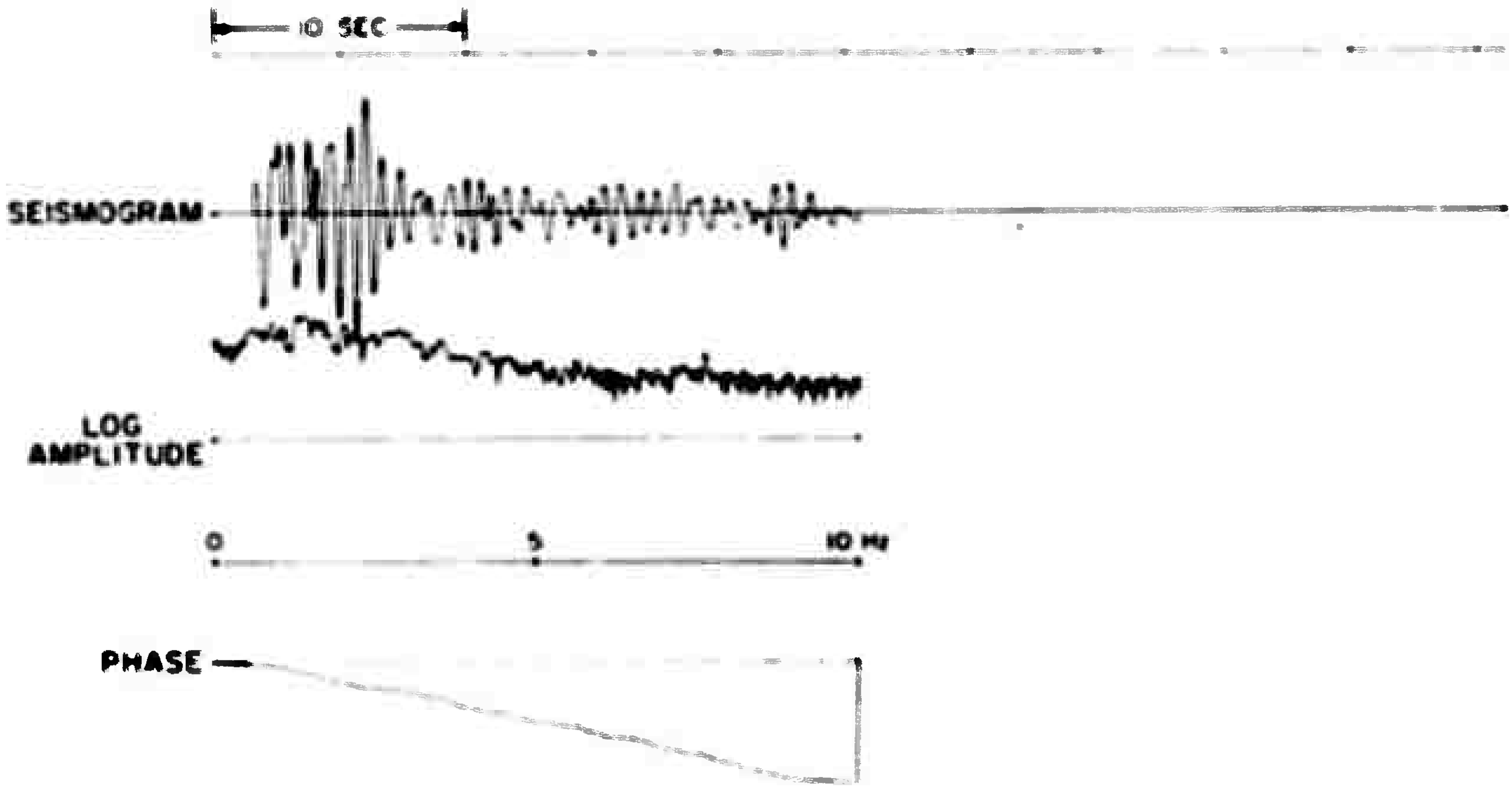

Figure [illegible]. [illegible], station [illegible] (a) Seismogram vs. time. (b) Log-amplitude vs. frequency. (c) Unwound phase vs. frequency.

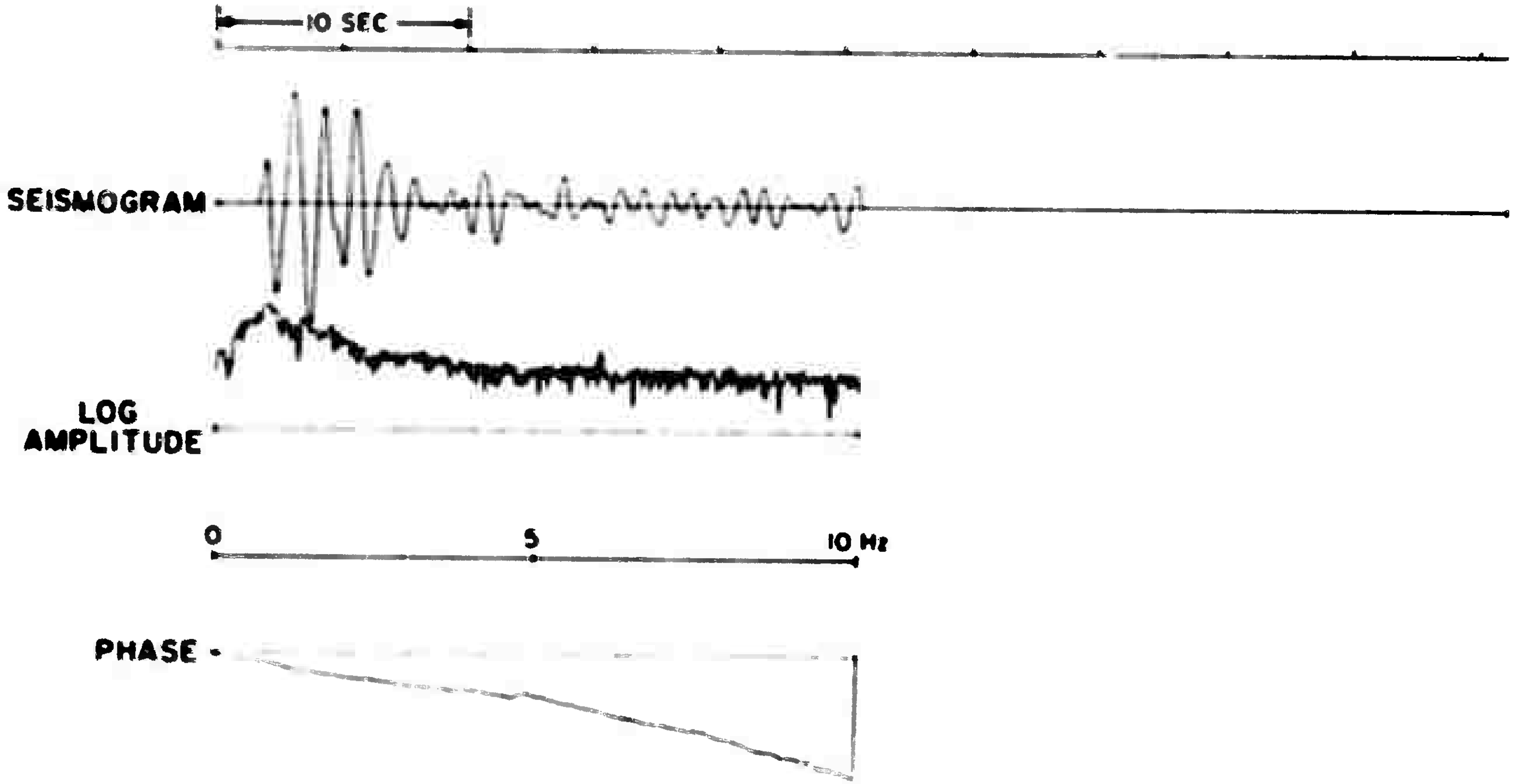

Figure [illegible]. [illegible], station [illegible] (a) Seismogram vs. time. (b) Log-amplitude vs. frequency, (c) Unwound phase vs. frequency.

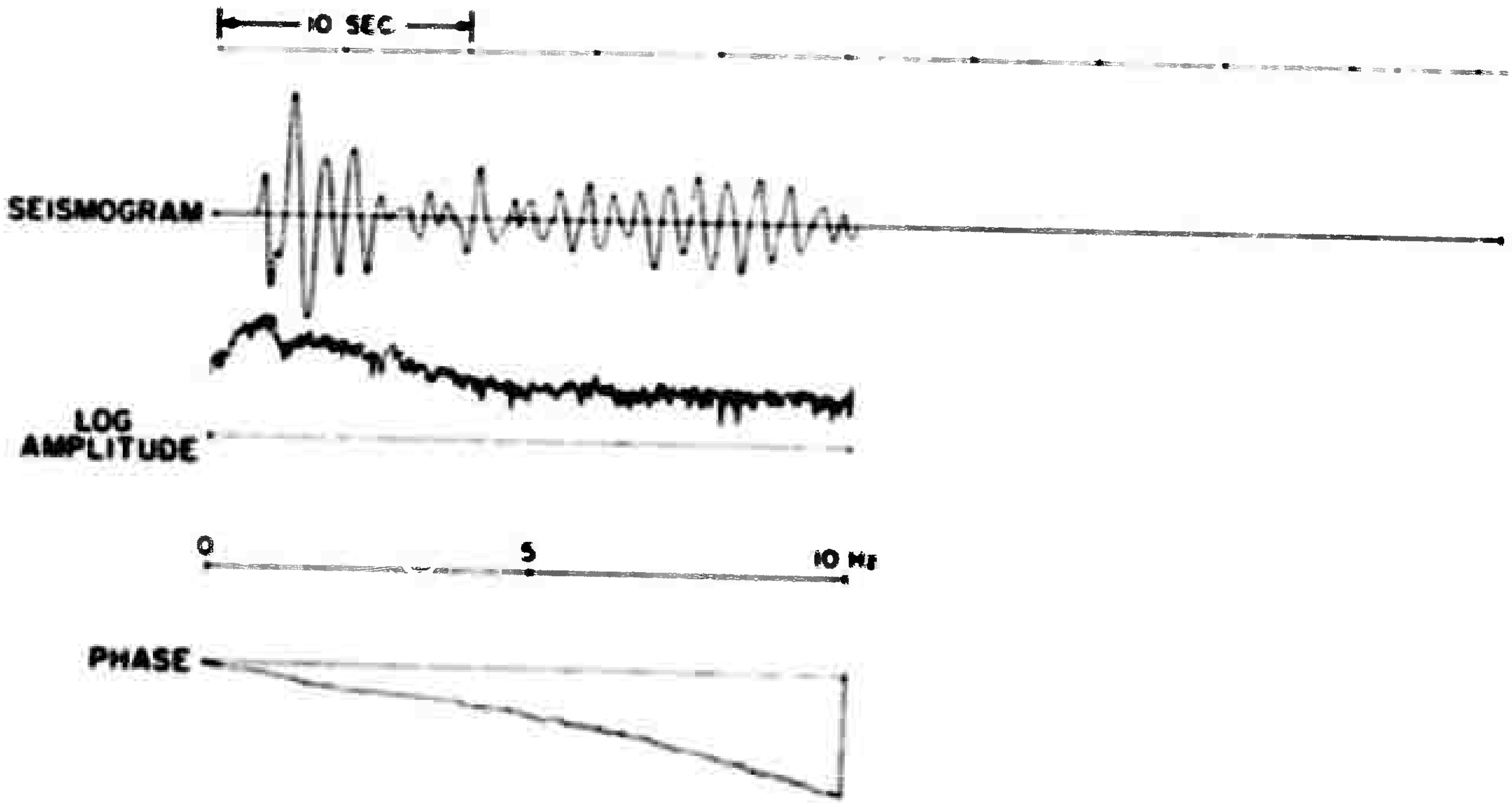

Figure [illegible]. [illegible], Station [illegible] (a) Seismogram vs. time. (b) Log-amplitude vs. frequency. (c) Unwound phase vs. frequency.

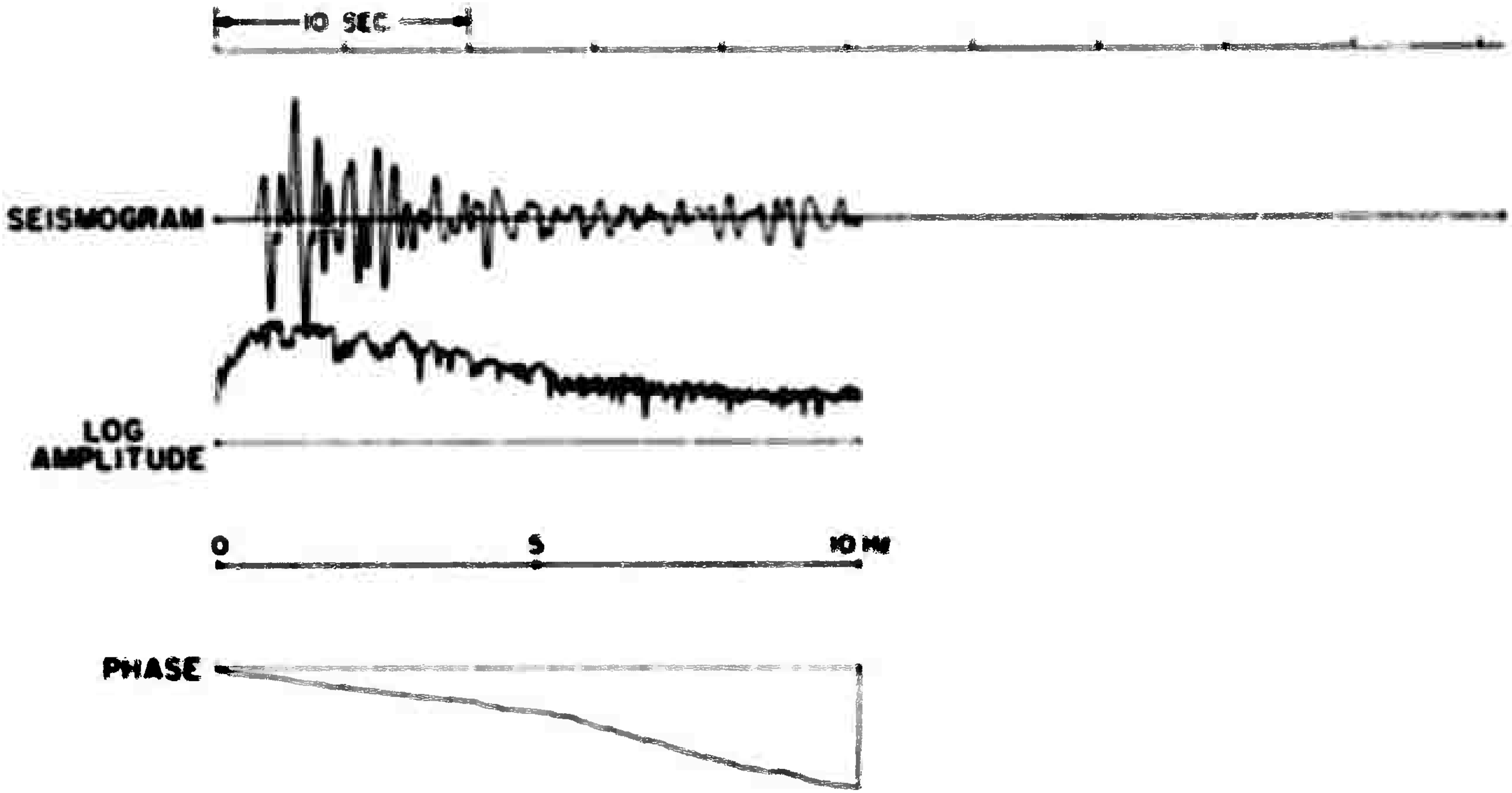

Figure [illegible]. [illegible], Station [illegible] (a) Seismogram vs. time. (b) Log-amplitude vs. frequency. (c) Unwound phase vs. frequency.

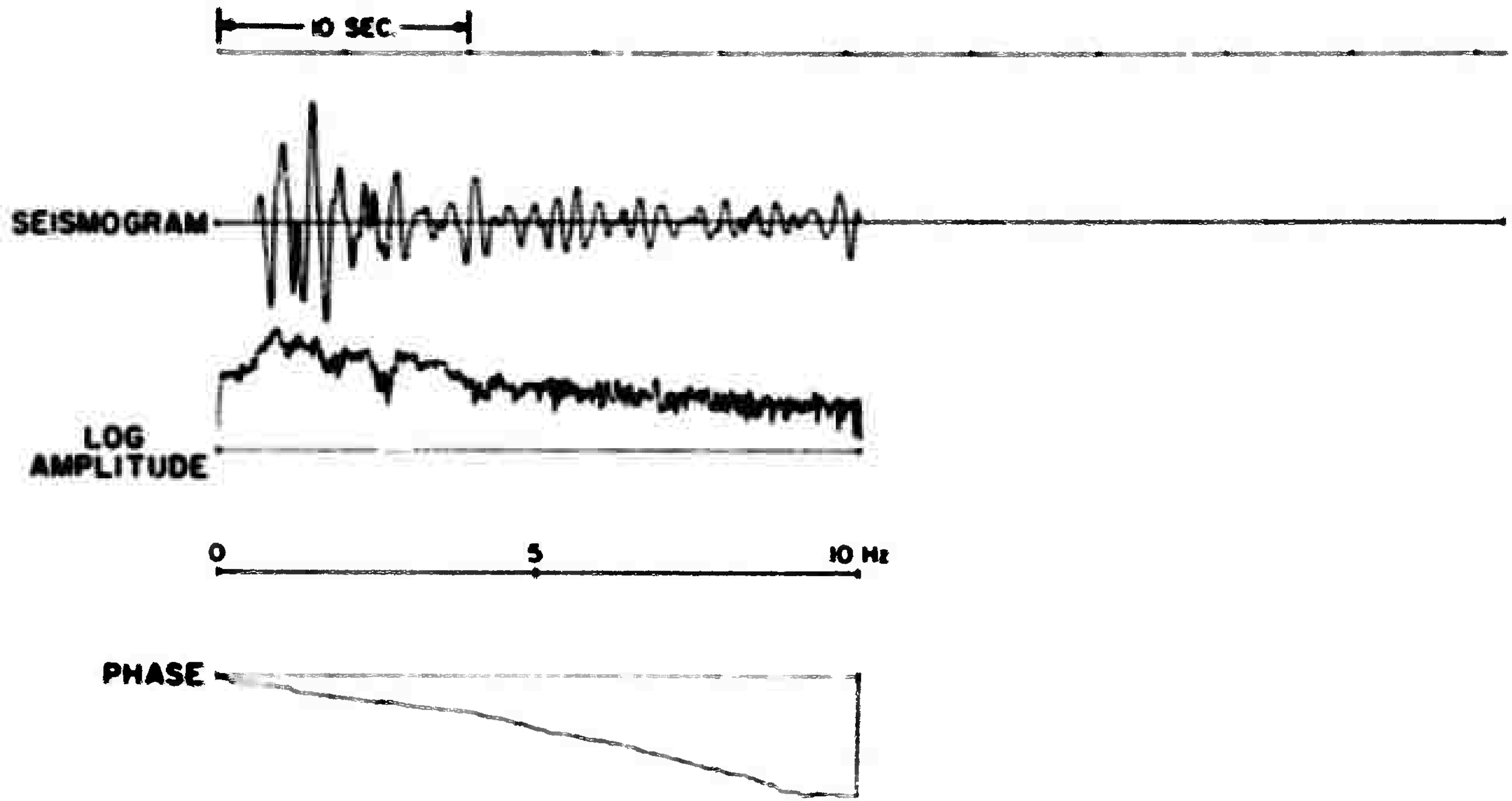

Figure 47. MILROW, Station LUZAL (a) Seismogram vs. time, (b) Log-amplitude vs. frequency, (c) Unwound phase vs. frequency.

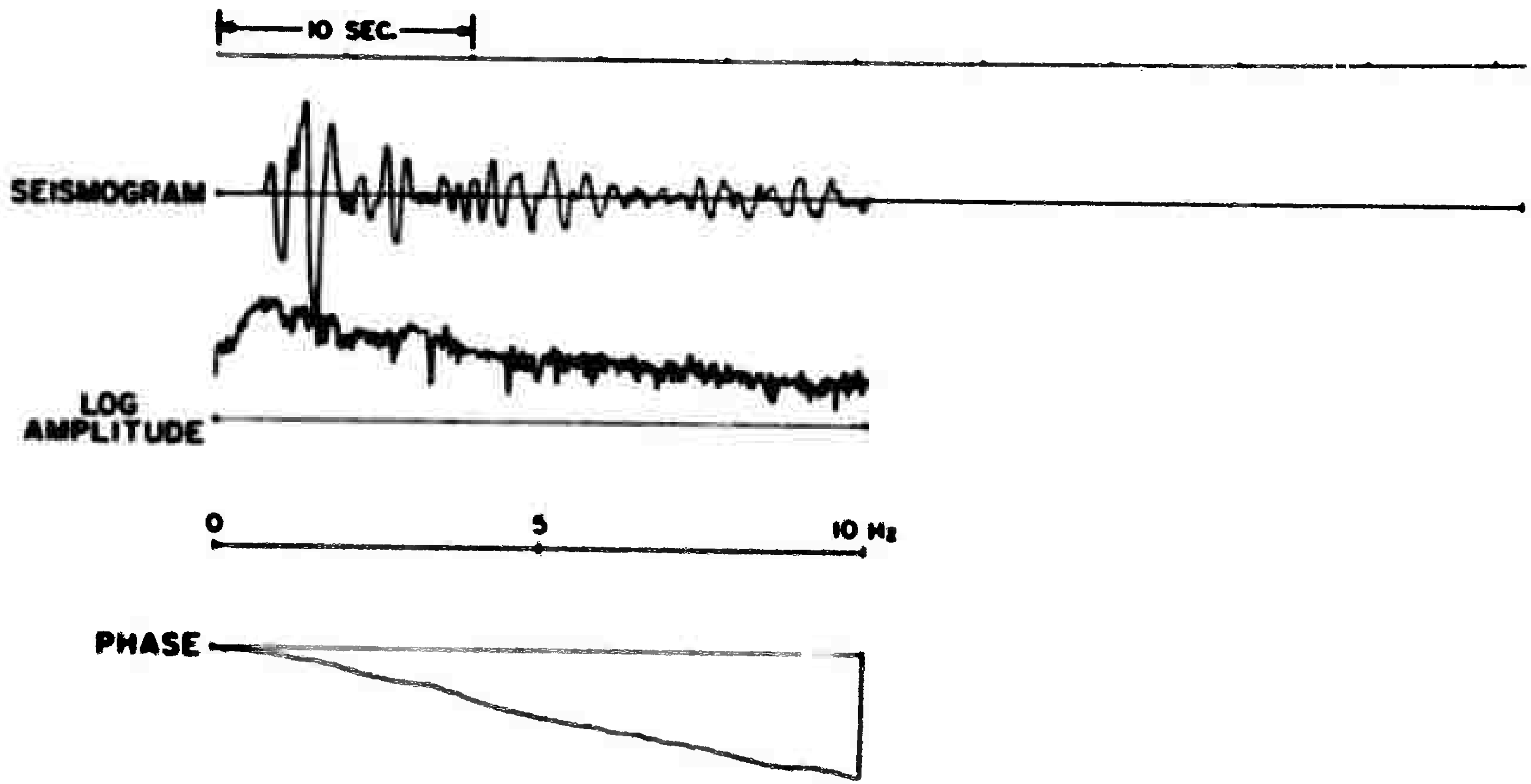

Figure 15. MILROW, Station PJ-FA (a) Seismogram vs. time, (b) Log-amplitude vs. frequency, (c) Unwound phase vs. frequency.

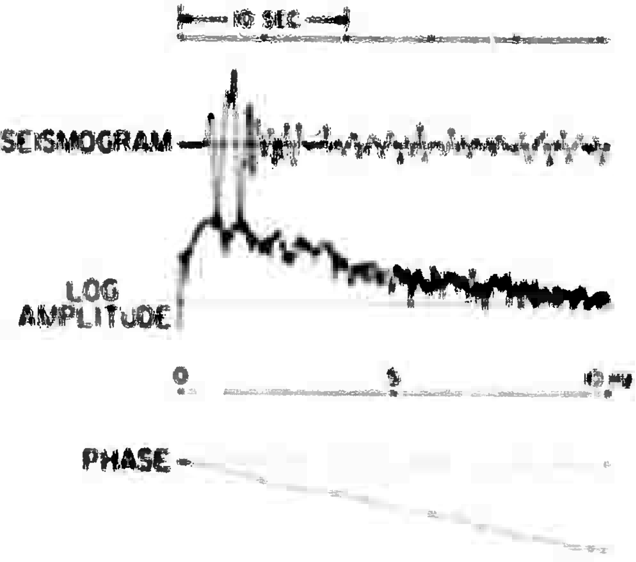

10 SEC
SEISMOGRAM
LOG
AMPLITUDE
0
5
PHASE

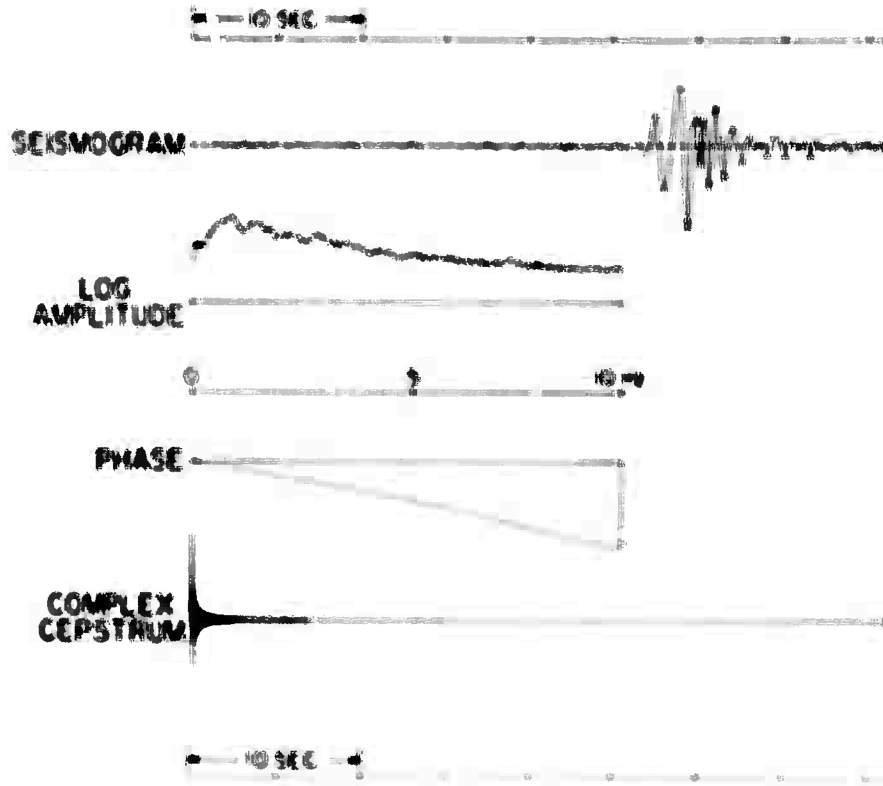

10 SEC
SEISMOGRAM
LOG
AMPLITUDE
0
5
PHASE
COMPLEX
CEPSTRUM
10 SEC

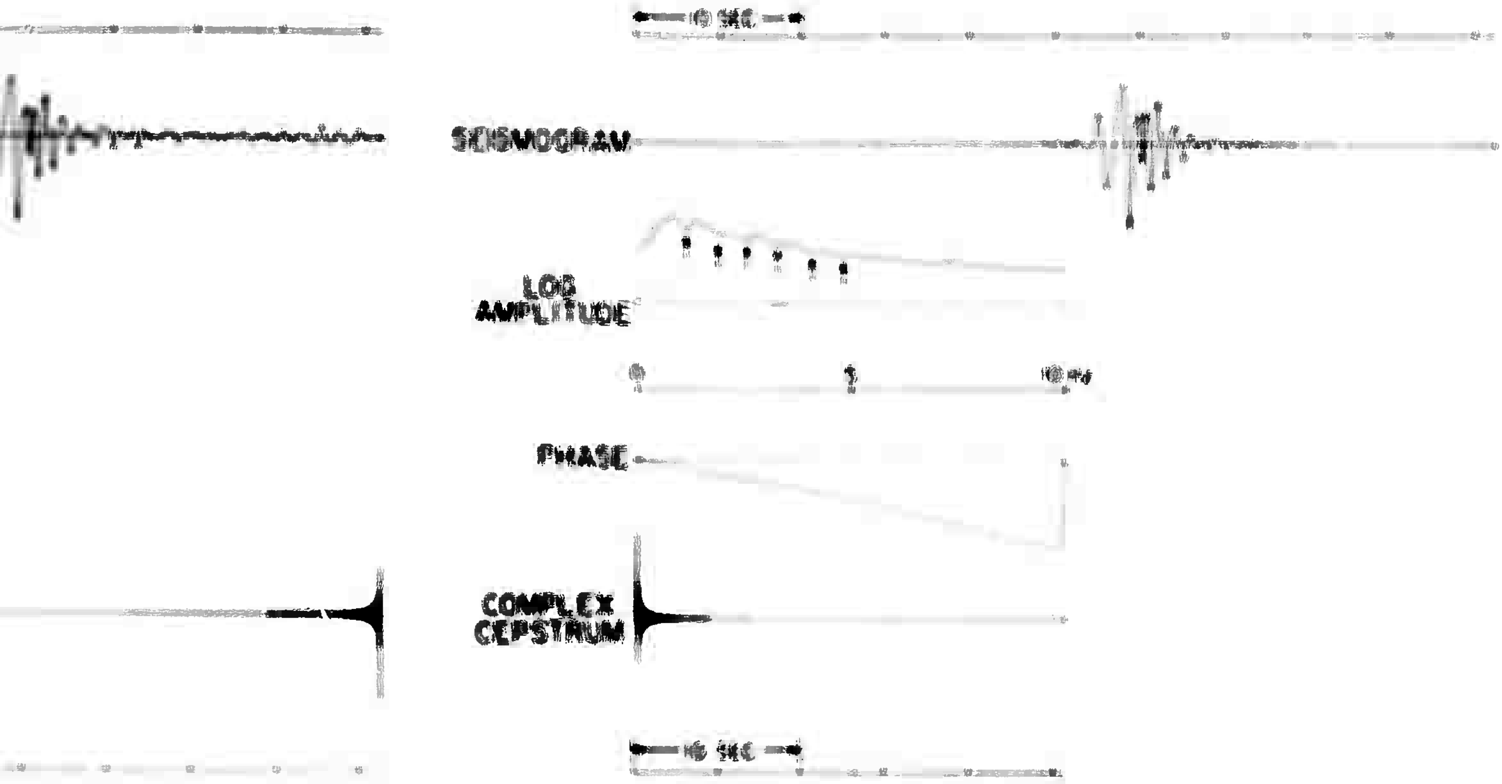

Figure 49. Processing results for MILROW
(a) Beamforming
1. Seismogram vs. time
2. Log-amplitude vs. frequency
3. Unwound phase vs. frequency
(b) Generalized linear filter 1
1. Seismogram vs. time
2. Log-amplitude vs. frequency
3. Unwound phase vs. frequency
4. Complex cepstrum vs. time
(c) Generalized linear filter 2
1. Seismogram vs. time
2. Log-amplitude vs. frequency
3. Unwound phase vs. frequency
4. Tapered complex cepstrum.

B

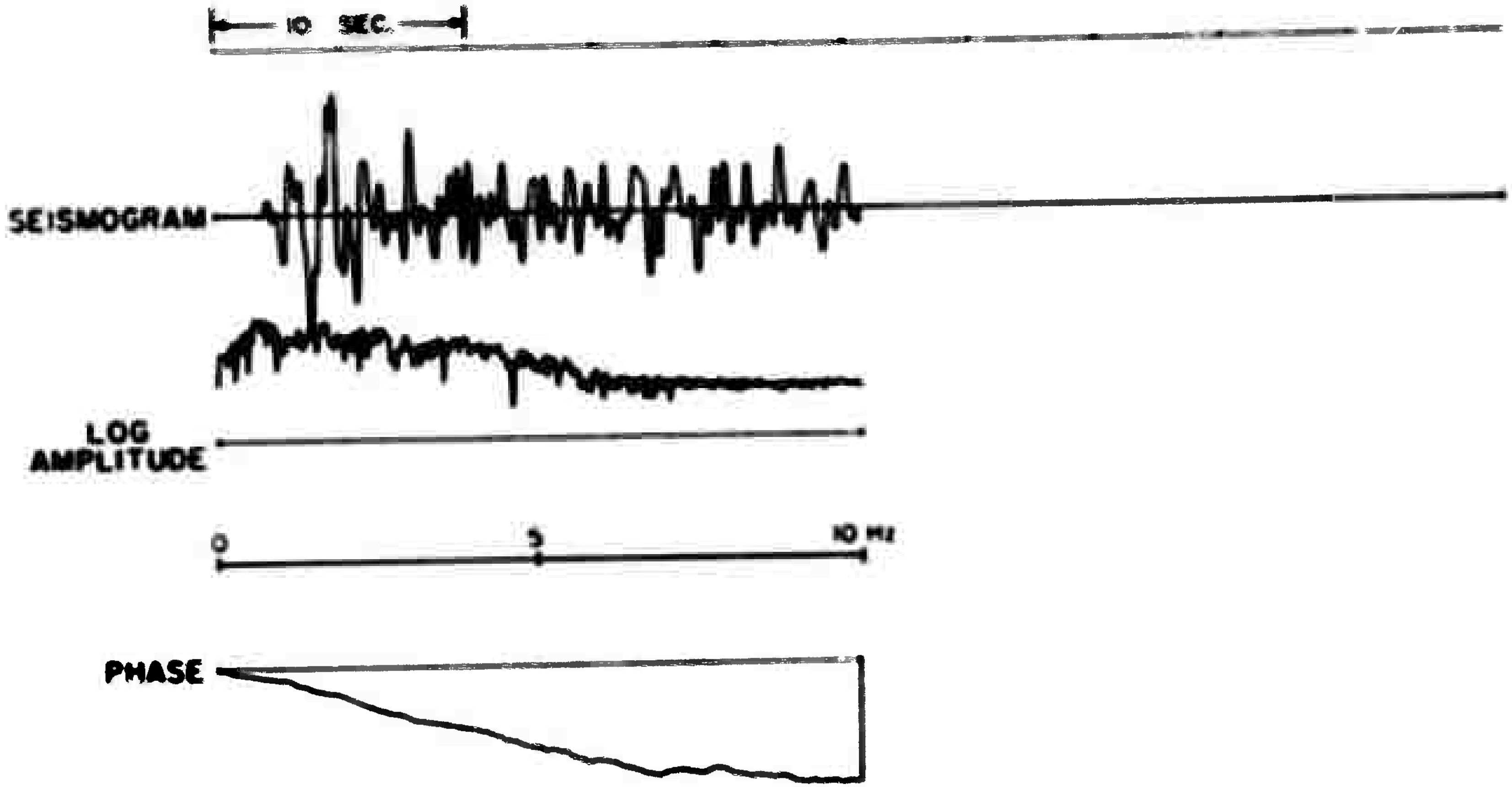

Figure 30. [illegible] Nov. 1965 Andreanoff Islands event. Station [illegible] (a) Seismogram vs. time. (b) Log-amplitude vs. frequency. (c) Unwound phase vs. frequency.

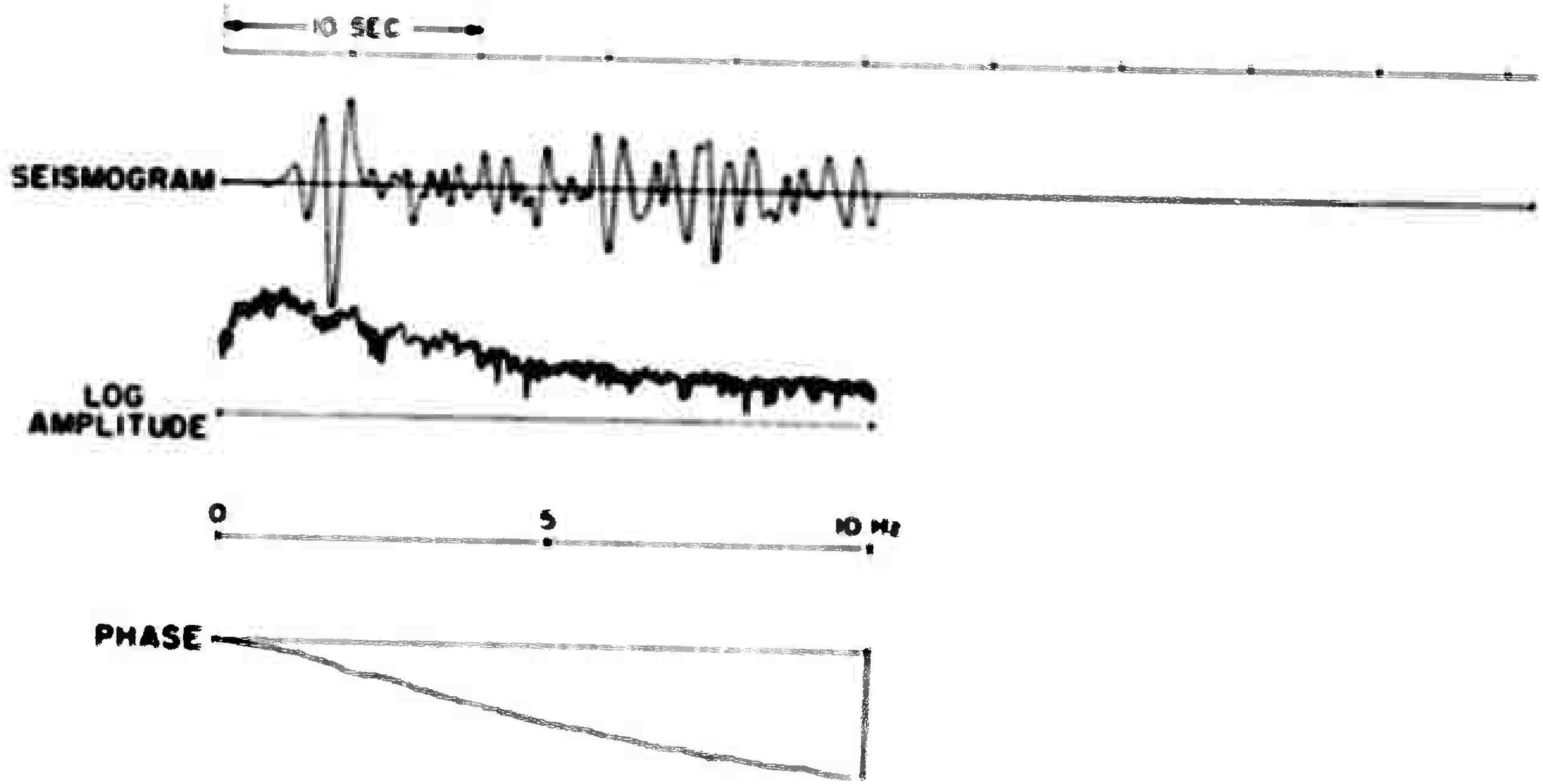

Figure 31. [illegible] Andreanoff Islands event, Station [illegible] (a) Seismogram vs. time. (b) Log-amplitude vs. frequency. (c) Unwound phase vs. frequency.

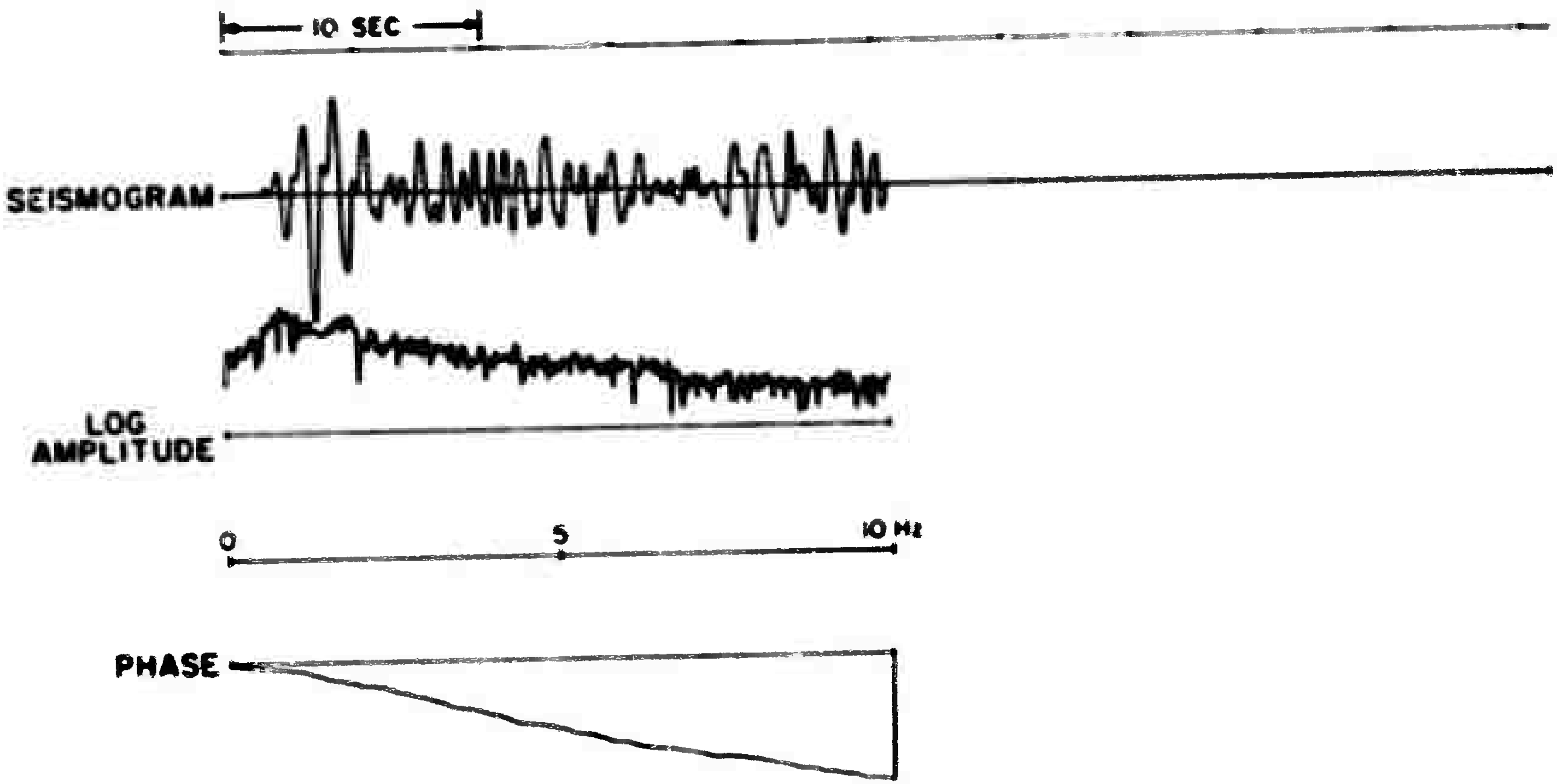

Figure [illegible]. [illegible] Nov. 1965 Andreanoff Islands event. Station KC-[illegible] (a) Seismogram vs. time, (b) Log-amplitude vs. frequency. (c) Unwound phase vs. frequency.

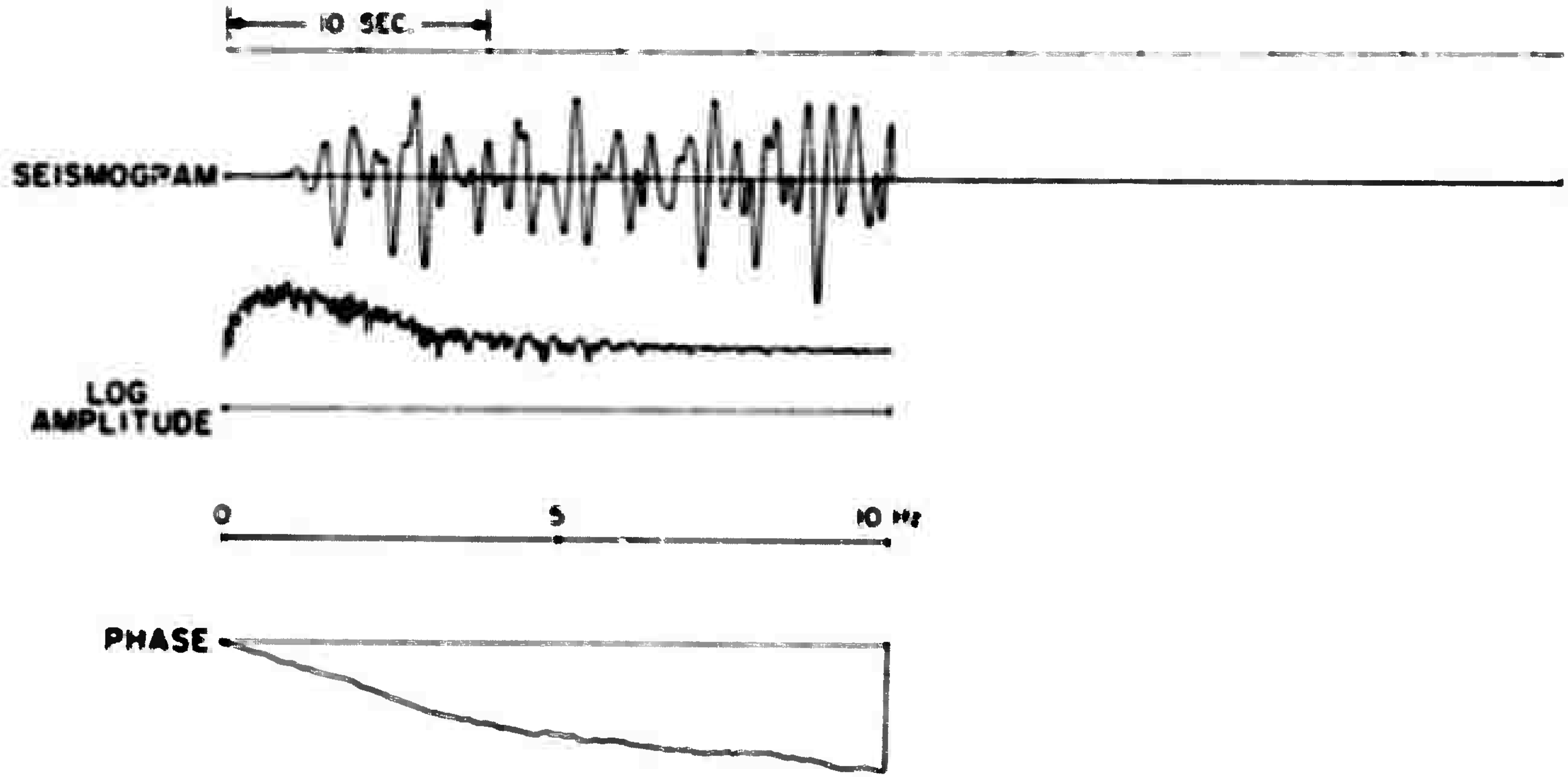

Figure [illegible]. [illegible] Nov. 196[illegible] Andreanoff Islands event, Station [illegible] (a) Seismogram vs. time, (b) Log-amplitude vs. frequency, (c) Unwound phase vs. frequency.

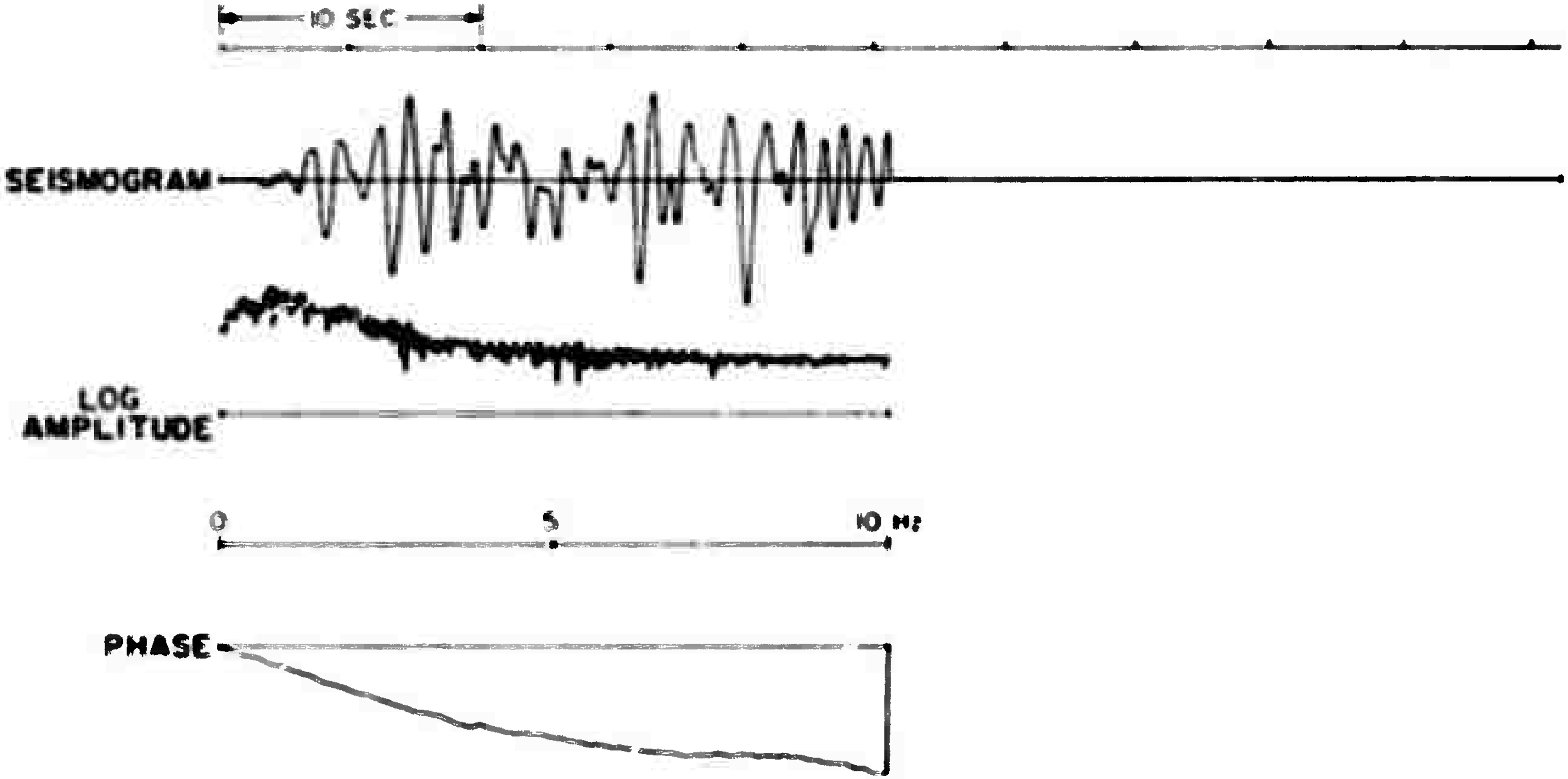

Figure [illegible]. [illegible] Nov. [illegible] Andreanoff Islands event, Station [illegible] (a) Seismogram vs. time. (b) Log-amplitude vs. frequency. (c) Unwound phase vs. frequency.

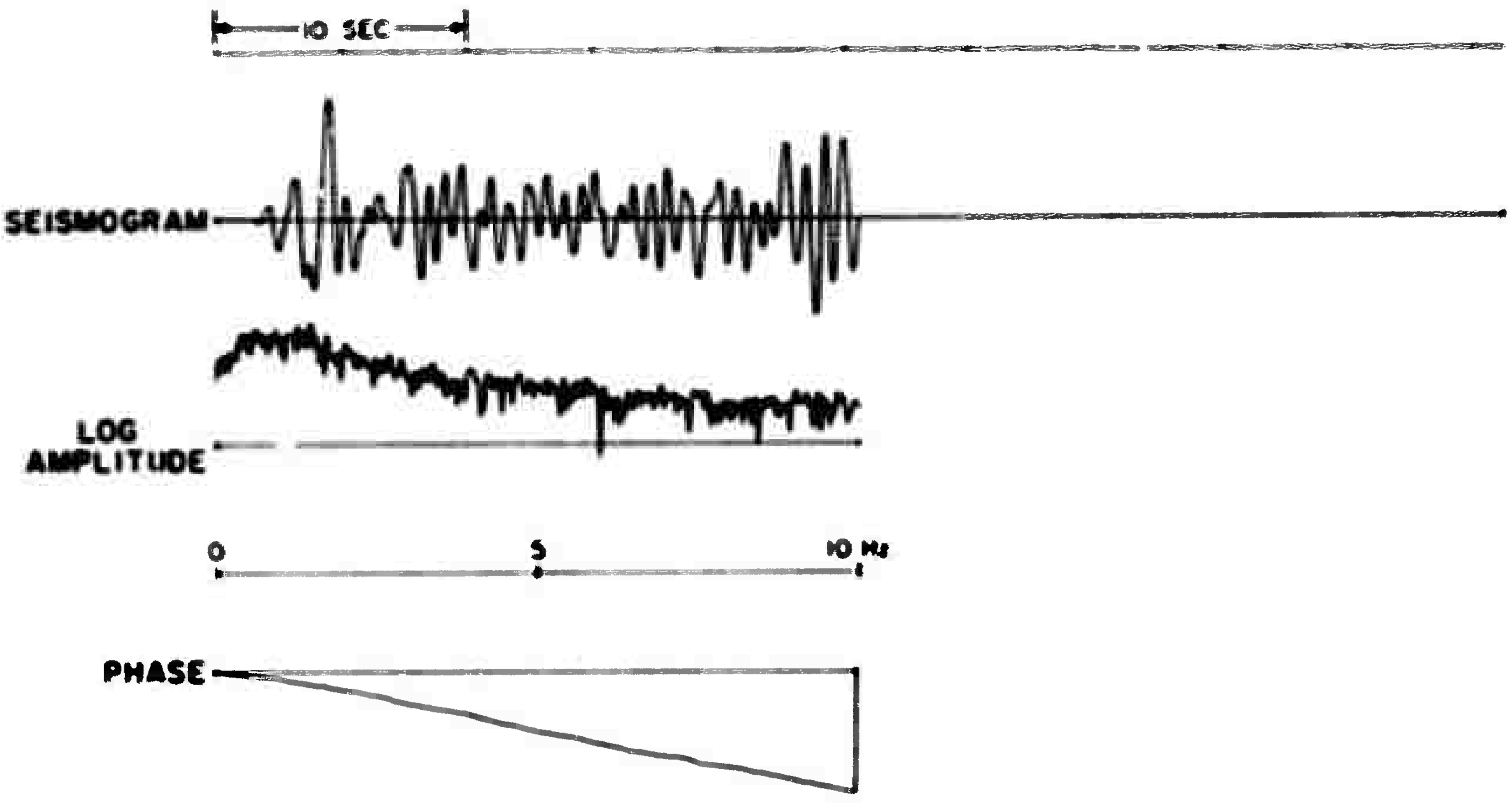

Figure [illegible]. [illegible] Nov. [illegible] Andreanoff Islands event, station [illegible] (a) Seismogram vs. time. (b) Log-amplitude vs. frequency. (c) Unwound phase vs. frequency.

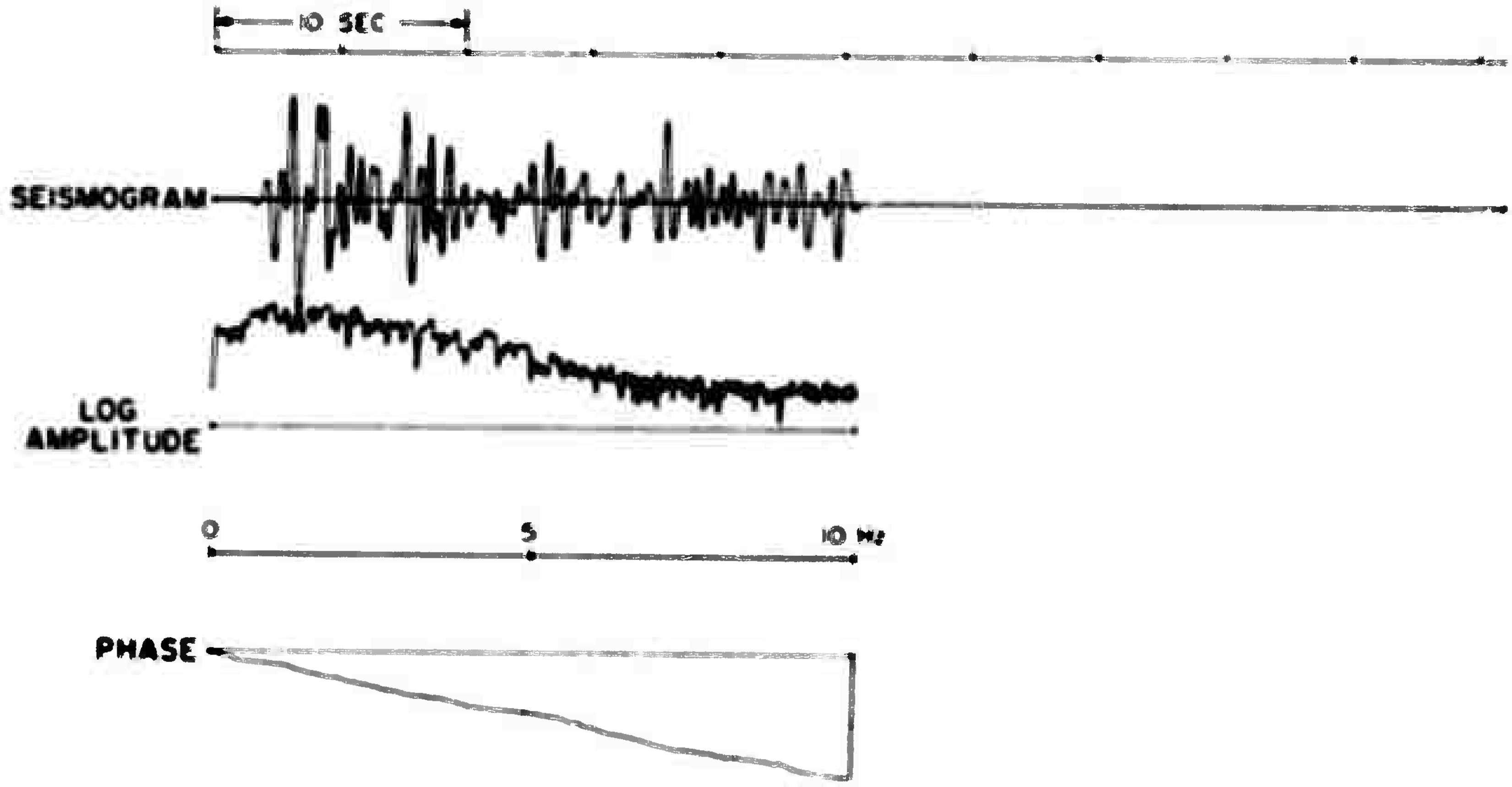

Figure [illegible]. [illegible] Nov. 1965 [illegible] Islands event, Station [illegible]. (a) Seismogram vs. time. (b) Log-amplitude vs. frequency. (c) Unwound phase vs. frequency.

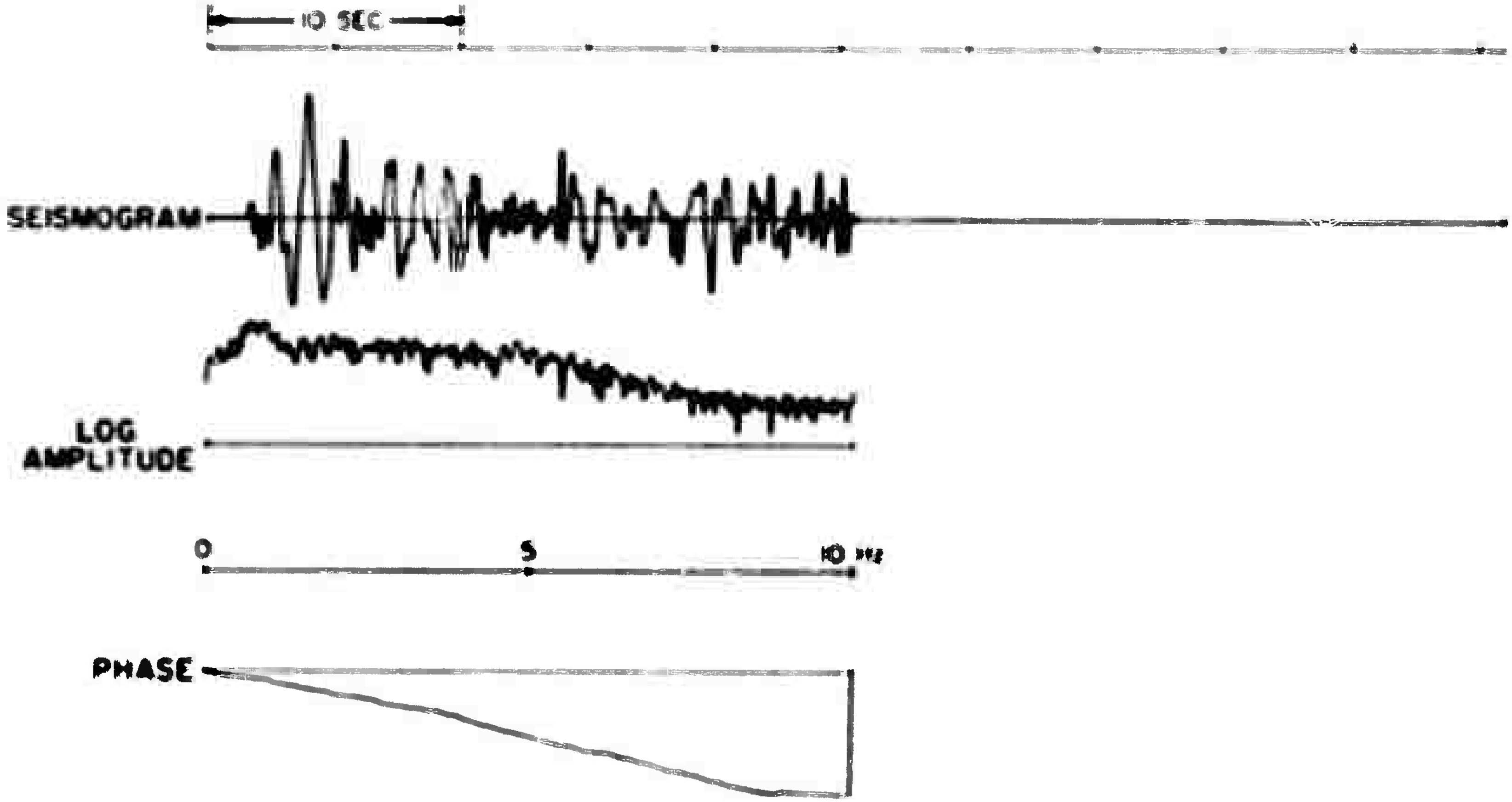

Figure [illegible]. [illegible] Nov. [illegible] Andreanoff Islands event. Station [illegible] (a) Seismogram vs. time. (b) Log-amplitude vs. frequency. (c) Unwound phase vs. frequency.

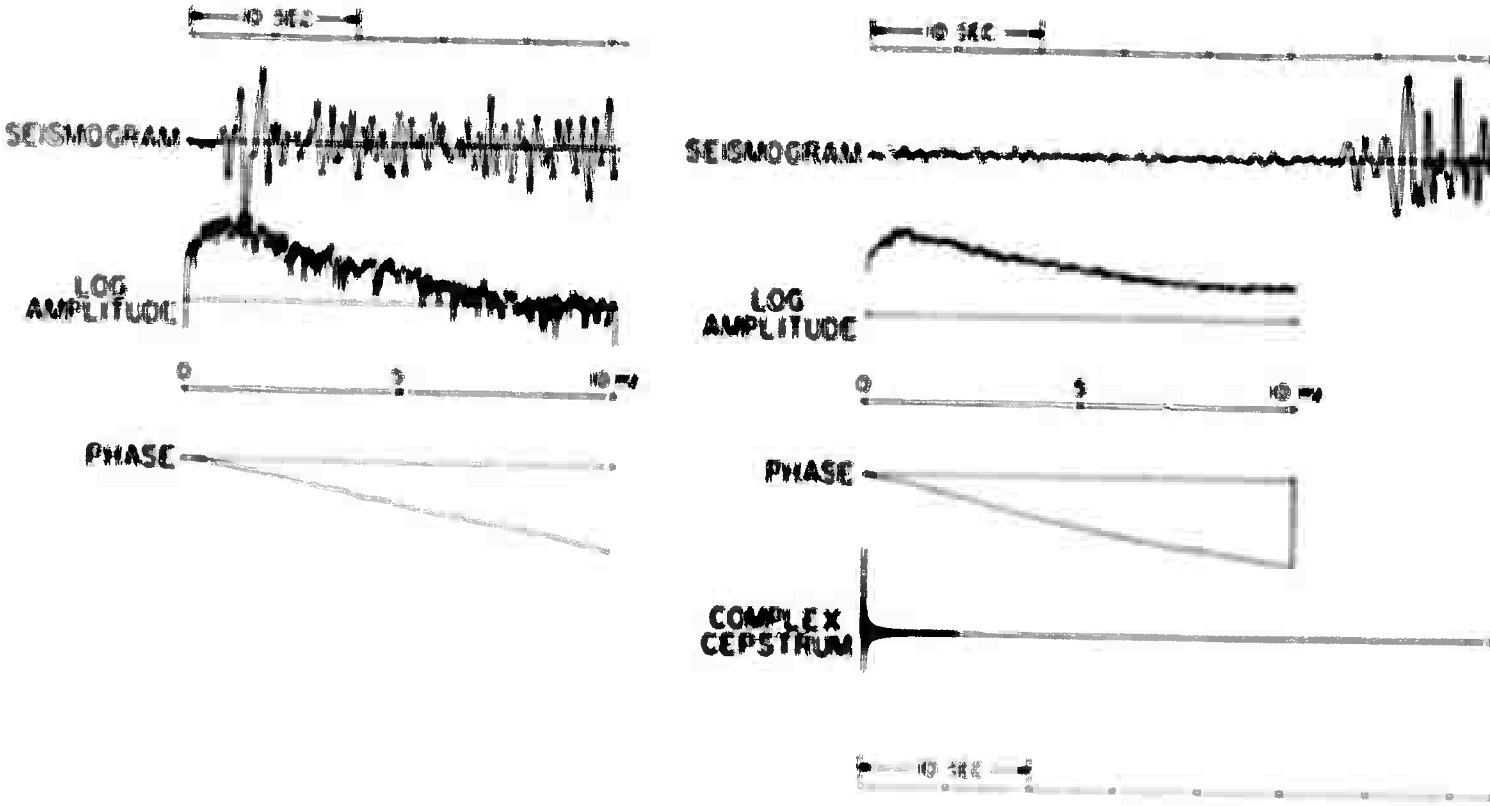
SEISMOGRAM
LOG AMPLITUDE
PHASE
0
5
SEISMOGRAM
LOG AMPLITUDE
0
5
PHASE
COMPLEX CEPSTRUM

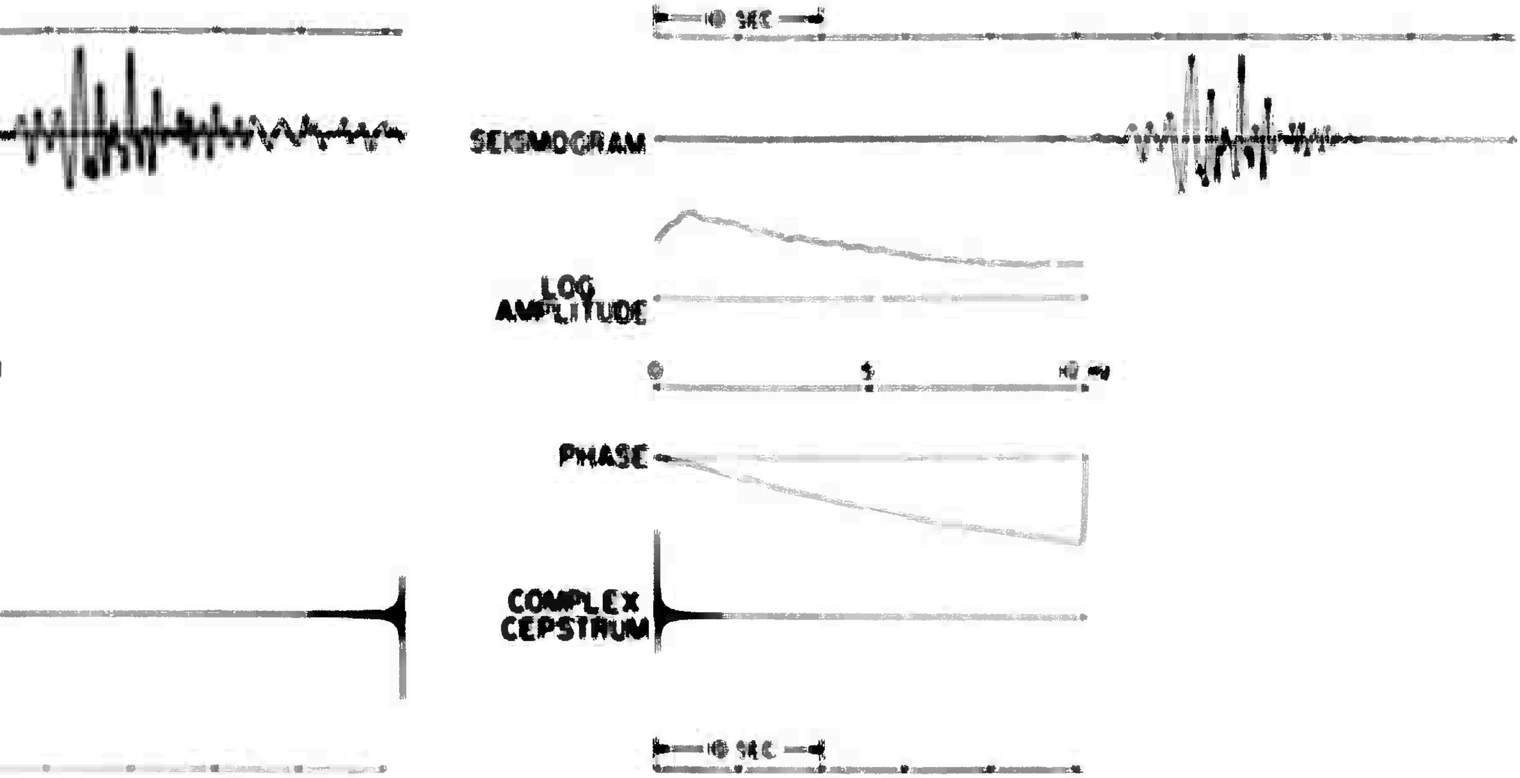

Figure 58. Processing results for 22 Nov. 196
Andreanoff Islands event
(a) Beamforming
1. Seismogram vs. time
2. Log-amplitude vs. frequency
3. Unwound phase vs. frequency
(b) Generalized linear filter 1
1. Seismogram vs. time
2. Log-amplitude vs. frequency
3. Unwound phase vs. frequency
4. Complex cepstrum vs. time

b

(c) Generalized linear filter 2
1. Seismogram vs. time
2. Log-amplitude vs. frequency
3. Unwound phase vs. frequency
4. Tapered complex cepstrum.